RESPONSE OF KARST AQUIFERS TO RECHARGE

by

WALTER G. KNISEL

December 1972

HYDROLOGY PAPERS
COLORADO STATE UNIVERSITY
Fort Collins, Colorado

60

RESPONSE OF KARST AQUIFERS TO RECHARGE

BY

Walter G. Knisel

HYDROLOGY PAPERS
COLORADO STATE UNIVERSITY
FORT COLLINS, COLORADO 80521

December 1972 No. 60

TABLE OF CONTENTS

ABSTRACT

RESPONSE OF KARST AQUIFERS TO RECHARGE

Three springflow measuring stations were selected for study where ground-water discharges from karstified limestone. The measured flow consisted only of ground-water outflow. Two springs were located in the Edwards Plateau of Texas and the third in south central Missouri. Rain gages near the springs were selected for study of associated rainfall.

Daily rainfall and mean daily springflow data were analyzed to determine the structure of the time series. Harmonic analysis was made to determine significant periodicity for 1-, 3-, 7-, and 14-day mean rainfall and springflow. Stochastic models of rainfall and springflow were developed for 1-day values of each time series.

Recharge of karst aquifers was estimated from rainfall by fitting a serpentine curve based on physical relations. Recharge was related to rainfall by the general expression $R = abP/(a^2 + p^2)$ in which R is recharge in percent, P is rainfall in inches, and a and b are constants.

Ground-water discharge data were analyzed to determine sustained recession characteristics and to discern characteristics of the aquifer systems. Recessions were found to be approximated by an expression of the form $q_t = q_o e^{-ct}$, in which q is discharge rate in cubic feet per second, t is time, and c is a constant.

Systems analysis was applied to determine system identification for springflow simulation. Convolution transfer functions were estimated by four methods: (1) optimization by the Wiener-Hopf equation, (2) optimization by multiple regression techniques, (3) harmonic series for total springflow, and (4) two-parameter gamma function. Recharge-response hydrographs, above extrapolated recessions, were used with methods 1, 2, and 4. Average convolution transfer functions were determined from the Wiener-Hopf equations and from multiple regression techniques with estimated recharge as input. Parameters of the gamma function were estimated from hydrograph analysis. Aquifer constants were determined for each springflow station using estimated parameters and hydrograph peak discharges. One-to-one correspondence of rainfall and springflow enabled determination of springflow contributing area. A linear relation was developed between size of area and aquifer constant.

Springflow simulation was made with convolution transfer functions determined for rainfall and for recharge using the optimized Wiener-Hopf equation. The chi-square test of goodness of fit was made to determine that recharge which as input gave the better results.

The two-parameter gamma function with estimated recharge provided the best results of simulation as determined by the computed chi-square. The harmonic function was the least accurate of the simulation procedures.

ACKNOWLEDGMENTS

The author gratefully acknowledges the encouragement, guidance, and patience of his adviser, Dr. V. Yevjevich. His vast experience of karst hydrology and analyses methodology has been invaluable in guiding the pursuit of the study.

Drs. D. B. Simons and D. C. Boes, members of long standing on the graduate committee, are acknowledged for their patience, comments, and suggestions. Special thanks is given to Drs. D. A. Woolhiser and C. F. Nordin for their gracious consent to serve on the committee in place of a member who had resigned from the C.S.U. staff. Despite their short tenure on the committee, their concerted efforts, comments, and suggestions are greatly appreciated.

Dr. Earl Burnett, Director of the Blackland Conservation Research Center, Temple-Riesel, Texas, is acknowledged for making digital computer time available for the study. Without such computer availability, the dissertation topic could not have been pursued.

Dr. Walter G. Knisel
U.S. Department of Agriculture - ARS
Southeast Watershed Research Center
Athens, GA 30601

PREFACE

To investigate responses of well-defined hydrologic environments, the current practice is to apply a systems approach. The response function thus derived is then applied in practice to determine the environment's output from a known input, or to determine an input for a known output. In addition, the response function is frequently used to predict the system output several days or weeks following an observed set of input variables.

The system is conceived as a well-defined area or space, usually with multiple inputs and outputs, since hydrologic system problems that require practical solution are seldom single-input, single-output relationships. This approach requires two of three factors (input, response, output) to be well known in order to determine the third factor.

Many techniques were developed or tried to solve such simplified problems. In particular, efforts have been invested in hydrologic studies to develop methods of determining the average response of a system to a given input and a given output. Among the factors which complicate such studies are the response function's non-stationarity that arises from periodic system characteristics affecting the response; randomness in the response, attributable to randomness in factors affecting the system response; errors in input and/or output computation; errors in assessing system characteristics; and variations in the accuracy of complex multiple input and/or complex multiple output measurements.

It is common for many hydrologic environments, conceived as systems, to have a good information on a concentrated single output, to have some information about the type of system response because of some known characteristics of the system, and to have some but not complete information on the input. In the case of response of a surface in the rainfall-runoff relationship, for example, the runoff is usually the best known of the three factors. The general surface features are known to a sufficient extent that something may be inferred about the type of response, while the precipitation is only partially known through temporal and areal sampling of its time-area distribution. When evaluating effective precipitation, the surface runoff portion and/or the ground water recharge portion must be determined, the information on effective precipitation is even less reliable than information on precipitation because of various errors in estimating evaporation, evapotranspiration, infiltration to ground water, and ground water portion of the runoff.

Hydrologic systems may be roughly classified into systems either open or closed to inspection. Here, the concept of "open systems" means that something about a system is known, either by visiting the area or by using maps and other sources of information. Therefore, it is either difficult or undesirable to apply the simple black-box system approach to an "open system," because the "box" is not black but grey, particularly as the inputs are only partially known, with relatively large errors in estimating their information, while the outputs are well known within the limits of measuring errors. This is the case of one well known factor, and of the partial knowledge on the two other factors, in the three-factor or the input-response-output approach. The hydrologic system that is "closed" to visual inspection, say, such systems as deep underground water aquifers, is an ideal case for the application of the black-box approach when very little is known quantitatively and objectively about the system itself, regardless of the fact that potentially a wealth of hypotheses and inferences resulting from the general hydrogeologic studies of aquifers may exist. When an underground water resources aquifer has a concentrated output in the form of a large spring, as in the case of many karst aquifers, the outflow is usually well measured. Uncertainties in determining the surface which contributes water to recharge and the recharge itself to ground water, make the black-box application relatively difficult. The case is usually reduced to knowing fully only the output and knowing only partially the recharge surface and its precipitation. For karst aquifers as hydrologic closed systems, the output is a good integration of areal and temporal inputs. It is then often feasible to derive some information about the input from the characteristics of the output.

Mathematical analysis of hydrologic systems in karst areas has been a relatively neglected subject when compared with efforts in studying other hydrologic systems, particularly the response of non-karst small river basins, urban areas, and larger river basins. However, karst areas may be very important; the total surface of karst formations in the United States, as shown in Fig. 1 of this paper, approximates the combined area of Texas, Oklahoma, and Kansas. Because the natural resources are relatively poor (say land, forest, and mineral resources) in most karst areas of the world, and because the water may be one of the most important resources for development, or its availability is a precondition for developing all other resources, the investigation of characteristics and responses of karst aquifers has high economic and social value. It can be also shown that hydrologic properties of highly permeable lava formations are very similar to properties of some karstified limestone or dolomite formations.

There is a general reluctance in many countries to construct water storage capacities in karst areas, because of the problem of securing the reservoir imperviousness. The development of water resources in karst areas is often delayed due to this understandable hesitation. However, since World War II very successful large storage reservoirs have been constructed in some of the most typical karst areas of the world. High permeability of karst formations and limited purifying capacity of underground karst aquifers have made it difficult to maintain clean outflowing waters from karst areas when the recharge surface waters are subject to natural or man-made pollution. This problem has been compounded in recent decades in many parts of the world. The study of karst aquifers becomes attractive from all three vantage points: development of scarce natural resources in karst areas, finding economical methods of regulating waters regardless of high permeability of karst formations, and the need for controlling water quality of karst aquifers under natural or changed conditions of recharge.

The doctoral thesis by Walter G. Knisel, Jr., under the title "Response of Karst Aquifers to Recharge," presented as this hydrology paper, was aimed at applying and extending various methods of systems approach to natural hydrologic environments for the

case of karst aquifers, particularly for the relatively deeper aquifers. This is the case in which only the output is well known, while the input or inputs can be estimated only with relatively large errors. This study is divided basically into three parts: (a) the analysis of input in the form of total precipitation, as well as the effective rainfall which recharges a karst aquifer; (b) the study of characteristics of output, in the form of concentrated karst spring outflows; and (c) the system identification in assessing the karst aquifer response functions in the form of unit hydrographs. The three examples used are from different karst areas in the United States. These examples clearly show that the reliability of determining responses of karst aquifers to recharge depends on both the type of karst aquifer and the reliability of data on both the output and the input.

It may be inferred from the study that the reliability of derived response functions may be significantly increased with the progress in collecting new data on recharge areas and on water recharge to and outflow from the karst aquifers. It may be expected also that the measurements of various properties of water of karst springs, not only of discharge, but also of temperature and various other water quality parameters (turbidity, mineralization, biological quality, etc.) would significantly increase the reliability of inferences about the types and characteristics of karst aquifers. In other words, the characteristics of quantity and quality of outflowing water from a karst formation, and the black-box systems approach in studying the responses of aquifers, can add new and reliable information to be combined with the general hydrogeologic information on these aquifers.

The study presented in this hydrology paper is sponsored by the U. S. Agricultural Research Service, with the cooperation of Colorado State University Experiment Station in the form of contributions by advisors. This paper is also a contribution to the ongoing bilateral cooperative U.S.-Yugoslavia research project on karst hydrology and water resources systems. This karst project is an attempt to combine in a cooperative endeavor the Yugoslav experience, accumulated data and other information on karst hydrology and water resources systems with the advanced U. S. research methodology and technology, for the mutual benefit of both cooperating parties. The Yugoslav part of the project is sponsored by the U. S. National Science Foundation Grant GF-29930X1, in using the PL-480 counterpart funds in Yugoslavia, with the University of Sarajevo, Sarajevo, Yugoslavia, responsible for the Yugoslav part of cooperation, and Colorado State University, Fort Collins, Colorado, U.S.A., responsible for the U. S. part of cooperation under the Karst Research Project sponsored by National Science Foundation, Grant GK-31529X.

Vujica Yevjevich
Professor of Civil Engineering
and Professor-in-Charge
November 1972 Hydrology and Water Resources
Program
Department of Civil
Engineering
Colorado State University
Fort Collins, Colorado, U.S.A.

CHAPTER I

INTRODUCTION

Streamflow simulation models of rainfall-runoff relations generally give little consideration to ground-water components of the hydrograph. Surface runoff prediction methods assume hydrograph separation techniques that are arbitrary and are rarely based on experimental data. Such separation techniques force specific characteristics of the ground-water flow without giving any consideration to aquifer properties or performance characteristics. Ground-water flow may be an important quantity of total streamflow for water supply and pollution abatement. Karst aquifers are known for their large storativity and transmissivity, yet simulation models treat such aquifers in the same manner as sandstone, shale, alluvium, lavas and other types of aquifers.

Mathematical models treat ground water as a residual of evaporation, surface flow, and soil water. Little effort has been made to simulate ground-water recharge and response. Aquifers in geologic mantles having high transmission and low storage capacity may behave quite differently from those having massive storage materials. Measurements of springflow as an entity provide an opportunity to study aquifer characteristics. An inherent problem in such a study is the uncertainties in determining areal extent of the springflow contribution and thus the area of system input; i.e., areal infiltrating rainfall.

Areal rainfall is highly variable, especially in semiarid regions. Weather Bureau rain gage networks are oftentimes very sparse. One rain gage per county is common in most states except in large metropolitan areas or in areas of specific studies. Such sparse rain gages provide meager input data for a hydrologic system. Sufficient rainfall may occur between gages to produce significant recharge of ground water, yet there may be no rainfall measured at the gages. Comparison of the rainfall and springflow records often times indicates increased discharge without observed rainfall. Also, large amounts of rainfall may be recorded at a single gage, but areal coverage is not sufficient to provide significant recharge and ground-water response. System modeling and simulation are no better than the information available, and lack of adequate input data severely handicaps any analysis.

Conversely, the measurement of total flow passing a gaging station provides a maximum of information about the flow characteristics at the gaging station. Continuous stage records and good stage-discharge relationships provide accurate estimates of total system response. Although the data are highly accurate, springflow is an integrator of the aquifer properties, and characteristics of the detailed system are masked. Particularly in a karst system, there is a high degree of variability between individual aquifers and within aquifers as parts of the total karst system of a large karst spring. A spring at one location may discharge only a trickle flow; whereas, another spring in the general vicinity may discharge large rates and volumes of ground water. Without a knowledge of the system, the measurement of input and output makes it difficult to study the cause and effect.

A ground-water karst system is unlike a surface-water system in that physical dimensions of the contributing area are unattainable for the most part. The ability to observe overland flow, measure surface channels, observe types of flow, determine flow resistance factors, etc., is nonaccessible in ground-water investigations. Logs of observation wells provide little information about the system, especially a karst system. The random occurrence of solution channels, fissures, caverns, and various deposits of transported materials, etc., makes well logs applicable only to the local area of logging. In the words of Stringfield and LeGrande [29]:

"Limestone and other carbonate rocks are characterized by many unusual features and extreme conditions, either involving the hydrologic system within them or wrought by hydrologic conditions on them or through them. Perhaps there could be little agreement as to what is typical or average for the many features of carbonate rocks, as indicated by the following conditions: bare rock and thin soils are common, but so are thick soils; very highly permeable limestones are common, but so are poorly permeable ones; and rugged karst topographic features with underlying solution caverns are common, but so are flat, nearly featureless conditions."

Therein lies reason enough why the literature noticeably lacks general description of karst ground-water flow phenomena. However, the widespread occurrence of karst areas in the United States, as shown by Fig. 1, indicates the need to understand and quantify karst ground-water flow.

This study is directed toward a better understanding of the karst ground-water flow phenomena. The three major objectives to be considered in the study are:

1. description of geohydrology of karst ground-water phenomena,
2. prediction of ground-water flow,
3. design of better prediction models of ground-water flow than are currently available.

The objectives are interdependent in that an understanding of the geohydrology is necessary to develop adequate models for ground-water flow prediction. Likewise, the investigation of theoretical models leads to a better understanding of the geohydrology.

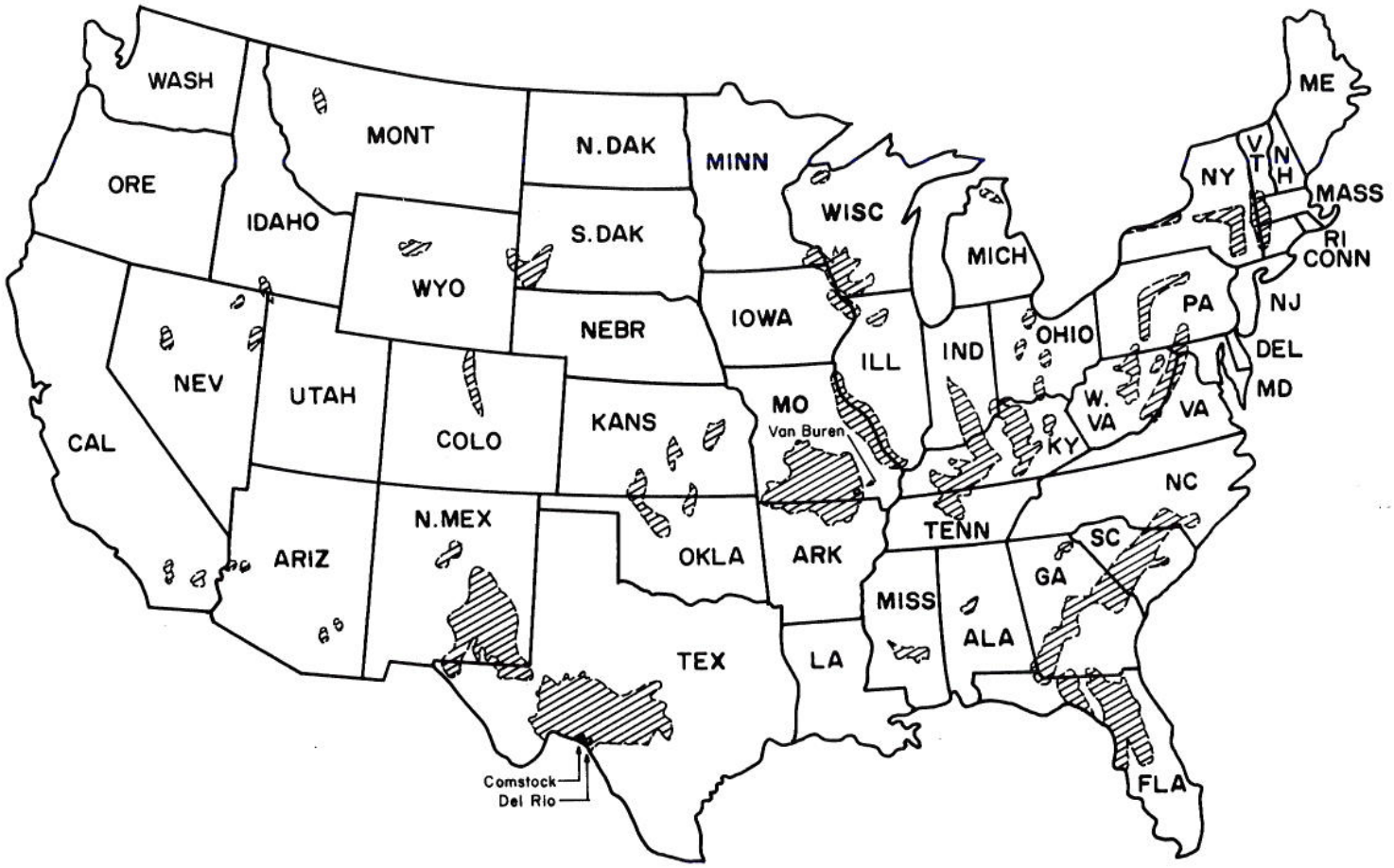

Fig. 1 Map of United States showing major karst areas. (Adapted from Stringfield and LeGrande [29])

CHAPTER II

REVIEW OF LITERATURE

Hydrograph separation techniques described by Linsley, Kohler, and Paulhus [21] have been used to separate storm and base flows for the purpose of studying aquifer characteristics. Probably the most used method, because of its simplicity, is depicted in Fig. 2, upper graph. Baseflow is assumed to decline to a time coincident with the storm flow peak and then increase to a point on the hydrograph recession known to be true baseflow. The method forces a specific aquifer performance. Knisel [19] found experimentally that baseflow begins to increase when storm flow begins and peaks at the approximate time of hydrograph inflection and continues along the backward extension of the true baseflow recession. The experimental data agree well with a method presented by Linsley, Kohler, and Paulhus [21], and is depicted in Fig. 2, lower graph. The second method more nearly describes the true aquifer behavior. Nevertheless, any type of flow separation forces that specific shape of the ground-water flow and any characteristic features of the aquifer are often completely masked.

Hydrograph recession analyses have been used to determine aquifer characteristics. The method described by Barnes [3] and later used by Knisel [17] relates aquifer discharge at some time, t, to an initial discharge by a recession constant, K_r, raised to a power of time. The relationship is

$$q_t = q_o K_r^t \quad . \tag{1}$$

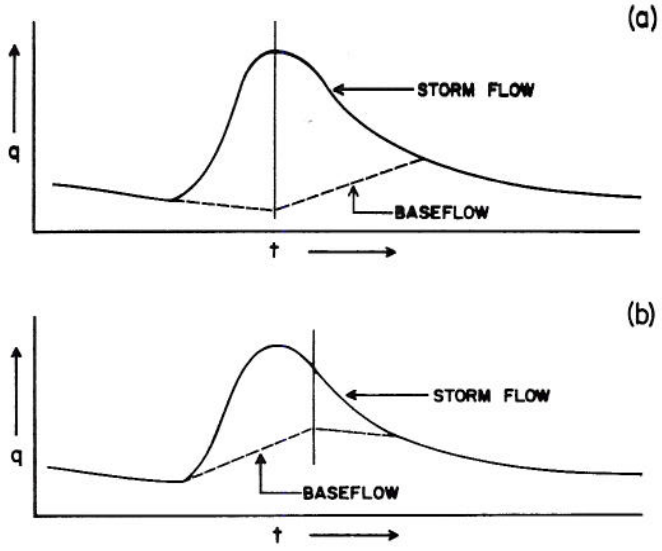

Fig. 2 Hydrograph separation techniques.

Recharge of the aquifer was not considered in the analysis, but aquifer storage was given as

$$S = \frac{-q_o}{\ln K_r} \quad , \tag{2}$$

where q_o and K_r were chosen to provide an estimate of maximum storage.

Analytical integration of differential equations of water storage was investigated by Yevjevich [40] to fit curves to outflow hydrographs for reservoir and channel reaches. It was found that for zero inflow, i.e., sustained recession, an exponential equation adequately represented the recession. The equation related discharge, q, at some time, t, to an initial discharge, q_o, as

$$q_t = q_o e^{-ct} \quad , \tag{3}$$

where c is the slope of the recession, and e is the base of natural logarithms.

Equation (3) represents a special case when the ratio of exponents of storage function and outflow rating curve was unity. The representation of recession by the exponential equation is an approximation of the ground-water flow portion of the total hydrograph.

Dooge [10] considered aquifer recharge in his theoretical development of aquifer performance. Two equations were theorized to describe the shape of the hydrograph, shown in Fig. 3. The discharge equations are

$$q = r\left(1-e^{-t/K}\right) \quad , \quad 0 < t < T \quad , \tag{4}$$

and

$$q = r\left(e^{T/K}-1\right)e^{-t/K} \quad , \quad T < t < \infty, \tag{5}$$

where r is the rate of recharge, T is the duration of uniform recharge, t is the time, and K is the storage delay time of an element.

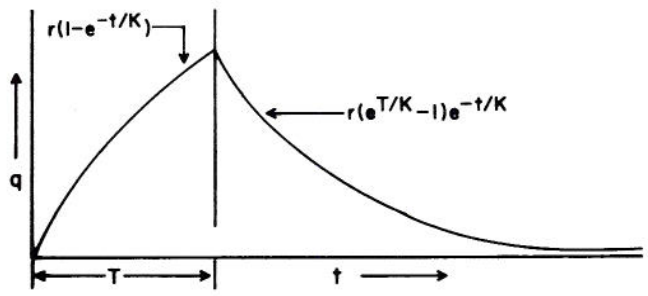

Fig. 3 Aquifer recharge and recession.

The K term in Eqs. (4) and (5) is merely a convenient term and is not the same as the recession constant, K_r, of Eqs. (1) and (2). In Eqs. (4) and (5), r is a scale factor, and T and K are shape factors. The necessity of two equations to describe the hydrograph indicates Dooge's recognition of the complexity of ground-water recharge and discharge.

A two-stage convolution was developed by Snyder et al [28] to provide a nonconstant response model of storm runoff for coastal plain watersheds. The nonconstancy of watershed response was attributed to permeable sandy soils, high water tables, and low relief. Snyder stated,

"...if rain falls on permeable soil when the water table is some distance below the surface, infiltration will be high. The net effect of the rain is to raise the water table, which in turn increases streamflow from ground water."

The permeable soil of coastal plain watersheds is equivalent to fractured limestone with a thin mantle of soil in a karst system. The resulting recharge and response is somewhat analogous to the condition of permeable sandy soil.

Snyder's [28] response function was given in two parts as

$$q_t = a\left(1-e^{-At}\right), \qquad 0 < t < b \ ,$$

$$q_t = a\left(e^{Ab}-1\right)e^{-At}, \qquad b < t \tag{6}$$

where A is the parameter of drainage basin wetness, a is a constant value of the core function, $C(\tau)$, and b is the time base of the core function. Snyder's two-part response function of surface flow is analogous to that theorized for ground-water flow by Dooge [10]. Snyder's terms a, A, and b in Eq. (6) are equivalent to Dooge's terms r, 1/K, and T in Eqs. (4) and (5), respectively.

Kraijenhoff van de Leur [20] used aquifer characteristics in an expression for ground-water hydrograph recession. The equation is

$$q_t = \frac{8}{\pi^2} pL\left(e^{b/j}-1\right)e^{-t/j} \tag{7}$$

where q_t is the discharge at time t, p is the rate of percolation to the saturated zone, L is the distance between two outflow channels, b is the duration of steady percolation, t is the time, and j is the ground-water reservoir coefficient. The coefficient j is a time measure relating aquifer characteristics, expressed as

$$j = \frac{1}{\pi^2}\,\mu\,\frac{L^2}{KD} \tag{8}$$

where μ is the volume fraction of pores drained at a falling water table, assumed to be equal to the volume fraction of pores filled at a rising water table, K is the hydraulic conductivity as influenced by permeability of soil and viscosity of the ground water, and D is the mean depth of the impermeable layer below the water table. Eqs. (5) and (7) can be related to express Dooge's K term with respect to aquifer characteristics. Equating (5) to (7), using common synonymous terms gives

$$r\left(e^{T/K}-1\right)e^{-t/K} = \frac{8}{\pi^2} pL\left(e^{b/j}-1\right)e^{-t/j} \tag{9}$$

Then

$$r = \frac{8}{\pi^2} pL \tag{10}$$

which relates recharge rate, r, to channel spacing, L, and

$$K = j = \frac{1}{\pi^2}\,\mu\,\frac{L^2}{kD} \ . \tag{11}$$

The product of kD in Eq. (11) is transmissivity, T_r, described by Todd [31].

Green [14] describes the Edwards reservoir as having 30,000 acre-feet of water per foot of drawdown, and gave the size of reservoir as approximately 6,400 square miles. Then the fraction of drainable pores μ, would be approximately 0.0075. Holt [16] states that pumping tests in cavernous limestones are unreliable, but estimated the transmissivity from his pumping data to be 20,000 gallons per day per foot. Perennial streams occur in the Edwards Plateau at approximately 40,000-foot intervals. These values substituted in Eq. (11) result in a reservoir coefficient, j, of 60 days. The coefficient would also be appropriate for Dooge's delay time element, K.

A value of K = 60 days in Eqs. (5) and (7) results in a general hydrograph shape shown in Fig. 4. The relatively long delay time element attenuates the peak and also results in a slow recession.

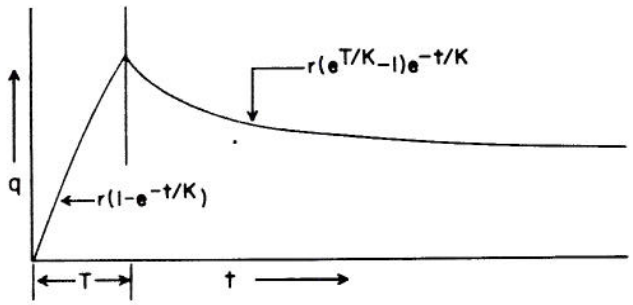

Fig. 4. General shape of hydrograph with a delay time element, K = 60 days.

Hydrograph rise is dominated by time of recharge, T, and a short rise time is depicted in Fig. 4.

Applying Eq. (1) to the recession of Fig. 4 and solving for K_r gives an average recession constant of 0.984. Knisel [17] found an average K_r of 0.939 for sustained baseflow from limestone geologic basins. However, Knisel found that recession constants vary considerably between basins, particularly when considering total streamflow.

Becker [4] related ground-water recharge to rainfall, season, and runoff by means of a coaxial graph for European basins. Recharge was considered to be a

residual of rainfall after (a) surface runoff and (b) abstraction from infiltration for soil water deficit. The relationship was independent of time in as much as rainfall values were total storm amounts. The theorizations by Dooge [10] and Kraijenhoff van de Leur [20] are the only attempts to express aquifer recharge and response by hydrographs.

Linearity of hydrologic systems was first assumed by Sherman [25] in his unit hydrograph concept for isolated pulses of uniform input. The unit hydrograph theory was applied to direct storm runoff. Since Sherman's work, numerous investigators have applied the unit hydrograph (linear) theory in the development of storm runoff models [8, 9, 33, 39]. Williams [39] made use of the relationship of Eq. (1) to describe the recession of direct runoff hydrographs for small ephemeral basins that did not have baseflow. The good results indicate the versatility of the equation to describe the phenomenon of flow recession, overland, or ground-water flow.

Since Sherman's [25] pioneering work, other investigators have employed various hydrograph fitting techniques to consider complex input systems. Linsley et al [21] suggested a numerical technique using all input and output data to describe the system. One objection to the method is the instability and oscillatory nature of the resulting hydrograph, except for truly linear systems.

Snyder [26] employed the method of least squares to fit storm hydrographs. Multiple regression analysis was made to relate hydrograph ordinates to rainfall amounts, distributed and combined in physical logic. The method failed to adequately fit observed hydrographs due to the inability of the regression constant to express a changing difference between rainfall and runoff during a storm. The failure occurred in the recession portion of the hydrograph which is the most predictable region of ground-water hydrographs.

For a watershed systems analysis, Amorocho [1] described three input-output-response function conditions.

1. If the input and output parameters, although distributed in space, can be lumped, the system is space invariant (lumped system).

2. If the response function of a watershed does not change during a storm or from season to season, the system is time invariant.

3. If the principle of superposition and its related principle of proportionality are applicable for a system, the system is linear. However, if past input elements influence present output such that the total of their effect is not the sum of their separate effects, the watershed is nonlinear.

Amorocho [1] stated that the linear behavior cannot be represented by hydrologic systems except in very special cases. The response of a ground-water system should not change during a particular storm, and since the aquifer is an integrator of the system, it should not change between storms. Therefore, in accordance with Amorocho's description, a ground-water system should act as a linear time-invariant system.

Cheng [6] presented the notion that the convolution equation exactly related the input and output time functions of a linear system. For a continuous linear system, the convolution equation is expressed as

$$g(t) = \int_{-\infty}^{\infty} h(\tau)\, f(t-\tau)\, d\tau \qquad (12)$$

where $g(t)$ is the system output, $f(t)$ is the system input, and $h(\tau)$ is the system unit impulse response. Such a system is illustrated in Fig. 5.

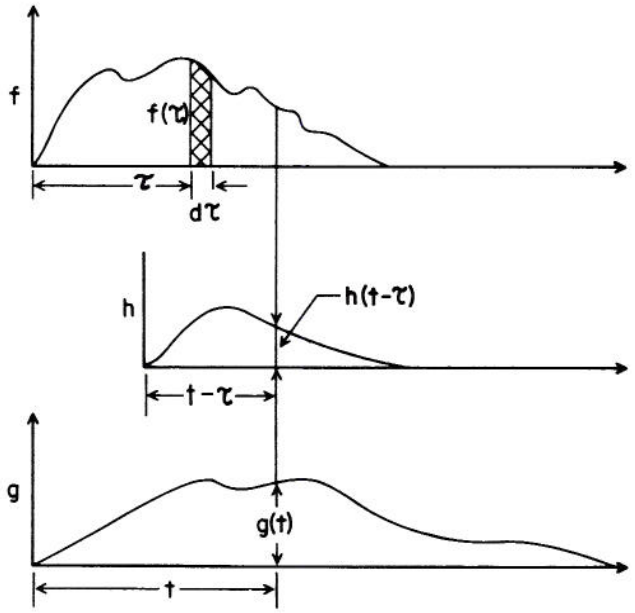

Fig. 5. Continuous linear system notation.

Eagleson et al [12] utilized the notion of convolution in their systems analysis of direct runoff from small urban catchments. Numerical values of input, $f(t)$, and output, $g(t)$, for a discrete time series, were used in the analysis. The discrete equivalent of the convolution integral, Eq. (12), is

$$g(i) = \sum_{k=-\infty}^{\infty} h(k)\, f(i-k+1)\, \Delta k \quad . \qquad (13)$$

Eq. (13) is readily solved by synthetic division for truly linear systems. Fig. 6 shows the linear system notation for the discrete time series. Hydrologic systems are recognized as not being true linear systems [1, 2]. Eagleson et al [12] demonstrated that in a truly linear system any errors of measurement cause unstable, oscillating unit impulse response functions as was the case with the method of least squares [26]. Eagleson [12] imposed requirements of a stable monotonic solution and followed the work by Wiener [38] to develop the discrete time form of the Wiener-Hopf equation

$$\phi_{fg}(j-1) = \sum_{k=1}^{\infty} h_{opt}(k)\, \phi_{ff}(j-k), \qquad j \geq +1. \qquad (14)$$

In Eq. (14), ϕ_{fg} is the cross correlation function of input and output, ϕ_{ff} is the autocorrelation function of input, and h_{opt} is the optimum unit impulse response function. Eagleson imposed the constraint that

$$h_{opt}(k) \geq 0 \qquad (15)$$

to determine stable unit impulse response functions. In order to impose Eq. (15), Eagleson developed an underdetermined set of simultaneous equations and used the simplex computational procedure [13] with linear programming to solve the equations. The procedure utilized "slack variables" to preserve the area under the impulse function. By imposing the condition that the sum of the slack variables was a minimum, the most feasible solution was obtained. The resulting characteristic of the impulse function was a hydrograph-shaped function with a "blip" displaced some time past the main response function: i.e., a normal shaped unit hydrograph followed by a smaller hydrograph. The unit response function can be used for a black-box type streamflow simulation, but such a function does not give any information about the system and it has no physical significance.

Snyder [27] applied multiple linear regression to the convolution equation to determine transfer function ordinates of surface runoff and thereby to infer characteristics of ground-water flow. A major advantage of the procedure over that of Eagleson's [12] is the resulting physical significance of the transfer function. Snyder [27] separated baseflow from storm runoff by extrapolating the baseflow exponentially to give an open-ended hydrograph, exemplified in Fig. 7. The example of Fig. 7 is characteristic of aquifer recharge and response superimposed on an extrapolated sustained recession. Snyder [27] gave the basic equations of convolution as

$$\begin{aligned}
r_1u_1 &= Q_1 \\
r_1u_2 + r_2u_1 &= Q_2 \\
r_1u_3 + r_2u_2 + r_3u_1 &= Q_3 \\
&\;\;\vdots \\
r_1u_n + r_2u_{n-1} + \ldots + r_mu_{n-m+1} + \ldots + r_nu_1 &= Q_n
\end{aligned} \qquad (16)$$

where r is the rainfall excess for a time interval, u is the unit impulse response ordinate, and Q is the discharge rate. The subscripts of Eqs. (16) are time increments. Equations (16) are, in essence, an expansion of Eq. (13). Snyder recognized that discrete transfer function ordinates represented a smooth continuous transfer function, and that it was impossible to represent the continuous function exactly by discrete ordinates. Due to errors of estimating rainfall excess, the input data represented erroneous discrete values and some optimization scheme, such as linear regression, was needed to provide a smoothing effect. Snyder represented the u's of Eqs. (16) as

$$\begin{aligned}
u_1 &= \phi_1 + e_1 \\
u_2 &= \phi_2 + e_2 \\
&\;\;\vdots \\
u_n &= \phi_n + e_n
\end{aligned} \qquad (17)$$

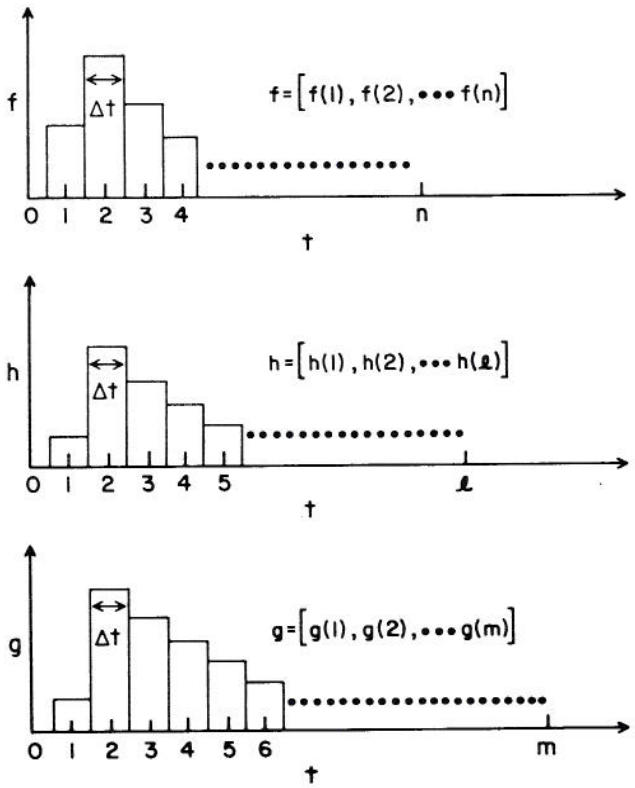

Fig. 6. Discrete linear system notation.

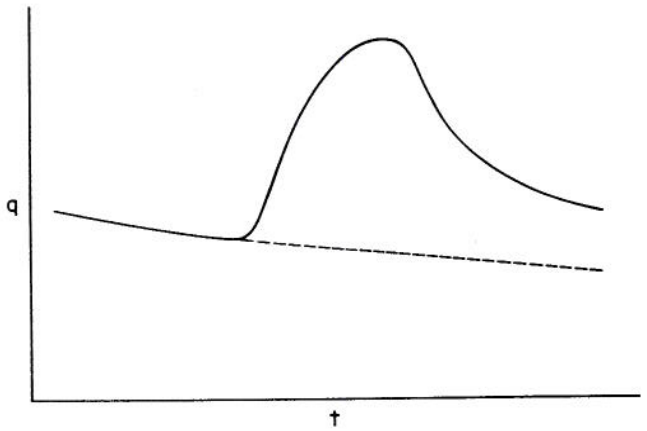

Fig. 7. Example of exponentially extrapolated baseflow to form open-ended hydrograph of direct runoff, or groundwater response to recharge.

where ϕ is the impulse function ordinate, and e is an error term. Snyder selected "angle points" on the transfer function and used linear interpolation between the angle points to distribute any error and provide a smoothing process. The angle points were closely spaced around the peak and spaced farther apart on the slowly changing recession. As an example, Snyder might select

ordinates at time units 1, 3, 4, 5, 7, and 9 as angle points to describe the shape of the transfer function. Then Eqs. (17) can be written,

$$
\begin{aligned}
u_1 &= \phi_1 + e_1 \\
u_2 &= \tfrac{1}{2}(\phi_1 + \phi_3) + e_2 \\
u_3 &= \phi_3 + e_3 \\
u_4 &= \phi_4 + e_4 \\
u_5 &= \phi_5 + e_5 \\
u_6 &= \tfrac{1}{2}(\phi_5 + \phi_7) + e_6 \\
u_7 &= \phi_7 + e_7 \\
u_8 &= \tfrac{1}{2}(\phi_7 + \phi_9) + e_8 \\
u_9 &= \phi_9 + e_9
\end{aligned}
\qquad (18)
$$

For the selected example, the peak of the hydrograph would be represented at time unit 4 and ordinates at times 3 and 5 are needed to adequately describe the hydrograph shape.

Eqs. (18) cannot be substituted into Eqs. (16) without increasing the total number of unknowns for ordinates and errors. However, there are errors in the discrete convolution and, when combined with the transfer function errors, errors in input, and errors in output, the error terms can be omitted. With omission of the error terms, e, in Eqs. (18), substitutions can be made into Eqs. (16) for four periods of rainfall excess to give

$$
\begin{aligned}
r_1\phi_1 &= Q_1 \\
\tfrac{1}{2} r_1(\phi_1 + \phi_3) + r_2\phi_1 &= Q_2 \\
r_1\phi_3 + \tfrac{1}{2} r_2(\phi_1 + \phi_3) + r_3\phi_1 &= Q_3 \\
r_1\phi_4 + r_2\phi_3 + \tfrac{1}{2} r_3(\phi_1 + \phi_3) + r_4\phi_1 &= Q_4 \\
r_1\phi_5 + r_2\phi_4 + r_3\phi_3 + \tfrac{1}{2} r_4(\phi_1 + \phi_3) &= Q_5 \\
\tfrac{1}{2} r_1(\phi_5 + \phi_7) + r_2\phi_5 + r_3\phi_4 + r_4\phi_3 &= Q_6 \\
r_1\phi_7 + \tfrac{1}{2} r_2(\phi_5 + \phi_7) + r_3\phi_5 + r_4\phi_4 &= Q_7 \\
\tfrac{1}{2} r_1(\phi_7 + \phi_9) + r_2\phi_7 + \tfrac{1}{2} r_3(\phi_5 + \phi_7) + r_4\phi_5 &= Q_8 \\
r_1\phi_9 + \tfrac{1}{2} r_2(\phi_7 + \phi_9) + r_3\phi_7 + \tfrac{1}{2} r_4(\phi_5 + \phi_7) &= Q_9
\end{aligned}
\qquad (19)
$$

Eqs. (19) have 9 equations and the number of unknowns has been reduced to 6. The values of r in Eqs. (19) provide the input for the multiple linear regression. The regression coefficients are the ordinates of the transfer function. The input data for the regression is shown in Table 1. Snyder's procedure [27] produced physically significant positive ordinates for the convolution equation.

Table 1. Coefficients for multiple regression grouped by ordinates.

Time Unit	ϕ_1	ϕ_3	ϕ_4	ϕ_5	ϕ_7	ϕ_9	
1	r_1						Q_1
2	$\frac{1}{2} r_1 + r_2$	$\frac{1}{2} r_1$					Q_2
3	$\frac{1}{2} r_2 + r_3$	$r_1 + \frac{1}{2} r_2$					Q_3
4	$\frac{1}{2} r_3 + r_4$	$r_2 + \frac{1}{2} r_3$	r_1				Q_4
5	$\frac{1}{2} r_4$	$r_3 + \frac{1}{2} r_4$	r_2	r_1			Q_5
6		r_4	r_3	$\frac{1}{2} r_1 + r_2$	$\frac{1}{2} r_1$		Q_6
7			r_4	$\frac{1}{2} r_2 + r_3$	$r_1 + \frac{1}{2} r_2$		Q_7
8				$\frac{1}{2} r_3 + r_4$	$\frac{1}{2} r_1 + r_2 + \frac{1}{2} r_3$	$\frac{1}{2} r_1$	Q_8
9				$\frac{1}{2} r_4$	$\frac{1}{2} r_2 + r_3 + \frac{1}{2} r_4$	$r_1 + \frac{1}{2} r_2$	Q_9

Dooge [10] referred to determination of unit impulse response functions in systems analysis as system identification. He stated that in truly linear systems in which input and output can be determined without error, all methods of system identification will give the same results, i.e., the same impulse response function. The optimization procedure, the least squares procedure, and the synthetic division procedure would each be appropriate and the choice of method would resolve to the selection of the simplest computational procedure. However, if the data contain errors or the system is not a truly linear one, the resulting impulse function will vary from method to method. The relative accuracy of the results in simulation depend upon how the methods handle various errors and linearize any nonlinear properties of the system.

The least squares method of system identification presented by Snyder [27] was formulated with the

thought that errors are normally encountered and the method tends to average the errors by a smoothing process. On the other hand, Eagleson's [12] optimization procedure tends to lump errors in an isolated blip at the tail of the response function.

Precipitation characteristics were studied by Todorovic and Yevjevich [32] in an attempt to determine the underlying structure of precipitation time series. Daily rainfall data were analyzed for selected stations to determine if significant harmonics existed in the means, standard deviations, and coefficients of variation. The Fisher test was used to determine the significance for six harmonics.

Quimpo [24] studied mean daily total streamflow time series (storm runoff and baseflow) for a number of river basins to determine the structure of the time series. One consideration in the analysis was to determine the amount of variance about the mean and the amount of variance of the standard deviation explained by each of six harmonics. The amount of variance about the mean explained by six harmonics ranged from 2 to 68 percent for 17 river basins studied; whereas, 31 to 97 percent of the variance of the standard deviation was explained by six harmonics. The eventual small cyclicity in precipitation could be a factor in the small explained variance when studying total streamflow where isolated input events cause storm runoff. Sustained ground-water flow should exhibit more cyclicity than total streamflow, since ground-water flow persists over longer durations than does rainfall and tends to attenuate the chance variations about the cyclic movement.

Principles of harmonic, spectral and cross-spectral techniques were applied to precipitation-streamflow systems by Gupta [15]. Monthly values of precipitation and streamflow data were analyzed for some river basins in California. Transfer functions between significant harmonics of the two time series could not be generalized. The analysis showed the transfer functions were exponential with respect to frequency.

Downer [11] reviewed Edson's work and showed that the Pearson III probability distribution function, with appropriate conversions, can represent the discharge-time relationship as for a hydrograph. The expression, known as the two-parameter or incomplete gamma function, was written as

$$q = \frac{\beta V \delta^{\delta r+1}}{\Gamma(\delta r+1)} t^{\delta r} e^{-\delta t}, \qquad (19a)$$

where V is the volume of runoff in inches, q is the discharge rate in inches per hour, t is the time in minutes since flow began, r is the time of hydrograph rise in minutes, δ is the shape parameter with dimensions of reciprocal of time, and β is the factor for conversion of discharge rate in inches per minute to inches per hour. Let $k = 1/\delta$ and $n = \delta r + 1$. Then $\delta = 1/k$ and $\delta r = n-1$, and Eq. (19a) can be written as

$$q = \frac{\beta V (1/k)^{n}}{\Gamma(n)} t^{n-1} e^{-t/k}. \qquad (19b)$$

The term

$$\left(\frac{1}{k}\right)^{n} = \frac{1}{k}\left(\frac{1}{k}\right)^{n-1} \qquad (19c)$$

and Eq. (19b) reduces to

$$q = \frac{\beta V}{\Gamma(n)}\left(\frac{1}{k}\right)\left(\frac{t}{k}\right)^{n-1} e^{-t/k}. \qquad (19d)$$

Equation (19d) is equivalent to that given by Nash [22], and by combining terms then

$$q = \frac{(t/k)^{n-1} e^{-t/k}}{K\Gamma(n)} \qquad (19e)$$

where $K = k/\beta V$, and thus Eq. (19c) is a function of the shape parameter, area, and runoff volume.

CHAPTER III

DATA AVAILABLE FOR ANALYSIS

Data used in this study were selected on the basis of ready availability and representativeness of the study domain. Published daily records of precipitation and streamflow for selected stations are available in most engineering and scientific libraries. Streamflow data for time intervals less than one day are available only upon special request. Hourly rainfall data are available for only a few major cities.

Ground-water flow from karst aquifers is the primary concern in the study. Streamflow stations, maintained by the U. S. Geological Survey and U. S. International Boundary and Water Commission, were reviewed with respect to geologic location to select records from karst areas. The streamflow stations in karst areas were further examined for flow characteristics. In order not to impose specific hydrograph shape by baseflow separation techniques, the list of stations were further screened to find those where only springflow was measured. Such stations, although very limited in number, represented true ground-water outflow. This is not meant to imply that surface runoff did not occur from the recharge area, but that surface runoff was not a part of the flow measured at the streamflow station.

The selection process resulted in only three springflow stations. Two springs discharge from the Edwards and associated limestones of Texas and the third discharges from the Merrimac limestone of Missouri.

Goodenough Springs near Comstock, Texas, and San Felipe Springs at Del Rio, Texas (Fig. 1) are maintained by the U. S. Department of State, International Boundary and Water Commission. Both Springs are within the Rio Grande River Basin. Mean daily discharge records are published in Water Bulletins [37]. Data are available for Goodenough Springs for calendar years 1947 through 1966. Data for San Felipe Springs are available for calendar years 1962 through 1967.

Measurements of Big Springs near Van Buren, Missouri, (index No. 7-0675) are maintained by the U. S. Geological Survey. Data are published in Water Supply Papers, Part 7, and are available for water years (October 1 through September 30) 1944 through 1964 [36].

Rainfall data for the study were obtained for locations nearest the springflow stations. The sparsity of U. S. Weather Bureau stations and the uncertainty of areas contributing to recharge of springflow caused difficulty in obtaining adequate rainfall data. Only one gage was found in the vicinity of each springflow station. The U. S. Weather Bureau station at Del Rio (index No. 2360) was selected for both Goodenough Springs and San Felipe Springs. Del Rio is the only station in the vicinity of Goodenough Springs with daily records available [34], although Del Rio is considerable distance from Comstock. The U. S. Weather Bureau location at Van Buren, Missouri, (index No. 8569) is the only gage in the vicinity of Big Springs [35]. It is recognized that single rain gage representation of ground-water recharge is not adequate for accurate model development but does not affect the principles of the analyses. Also, hydrologists concerned with water resources planning are confronted with the same problem of inadequate rainfall data.

CHAPTER IV

SYSTEM INPUT--PRECIPITATION

Precipitation data as input to an aquifer system are highly important in systems analysis and aquifer simulation. The ability of a rain gage sample to adequately represent areal precipitation is a primary concern. As was mentioned in Chapter I, sparse rain gage networks that are generally available do not provide sufficient samples for averaging over a small area. Daily rainfall amounts published in Climatological Data [34, 35] are the best estimates of rainfall for county-wide areas. The chance occurrence of rainfall at a specific location may be representative of a very small area, particularly in arid and semiarid regions. However, there is also the chance of nonoccurrence of rainfall at that location when extensive areal rainfall occurs. Therefore, any given rain gage should be representative of a meteorologically homogeneous area over a long period of time even though individual days may be considerably in error.

In view of the inadequacy of areal coverage of precipitation data, time series analyses is necessary to determine the structure of the input series. Any characteristics discernible from the time series analyses will be helpful later in relating the input to aquifer performance. Precipitation data adjustment and time series analyses were made for the input data, and a discussion of each procedure will follow in separate sections. The ultimate relation to system identification and system output will be made in later chapters. Although some of the discussion in subsequent sections will also be appropriate for springflow analyses, the discussion will pertain only to precipitation.

1. Adjustment of Daily Precipitation Data. Daily rainfall data are published in Climatological Data [34, 35] for widely separated locations. Only one rainfall station is in the vicinity of the springflow stations selected for the study. The International Boundary and Water Commission has published monthly rainfall data for a large number of locations in the Rio Grande River Basin as a supplement to discharge data [37]. The daily records are not readily available. Daily rainfall amounts were published for the same monthly stations in Water Bulletins for the five years 1948-52. The 5-year period of record is not long enough for time series analysis, and a single long-term Weather Bureau station was used for daily data.

Rainfall data from a single location should be adjusted in some way to represent areal rainfall. Any adjustment should provide more accurate input information. The best estimate of areal rainfall would be obtained from averaging, or weighting by the Thiessen method, daily values from several gages in and around the area of concern. Since daily data are available for only a short period at several locations, an alternate method would be to adjust daily values on the basis of ratios of monthly averages of several locations over the area. Monthly rainfall for several stations, including the station with the daily record, can be averaged arithmetically or by the Thiessen method. A ratio of the monthly average rainfall for the area, $\overline{P}_m$, to monthly total rainfall for the station with the daily record, P_m, can be determined for each month of record. Then the ratio can be multiplied by the recorded daily rainfall, P_d, to give the adjusted daily rainfall ${}_aP_d$. The adjustment can be expressed as

$$ {}_aP_d = \frac{\overline{P}_m}{P_m} P_d \quad . \qquad (20) $$

Daily rainfall is adjusted for the appropriate month for which the monthly ratio was determined. Equation (20) adjusts the observed rainfall amount, but has the disadvantage that the days with recorded daily rainfall may not be the only days on which rainfall occurred over the area.

To determine the probable accuracy of the described adjustment method, a comparison was made with daily averages of the several gages for the 5-year period 1948-52. Four stations were used in the arithmetic averaging procedure. Since the actual area contributing to aquifer recharge is not known, an arithmetic average has less bias than the Thiessen weighting method with a highly fictitious area.

Results of the comparison of the rainfall adjustment and the rainfall averaging are summarized in Fig. 8. In general, it appears that daily rainfall at a single gage adjusted by averages of monthly totals gives larger rainfall amounts for large storms and less for smaller storms than that determined from averaging daily amounts from four gages. The most noticeable difference is that numerous points are on the abscissa of Fig. 8, that is, measurable rainfall at one or more gages other than the one for which the daily record is available and none at the daily-record gage.

Theoretically, if the rainfall station for which the daily record is available is located at the center of a meteorologically homogeneous area, the scatter of points in Fig. 8 would be equivalent above and below the line of equal values. The four gages used in the comparative study are in a meteorologically homogeneous area in that the probability of measurable rainfall at each gage is the same. However, there is some difference in annual rainfall. The average annual rainfall at the daily-record station at Del Rio is 17.83 inches as compared with 15.35 inches, 15.60 inches, and 15.68 inches at the other three locations. In this particular case, the daily-record gage at Del Rio has higher annual rainfall than the surrounding locations and the adjustment of daily rainfall may be biased.

A regression analysis of the data in Fig. 8 was made to determine if a least squares line is significantly different from the line of equal values. The least squares regression equation is

$$ y = 0.9428x + 0.0109 \qquad (21) $$

where x is the daily rainfall, average of four gages, and y is the daily rainfall, single gage adjusted by the ratio of monthly totals.

The linear correlation coefficient is 0.798, the means of x's and y's are 0.1982 and 0.1978, respectively, and the standard deviation is 0.2464. Tests of significance were made to determine if the y-intercept is significantly different from zero and if the slope is significantly different from unity. There are 338 data points, all of which obviously do not appear in Fig. 8. The tests revealed that the y-intercept is not significantly different from zero and the slope is not significantly different from unity.

Based on the data shown in Fig. 8 and the significance tests made, daily rainfall adjusted by ratios of average monthly rainfall is not biased in the particular case presented. Although averages of daily rainfall are the best estimates of input, the method described for adjusting daily rainfall at a single gage provides an adjustment that could not have been made by averaging daily rainfall for several gages.

2. Autocorrelation of Precipitation. The dependence in time of the daily rainfall time series was determined for the three rainfall stations used in the study. Autocorrelation coefficients [7] were computed by the relationship

$$r_k = \frac{\frac{1}{N-k}\sum_{i=1}^{N-k} X_i X_{i+k} - \frac{1}{(N-k)^2}\left(\sum_{i=1}^{N-k} X_i\right)\left(\sum_{i=1}^{N-k} X_{i+k}\right)}{\left[\frac{1}{N-k}\sum_{i=1}^{N-k} X_i^2 - \frac{1}{(N-k)^2}\left(\sum_{i=1}^{N-k} X_i\right)^2\right]^{1/2}\left[\frac{1}{N-k}\sum_{i=1}^{N-k} X_{i+k}^2 - \frac{1}{(N-k)^2}\left(\sum_{i=1}^{N-k} X_{i+k}\right)^2\right]^{1/2}} \quad (22)$$

for $k = 1,2,\ldots N$ where r_k is the k-th autocorrelation coefficient, N is the length of record, k is the units of lag, and X is the daily precipitation.

The first 30 autocorrelation coefficients were determined for each rainfall station and the correlograms are shown in Figs. 9, 10, and 11. Daily rainfall for the three springflow precipitation stations is practically independent. The first autocorrelation coefficient is 0.20, 0.25, and 0.10 for Goodenough Springs, San Felipe Springs, and Big Springs, respectively. The serial correlation analyses were made for adjusted precipitation at Goodenough Springs and San Felipe Springs. There were no rainfall stations in the near vicinity of Van Buren, Missouri, and therefore the precipitation for Big Springs was not adjusted.

3. Harmonics in Precipitation. Harmonic analyses were made to determine if the precipitation time series contained significant periodicities in their structure. Since there are many days each year with zero rainfall, the zero-valued days may tend to mask periodicities. Therefore, time intervals of 1, 3, 7, and 14 days were considered, over which the precipitation was averaged. The time intervals selected would provide a means of extrapolation of data to shorter time intervals if any significant characteristic was discerned.

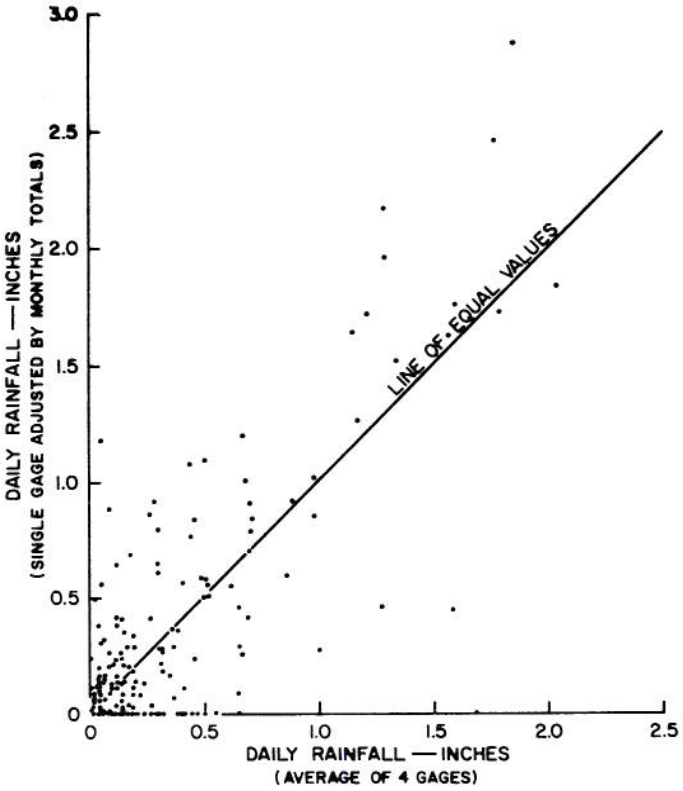

Fig. 8. Comparison of average daily rainfall for 4 gages and daily rainfall for a single gage adjusted by average of monthly totals for the 4 gages, Goodenough Springs area, Texas, 1948-52.

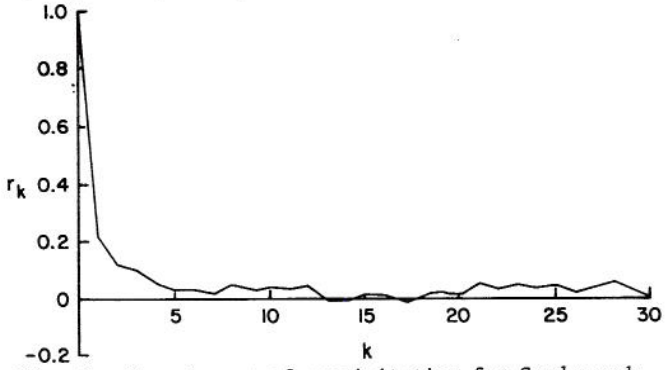

Fig. 9. Correlogram of precipitation for Goodenough Springs, Comstock, Texas, 1947-66.

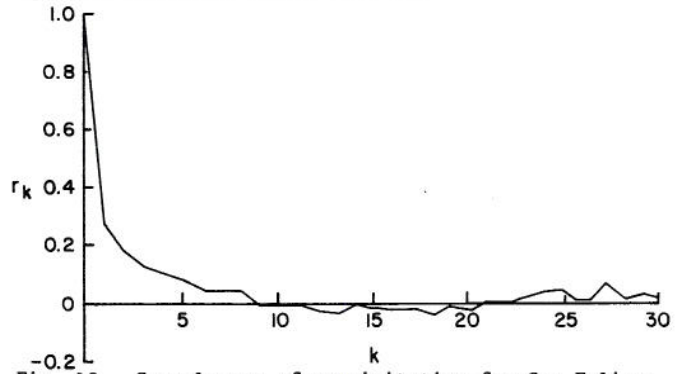

Fig. 10. Correlogram of precipitation for San Felipe Springs, Del Rio, Texas, 1961-67.

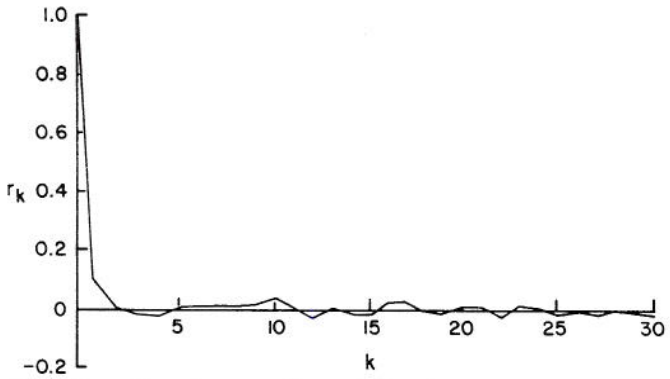

Fig. 11. Correlogram of precipitation for Big Springs, Van Buren, Missouri, 1945-64.

The basic data considered in the analyses were the means, the standard deviations, and the coefficients of variation. The three statistics were determined from the following equations, [32]:

$$m_\tau = \frac{1}{n} \sum_{p=1}^{n} x_{p,\tau} , \tag{23}$$

$$s_\tau = \left[\frac{1}{n} \sum_{p=1}^{n} \left(x_{p,\tau} - m_\tau \right)^2 \right]^{1/2} , \tag{24}$$

and

$$Cv_\tau = \frac{s_\tau}{m\tau} \tag{25}$$

where m_τ is the mean, s_τ is the standard deviation, Cv_τ is the coefficient of variation, and τ is the position of interval along the year. For 1 day, $\tau = 1,2,\ldots 365$; for 3 days, $\tau = 1,2,\ldots 121$; for 7 days, $\tau = 1,2,\ldots 52$; and for 14 days, $\tau = 1,2,\ldots 26$. Further, p are the years, $p = 1,2,\ldots,n$, and n is the total years of record, and $x_{p,\tau}$ is the precipitation for the p-th year, τ-th interval.

Fourier series was used to describe the periodic component of each statistic. For any statistic under consideration, ν_τ, the periodic component can be expressed as [32]

$$\nu_\tau = \nu_x + \sum_{j=1}^{m} \left(A_j \cos\frac{2\pi j}{\omega}\tau + B_j \sin\frac{2\pi j}{\omega}\tau \right) \tag{26}$$

where ν_τ is the symbol for m_τ, s_τ, or Cv_τ, ν_x is the mean of ω values of ν_τ, τ is the interval of a given year, ω is the number of periods per year, A_j, B_j are the Fourier coefficients, and j is the index of harmonics. Todorovic and Yevjevich [32] stated that rarely is any harmonic beyond the sixth significant in hydrology. However, in this study 12 harmonics were considered in order to discern the most information. Therefore, the upper limit of summation in Eq. (26) is $m = 12$.

The Fourier coefficients were estimated by the eqs.

$$A_j = \frac{2}{\omega} \sum_{\tau=1}^{\omega} (\nu_\tau - \nu_x) \cos \frac{2\pi j\tau}{\omega} , \tag{27}$$

and

$$B_j = \frac{2}{\omega} \sum_{\tau=1}^{\omega} (\nu_\tau - \nu_x) \sin \frac{2\pi j\tau}{\omega} \tag{28}$$

with the terms as previously defined.

The square of the amplitude of any harmonic is

$$C_j^2 = A_j^2 + B_j^2 . \tag{29}$$

The variance of ν_τ is

$$\text{var } \nu_\tau = \frac{1}{\omega} \sum_{\tau=1}^{\omega} (\nu_\tau - \nu_x)^2 . \tag{30}$$

The Fisher test [32] was used to determine the significance of each computed harmonic. The Fisher parameter for the harmonic of maximum amplitude is

$$g = \frac{C_j^2}{2 \text{ var } \nu_\tau} . \tag{31}$$

The Fisher parameter for the second and higher harmonics is

$$g = \frac{C_j^2}{2 \text{ var } \nu_\tau - \sum_{i=1}^{j-1} C_i^2} \tag{32}$$

Results of the harmonic analyses of precipitation are summarized in Table 2. The table shows the number of harmonics determined to be significant by the Fisher test for each time increment for each springflow rainfall station. There were no significant harmonics for either of the three statistics at either springflow station for 1-, 3-, or 7-day intervals. Significant harmonics were found to exist in the 14-day interval only. This indicates that averaging over the longer interval provided sufficient smoothing of the precipitation time series for periodicities to be discerned as significant. Figs. 12, 13, and 14 show the interval means, standard deviations, and coefficients of variation, respectively, and the associated fitted periodic components for the significant harmonics in precipitation for Goodenough Springs, Texas. The precipitation amounts in Figs. 12 and 13 have been converted to equivalent springflow in cubic feet per second.

Lack of significance of harmonics may be due to inadequacy of the Fisher test in these cases. No significant harmonics in the mean 14-day rainfall at San Felipe Springs may be due to the short time series. Only six years of record are available for San Felipe Springs, and this may not provide sufficient smoothing of the data even for 14 days. The Weather Bureau station at Del Rio, Texas, was used for the daily rainfall record of Goodenough Springs and San Felipe Springs. The adjustment of the daily record made use of different monthly rainfall stations for the two springflow stations. However, in view of the data shown in Fig. 8 and the associated regression analysis, both areas are meteorologically homogeneous. A 20-year record for San Felipe Springs should have given results for harmonic analysis similar to that for precipitation at Goodenough Springs.

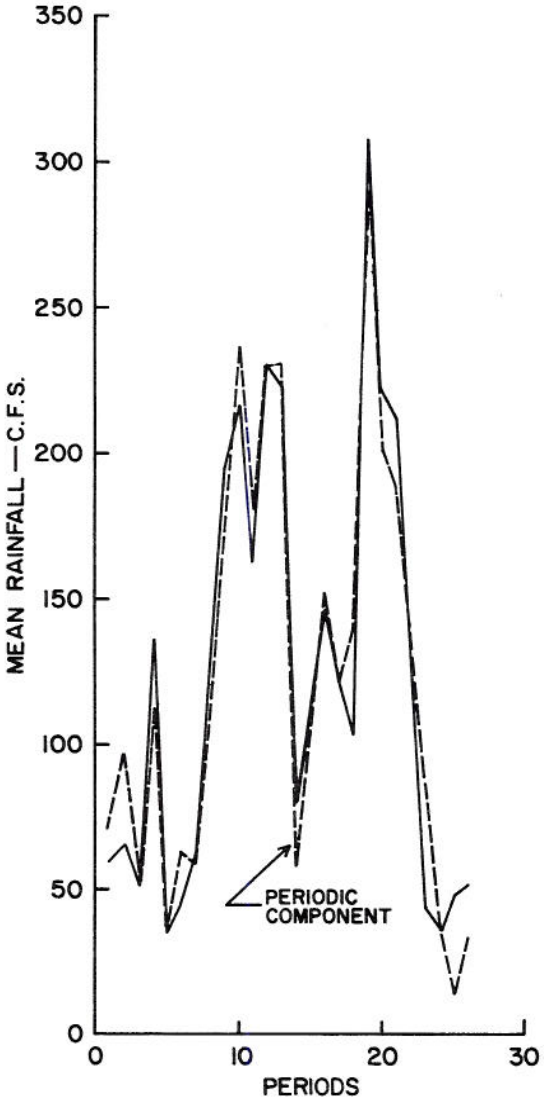

Fig. 12. Density of mean rainfall converted to equivalent springflow in cubic feet per second and fitted periodic component for 7 harmonics 26 periods 14 days long, Goodenough Springs, Texas.

The means of precipitation by time interval are of most interest in springflow simulation and are therefore given the most consideration in the harmonic analyses. The amount of variance of the means explained by each harmonic was determined for each time interval for all springflow rainfall stations. Results are shown comparatively for all time intervals in Figs. 15, 16, and 17 for Goodenough Springs, San Felipe Springs, and Big Springs rainfall stations, respectively. The time-interval lines are relatively uniformly spaced on Figs. 15 and 16, whereas the 14-day line is considerably above the 7-day line for Big Springs, Fig. 17. There is no apparent reason or logical explanation of the difference for Big Springs other than the rainfall at Big Springs was not adjusted due to lack of gages as explained earlier. This nonadjustment should not have caused the difference between the 7- and 14-day intervals since the means for both intervals came from the same daily record.

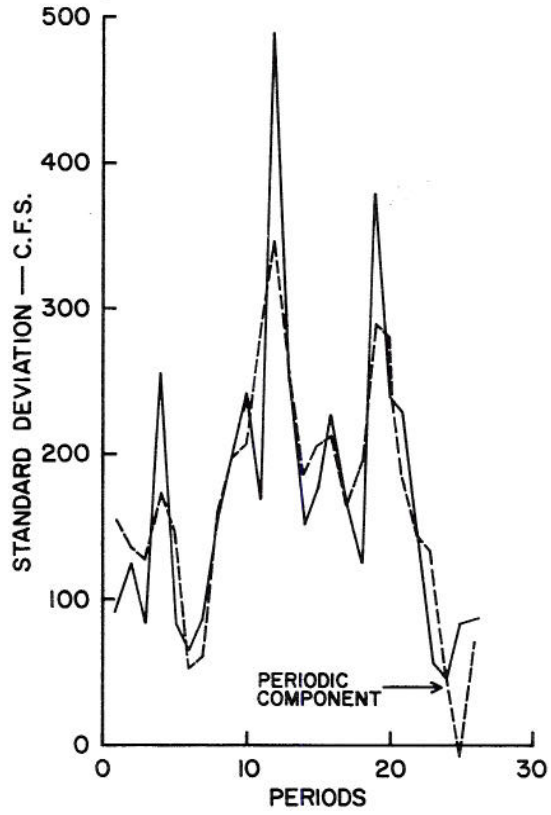

Fig. 13. Density of standard deviation of rainfall converted to equivalent springflow in cubic feet per second and fitted periodic component for 3 harmonics, 26 periods 14 days long, Goodenough Springs, Texas.

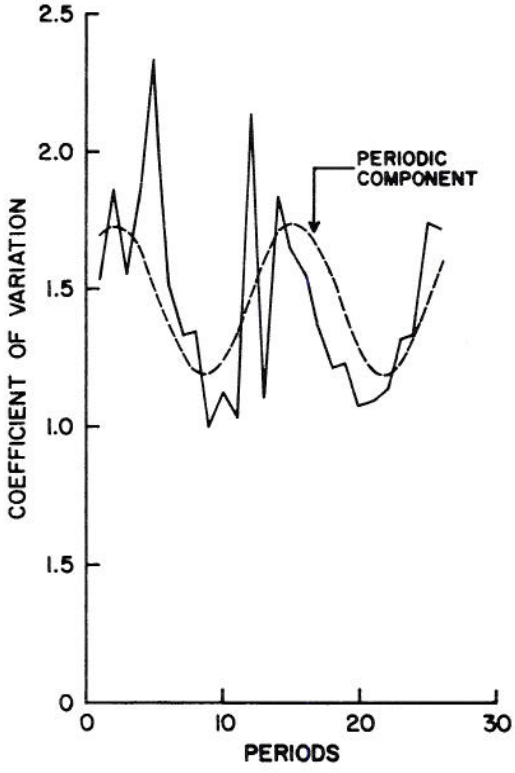

Fig. 14. Density of coefficient of variation of rainfall and fitted periodic component for 1 harmonic, 26 periods 14 days long, Goodenough Springs, Texas.

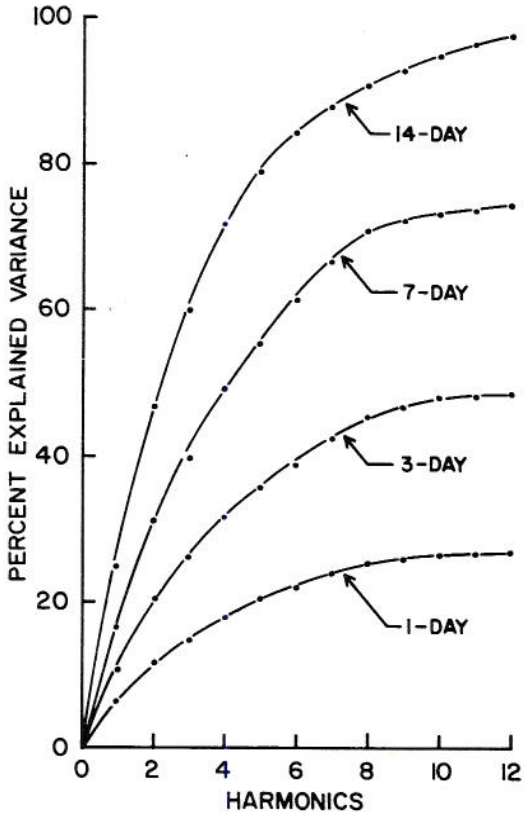

Fig. 15. Amount of variance of the mean rainfall time series explained by harmonics for Goodenough Spring, Texas.

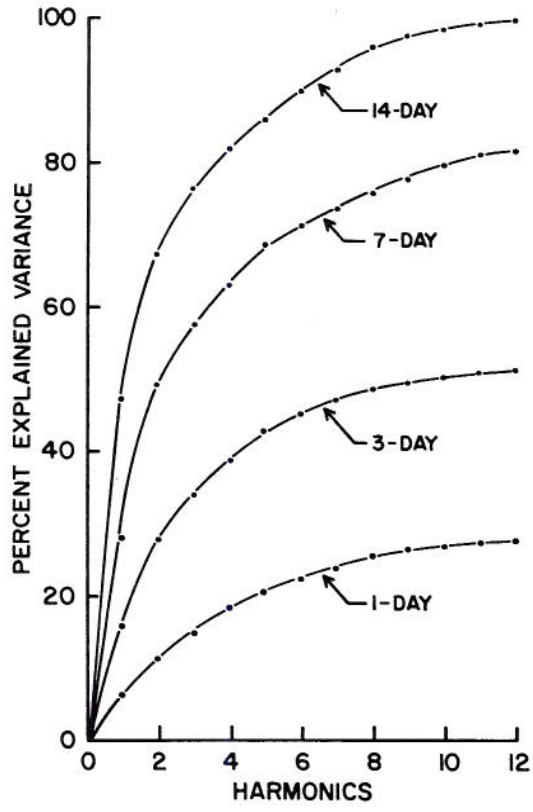

ig. 16. Amount of variance of the mean rainfall time eries explained by harmonics for San Felipe Springs, exas.

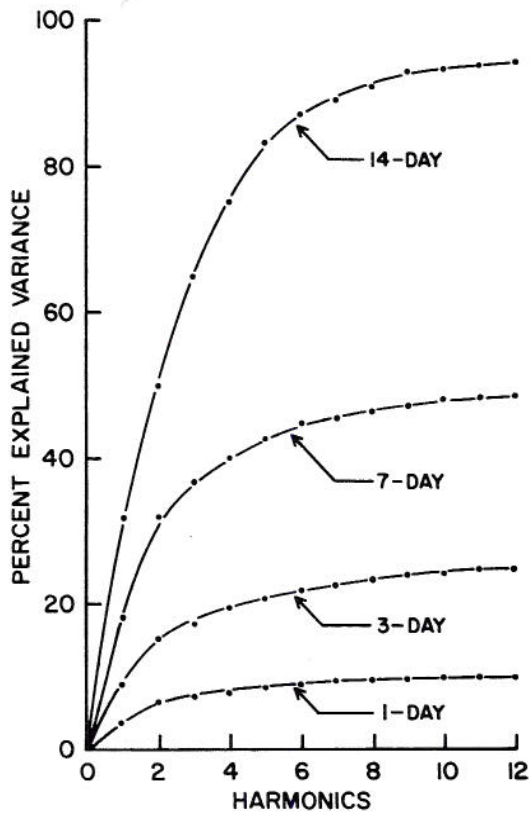

Fig. 17. Amount of variance of the mean rainfall time series explained by harmonics for Big Springs, Missouri.

Table 2. The number of significant harmonics in precipitation at three springflow stations by time interval for mean, standard deviation, and coefficient of variation.

Time Interval (days)	Parameter 1/	Number of Significant Harmonics for Goodenough Springs	San Felipe Springs	Big Springs
1	m	0	0	0
	s	0	0	0
	Cv	0	0	0
3	m	0	0	0
	s	0	0	0
	Cv	0	0	0
7	m	0	0	0
	s	0	0	0
	Cv	0	0	0
14	m	7	0	1
	s	3	2	2
	Cv	1	5	3

1/ The symbols for parameter are defined as follows: m is the mean, s is the standard deviation and Cv is the coefficient of variation.

Fig. 15 shows that for the 14-day time interval, the seven significant harmonics explain approximately 93 percent of the variance for precipitation at Goodenough Springs. However, Table 2 shows no significant harmonics for the San Felipe Springs location where nine harmonics explain 93 percent of the variance. Nine harmonics account for 93 percent of the variance at the Big Springs location and Table 2 shows one significant harmonic (32 percent explained variance). This shows that the tests by Fisher's statistic g may not be proper due to the periodicities in all three parameters, m, s, and Cv.

The Fisher test has been used in periodic analysis in other studies to determine significant harmonics. Time intervals of 1 month or 1 year may lend better to the Fisher test than the shorter intervals used in this study. For short time intervals, $t < 30$ days, somewhat relaxed criteria might well be in order. One consideration could be that significance be based on amount of variance explained by harmonics. A predetermined percent of variance explained by harmonics, with a lower percentage for the shorter time intervals, may provide a more useful criteria for significance. In reviewing the results of this study, the amount of variance explained by harmonics is very low for the 1-day interval. The three rainfall stations used in this study does not provide sufficient representation for drawing conclusions, but further consideration in other studies would be profitable.

4. Random Component of Precipitation. It was shown in section 2 that precipitation is nearly independent in time by reflecting the small lag autocorrelation of the order of $r_1 = 0.20$. However, this does not preclude a nonrandom internal structure of some periodicity and other time dependence. Such a random or nonrandom occurrence may be important later in the convolution of rainfall and springflow to determine the impulse response function. Therefore, the interval structure of the precipitation time series was analyzed.

From the harmonic analyses, the periodic means m_τ, and standard deviations, s_τ, are known for all τ. The coefficient of variation was given by Eq. (25) as

$$Cv_\tau = s_\tau / m_\tau \quad .$$

Eq. (25) can be rewritten as

$$s_\tau = Cv_\tau \; m_\tau \quad . \tag{33}$$

The periodicity can be removed by standardizing the time series as

$$\xi_{p,\tau} = \frac{X_{p,\tau} - m_\tau}{s_\tau} \quad , \tag{34}$$

which can be rewritten as

$$X_{p,\tau} = m_\tau + s_\tau \; \xi_{p,\tau} \quad . \tag{35}$$

Substituting Eq. (33) for the standard deviation in Eq. (35) gives

$$X_{p,\tau} = m_\tau + m_\tau \; Cv_\tau \; \xi_{p,\tau} \quad . \tag{36}$$

The right term of Eq. (36) can be factored, assuming that $Cv_\tau = Cv$ is a constant, then

$$X_{p,\tau} = m_\tau \left(1 + Cv_\tau \; \xi_{p,\tau}\right) \quad , \tag{37}$$

where $E(\xi) = 0$ and var $\xi = 1$. Let

$$\eta_{p,\tau} = 1 + Cv_\tau \; \xi_{p,\tau} \tag{38}$$

where the $E(\eta) = 1$ and var $\eta = Cv^2$. Substituting $\eta_{p,\tau}$ for its equivalent in Eq. (37) gives

$$X_{p,\tau} = m_\tau \; \eta_{p,\tau} \quad . \tag{39}$$

Taking logarithms of Eq. (39) gives

$$\ln X_{p,\tau} = \ln m_\tau + \ln \eta_{p,\tau} \tag{40}$$

for which $\mu_\tau = \ln m_\tau$, or $m_\tau = e^{\mu_\tau}$. Then Eq. (40) can be written as

$$X_{p,\tau} = e^{\mu_\tau} \; \eta_{p,\tau} \quad . \tag{41}$$

From Eq. (41) a new series of η was computed for the daily precipitation time series at each station.

The first serial correlation coefficient of the η-series was determined by Eq. (22). Results of the correlation showed that $r_1(\eta)$ was less than 0.10 for each of the springflow precipitation stations. Such low values indicate the η-series is nearly independent for practical purposes. The amount of variance that could be explained by a first order Markov model would be less than 1 percent. Therefore, Eq. (41) can be used as an approximation to express the precipitation time series.

CHAPTER V

RAINFALL EFFECTIVE FOR RECHARGE

All precipitation that occurs on an area is not effective for recharge of groundwater. Numerous elements affect the depletion of measured rainfall to that which ultimately reaches a karst aquifer. The abstraction from total rainfall among the various elements may be considered as loss with respect to recharge, but in reality represents transposition of water in the hydrologic cycle.

Since ground-water recharge represents a portion of the precipitation that infiltrates the earth's surface, rainfall intercepted by vegetation, surface detention (with later evaporation), and surface runoff are the first abstractions from recharge. Interception losses are recognized as being a small portion of the total rainfall. Evaporation from surface detention may also be quite small relative to the total input. Many karst areas do not experience surface runoff. In the strict definition of karst as given by Thornbury [30], i.e.,

> "a term applied to limestone or dolomite areas that possess a topography peculiar to and dependent upon underground solution and the diversion of surface waters to underground routes,"

surface runoff would not be expected to exist. However, depending upon the soil characteristics and rainfall intensity, surface runoff will occur on what is commonly termed karstic terrain. Runoff is known to result from intense storms in the Edwards Plateau of Texas and the limestone areas of Missouri. Therefore, runoff does represent an abstraction of rainfall from recharge.

Infiltrated water, that is the rainfall that infiltrates into the earth's surface, is further acted upon to abstract water from recharge. Although soils overlying limestone areas may be thin, there will be varying amounts of water stored for plant growth, transpiration, and evaporation from surface and underground. The amount of soil water abstraction is dependent upon the temporal distribution of storm events and season of occurrence. Several storms that produce small amounts of rain may not add recharge to the karst aquifer if several days elapse between storm events. Evaporation and transpiration may deplete the stored soil water and thereby provide renewed storage capacity during subsequent storms. If the soil mantle is sufficiently deep, considerable rainfall may be required to provide any ground-water recharge.

The separate estimation of the various abstraction components (interception, evaporation, transpiration, soil water accretion and depletion, and surface runoff) constitutes a problem of considerable undertaking in itself. Also, each component is a source of error and randomness that may be accumulative, and thereby cause considerable error in estimation of recharge. For the problem being studied, a lump sum estimate of the recharge will suffice and be less likely to contain large errors.

One method of estimating recharge from rainfall is to consider abstractions linear throughout the range of rainfall experienced. A simple means of treating linear losses is to relate average daily springflow discharge to average daily rainfall. Such a relation can be expressed as

$$R = \frac{\overline{Q}}{\overline{P}} P \qquad (42)$$

where R is the recharge rate in CFS, $\overline{Q}$ is the average daily springflow discharge in CFS, $\overline{P}$ is the average daily rainfall in inches, and P is the observed daily rainfall in inches. Eq. (42) considers losses to be linear for all values of P , and R includes any surface runoff that might occur. This may be far from the real relations.

In areas where surface runoff does not occur, as previously indicated, losses may be treated nonlinearly by applying an exponential curve as depicted in Fig. 18. The region under the curve in Fig. 18 would be representative of evaporation, transpiration, and changes in soil moisture. The amount of losses would be dependent upon the amount of rainfall available for possible loss. The exponential curve of Fig. 18 does not represent conditions where surface runoff occurs. Such representation could be made if the curve indicated increased losses with increased rainfall above some initial point.

A more meaningful depiction of nonlinear losses with surface runoff present would be shown in Fig. 19, where recharge is expressed as a function of precipitation. A relationship such as that shown in Fig. 19 provides a ready comparison of recharge and rainfall. The region to the left of the maximum recharge would be indicative of losses by evaporation, transpiration, and interception; whereas, the region to the right of maximum recharge also includes surface runoff.

Data available for this study are not sufficient for accurately describing the shape of the curve in Fig. 19. The Agricultural Research Service has made hydrologic measurements in the Edwards Plateau of Texas near Sonora [17]. The amount of rainfall necessary to produce surface runoff is not constant for all storms and is dependent upon several factors including antecedent rainfall, rainfall intensity, soil-cover complex, season of the year, and depth of soil, among others. However, the data indicate that approximately 3 inches of rainfall is required to initiate runoff. The data obtained by the ARS in the Edwards Plateau are not sufficient to define the rainfall-runoff relationship, but as much as 6 inches of rainfall produced only approximately 1 inch of surface runoff. The ARS data also indicate that the Edwards Plateau soils maintain a good transmission rate during prolonged rainfall periods. Thus, ground-water recharge would be expected to continue at a relatively high rate even for large rainfall amounts.

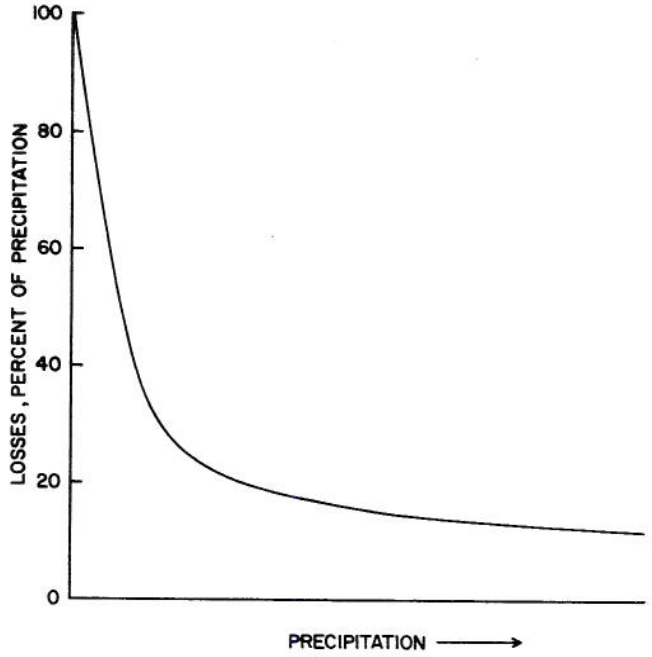

Fig. 18. Schematic representation of losses of rainfall from ground-water recharge exponentially related to rainfall.

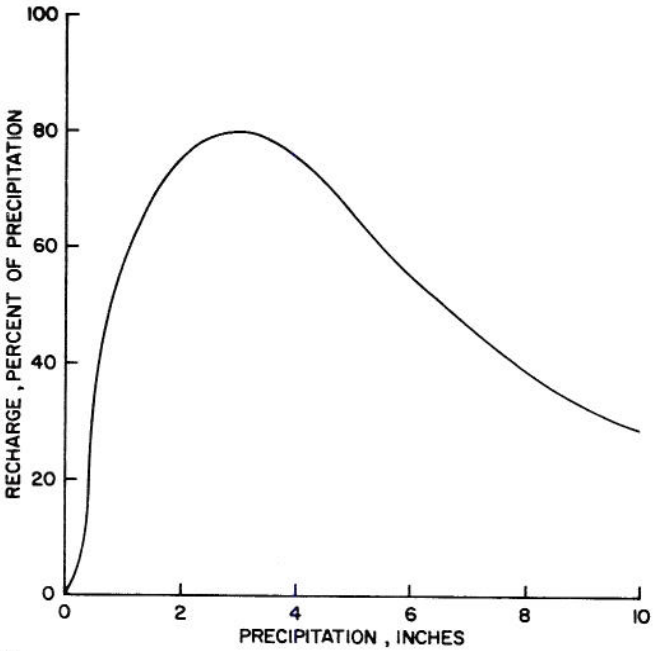

Fig. 19. Ground-water recharge as a function of rainfall when losses include surface runoff.

Due to high evaporation rates in the semiarid Edwards Plateau, rainfall loss due to evaporation from the soil surface can be quite high. Probably a maximum recharge before the point of runoff initiation would be in the order of 80 percent of the rainfall. Small rainfall amounts may largely be lost to evaporation. The lower limit of rainfall effective in recharge is not known but is assumed to be approximately 0.25 inch.

With the meager quantitative information available and assumptions previously stated, an estimated rainfall-recharge curve was hypothesized as shown by

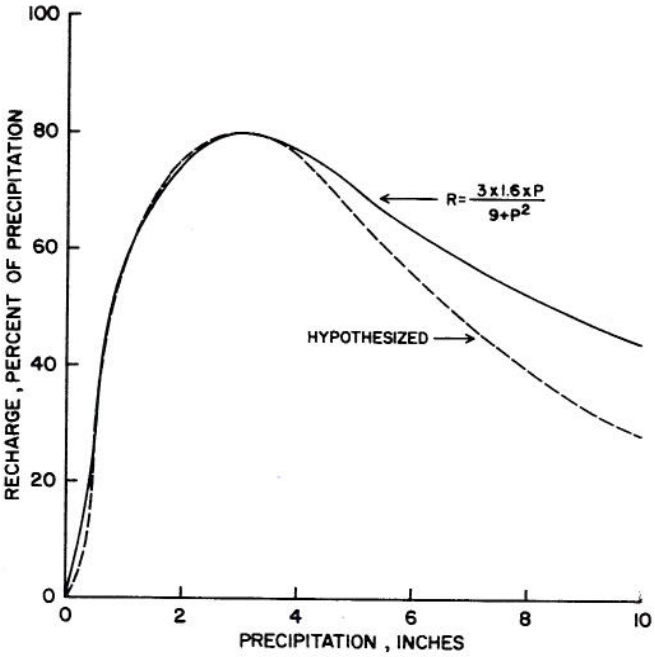

Fig. 20. Serpentine curve fitted to hypothesized recharge as a function of rainfall.

the sketch in Fig. 19. A two-parameter gamma function was thought to be representative of the conditions as outlined. The gamma distribution is expressed as

$$y = \frac{(x/\beta)^{\alpha-1} e^{-x/\beta}}{\beta\Gamma(\alpha)} , \qquad (43)$$

where α and β are the shape and scale parameters, respectively. A number of values were assumed for the parameters of the gamma function and the resulting curves were superimposed on the sketch of Fig. 19. The gamma function did not fit the hypothesized curve well at all. When the α parameter described the shape well, no value of the β parameter would permit large enough values of recharge. Likewise, when the β parameter described the maximum expected recharge, no value of the α parameter permitted the function to duplicate the recession portion of the curve or the expected abscissa value for the peak. The main difficulty was that the two-parameter gamma curve returned to near zero too quickly after the peak.

The positive portion of a serpentine curve was considered to describe the hypothesized rainfall-recharge curve of Fig. 19. The general form of the serpentine curve is

$$y = \frac{abx}{a^2 + x^2} \qquad (44)$$

where a is the shape parameter and b is the scale parameter. Substituting recharge (R) for y, where (R) is expressed as percent of precipitation, and precipitation (P) for x, Eq. (44) can be rewritten as

$$R = \frac{abP}{a^2 + P^2} , \quad \text{for } P \geq 0 . \qquad (45)$$

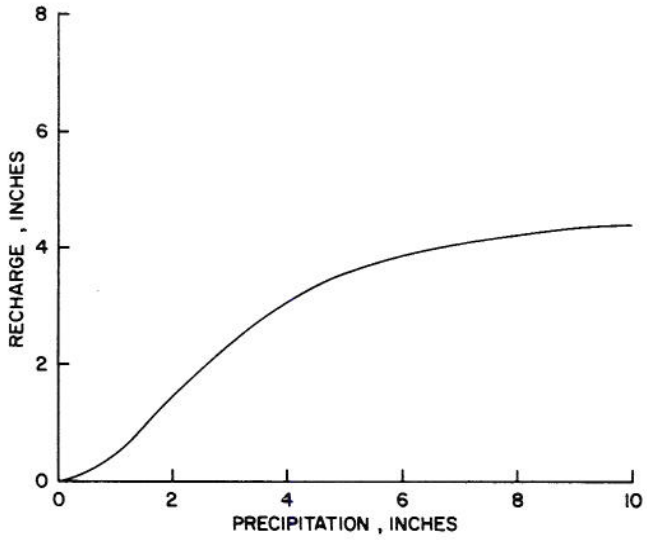

Fig. 21. Volume of ground-water recharge as a function of daily rainfall.

Precipitation cannot be negative and R is always positive, but the positive restriction of Eq. (45) is merely for definition purposes. Eq. (45) was fitted to selected points on the curve of Fig. 19 and values of a and b were determined to be 3.0 and 1.6, respectively. Substituting these values in Eq. (45) gives

$$R = \frac{4.8P}{9 + P^2} \qquad \text{for} \quad P \geq 0 \ . \qquad (46)$$

Eq. (46) was superimposed on Fig. 19 and the result is shown in Fig. 20. The fitted equation duplicates the rising side and peak of the hypothesized curve, but tends to diverge above the curve on the recession with approximately 16 percent difference for a rainfall of 10 inches. However, daily rainfall of 8 inches at the study locations is approximately a 100-year event according to Weather Bureau publications. An error of 16 percent for such an infrequent event is rather small.

Recharge is given as a percentage of rainfall in Eq. (46) and Fig. 20, but a direct comparison of rainfall and recharge in inches would be more meaningful. Multiplying both sides of Eq. (46) by P gives the total recharge as a function of rainfall and the equation can be written as

$$R = \frac{4.8P^2}{9 + P^2} \qquad \text{for} \quad P \geq 0 \ . \qquad (47)$$

Eq. (47) is shown in Fig. 21.

Although sufficient data are not available to accurately describe the rainfall-recharge relationship, the ARS data indicate that the curve in Fig. 20 is a reasonable estimate of the true relation. The range of ARS data is rather short and extrapolation of the Eq. (47) above approximately 6 inches may be erroneous.

Another method was considered for determining the rainfall-recharge relationship. Increased ground-water storage resulting from recharge was estimated for several recharge periods in the springflow record. The increased storage was estimated as the difference between the measured springflow and an extrapolated recession after the springflow rate increased. That is, the recession equation (Eq. 3) was integrated between time limits 0 and ∞ with q_o as: (a) the last discharge rate before increase, and (b) peak discharge after increase. The difference between values determined in (a) and (b) was the estimated recharge. The recharge was related to measured point rainfall. A high degree of variability resulted in the relation due to the apparently poor representation of actual areal rainfall by measured point rainfall. This method of determining the rainfall-recharge relation was rejected in favor of the previously described serpentine curve based on physical relations.

CHAPTER VI

SYSTEM OUTPUT - SPRINGFLOW

One of the objectives of this study, as showed in Chapter I, is to develop an understanding of karst ground-water flow phenomena. Since ground-water movement in the aquifer system cannot be studied in situ or modeled for laboratory study, the only recourse is to study the phenomena of ground-water flow at a springflow measuring station. Analyses of springflow data provide information about the characteristics and internal structure of the time series that leads to a better understanding of the flow phenomena. Such characteristics as flow recession, periodicity, time dependence, and stochastic component are all important and will be treated separately to aid in understanding the processes of ground-water flow and response to recharge.

1. Flow Recession. Several methods of ground-water recession analyses were cited in Chapter II [3, 17, 40]. The method used by Yevjevich [40] has the advantage of studying springflow relative to time; whereas, the methods of Barnes [3] and Knisel [17] obscure the time element as such. To reiterate Yevjevich's method, a semilogarithmic plotting of sustained recession discharge (log) versus time (arithmetic) will indicate the relationship of discharge and time. If the change in logarithms of discharge with time is linear, a simple relationship can be developed. That is, if the relation is linear, then

$$\ln q_t = \ln q_o - ct \qquad (48)$$

where q_t is the discharge rate at some time t, q_o is the discharge rate at an initial time o, t is the time, and c is the constant parameter. The negative sign preceeding the coefficient c indicates a decrease in discharge with an increase in time. Eq. (48) can be rewritten as

$$-ct = \ln q_t - \ln q_o \ , \qquad (49)$$

or

$$e^{ct} = \frac{q_o}{q_t} \ . \qquad (50)$$

Since q_t is of normal interest, Eq. (50) can be rearranged to

$$q_t = q_o / e^{ct} \ , \qquad (51)$$

or to

$$q_t = q_o \, e^{-ct} \ , \qquad (52)$$

which is recognized as the simple exponential flow recession equation.

Discharge data for the three springflow stations were plotted on semilog paper to discern flow characteristics. The plottings were made such that discharge indicated a continued decrease for many days although the recession was interrupted by recharge and increased discharge. The largest observed discharge was plotted at the zero time. When a recharge period was encountered, the peak discharge was plotted at the appropriate rate on the recession irrespective of time. An example will provide a better explanation of the plotting procedure. The typical data in Table 3 are used for the example. The data in the table are representative of published discharge data. Discharge decreases for January 1-16, increases on January 17, and decreases steadily to January 22. Consecutive time plottings ($t = o$ to $t = 16$) are made for days 1 through 16. The peak discharge on January 17 corresponds to the discharge of January 2, thus the discharge for January 17-22 are plotted at times 1 to 6. Fig. 22 shows the date for each plotted point.

Table 3. Typical discharge data to exemplify plotting procedure.

Date January	Discharge (CFS)
1	90
2	88
3	86
4	84
5	82
6	80
7	78
8	76
9	74
10	72
11	70
12	68
13	66
14	64
15	62
16	60
17	88
18	78
19	70
20	64
21	62
22	60

Fig. 23 is a semilog plotting of discharge versus time for Goodenough Springs near Comstock, Texas. The figure shows an erratic recession that changes slope numerous times over the time period shown. The change of slope along the recession is probably indicative of variable porosity throughout the thickness of saturated mantle. A steep portion of the recession would be indicative of the effect of low porosity layers, whereby the hydraulic gradient would decrease rapidly and cause a large change in discharge. On the other hand, high porosity layers would have little change of hydraulic gradient for a given discharge and the recession slope would be flatter relative to low

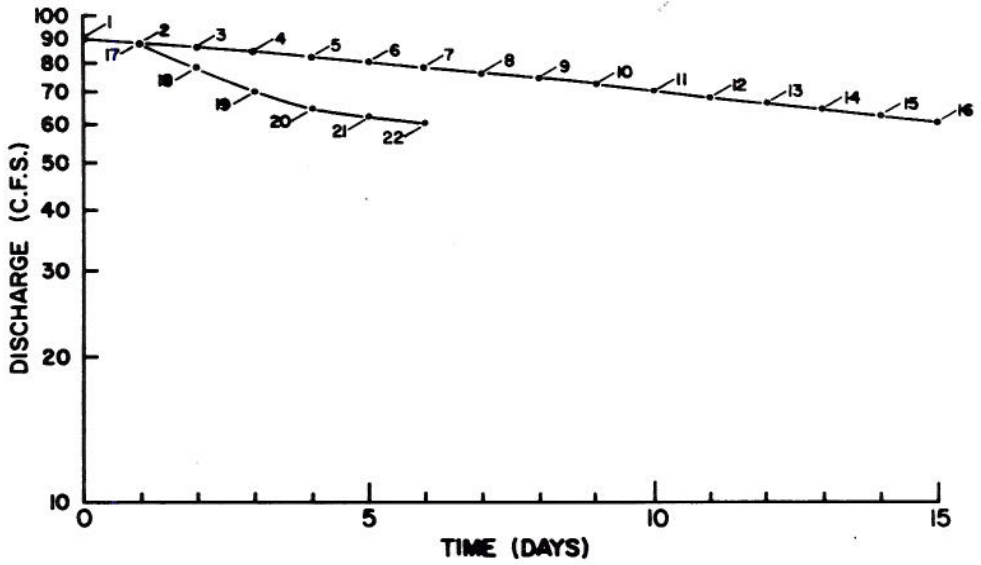

Fig. 22. Sample plotting of typical discharge data.

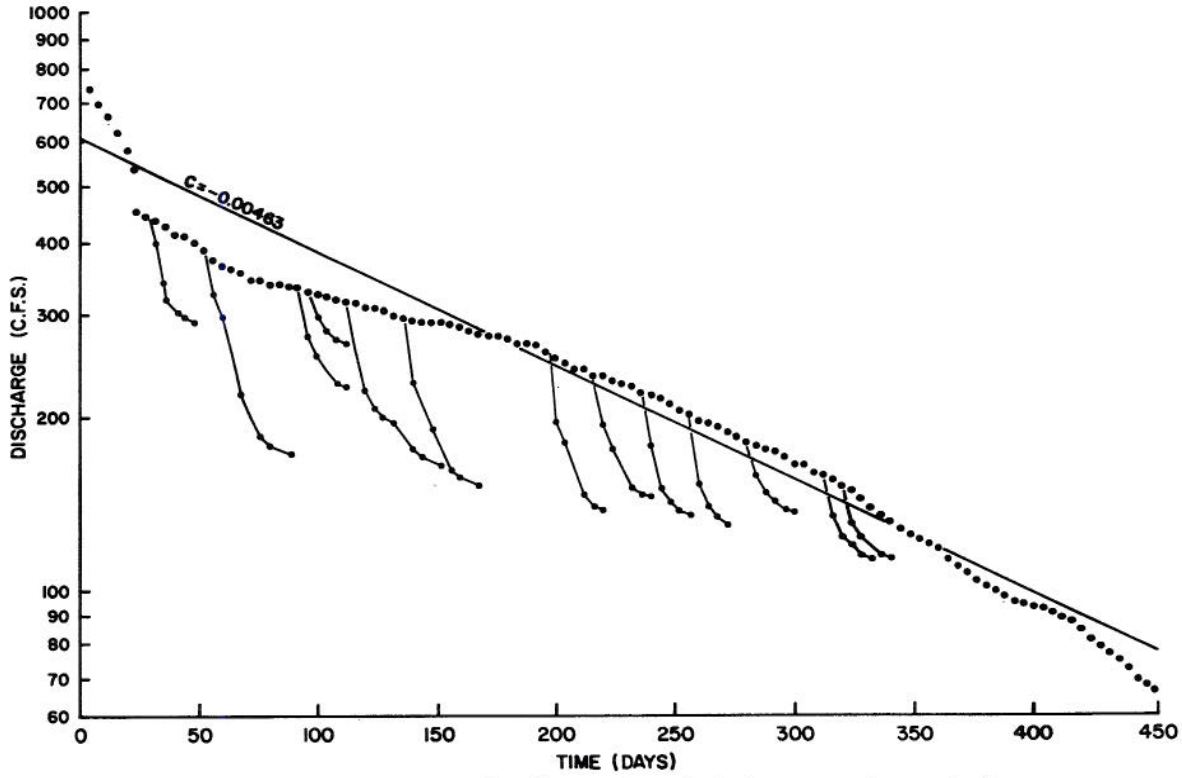

Fig. 23. Time discharge relation for Goodenough Springs near Comstock, Texas.

porosity layers. However, each so-called layer in the mantle is affected by the underlying layers and the discharge represents an integration of flow through the system. The observed recession may obscure stratification and the preceding discussion cannot be considered factual but only conjectural.

The recession shown in Fig. 23 seems to have the highest portion (t = 0-24) definitely with a steeper slope than the remainder of the recession. However, if a single recession constant, c in Eq. (52), is rejected on the basis of the steep portion, then probably a single recession constant should also be rejected for the remaining portion of the plotting. An "average" line was drawn by eye to approximate the overall recession with a slope of -0.00463. Such an average is very little in error as compared with two lines--one for the steep early portion and one for the average of the remaining recession. It can be seen that any springflow simulation method, using Eq. (52) for recession without recharge could produce erroneous results depending upon the actual recession.

The "stringers" of lines below the sustained recession in Fig. 23 is indicative of another type of flow phenomenon. The steep recessions immediately following periods of recharge indicate that infiltrated water, or recharge, moves from the surface to the aquifer very rapidly. Apparently channels in the karstified limestone carry large volumes of water at high velocity. The recharge mass may also quickly raise the water table, increasing the pressure head,

and thereby causing a quick increase in springflow. The stringers of recession in Fig. 23 changes slope rather quickly to approximate that of normal recession. This would indicate that some effects of recharge have rather short duration. Fig. 24 is an expanded plotting of a hydrograph showing dates and amounts of rainfall. The quick response of the aquifer and short duration of recharge effect is apparent in the figure. Some preliminary estimates indicate the size of contributing area is well in excess of 100 square miles. For a drainage area of this size, the springflow hydrograph of Fig. 24 is not vastly different from an expected surface runoff hydrograph from a similar size area. Obviously, the prolonged rise normally hypothesized for ground-water flow is not appropriate for karst systems.

Fig. 25 is the semi-log plot of discharge versus time for San Felipe Springs at Del Rio, Texas. The sustained recession for San Felipe Springs is much more uniform than that for Goodenough Springs. A single line is indicated for the entire range of data. The slope of the line, -0.0121, is much steeper than that for Goodenough Springs, -0.00463. As in the case of Goodenough Springs, rapid percolation of recharge to the water table is also exhibited for San Felipe Springs. The duration of increased discharge due to recharge is shorter at San Felipe Springs than at

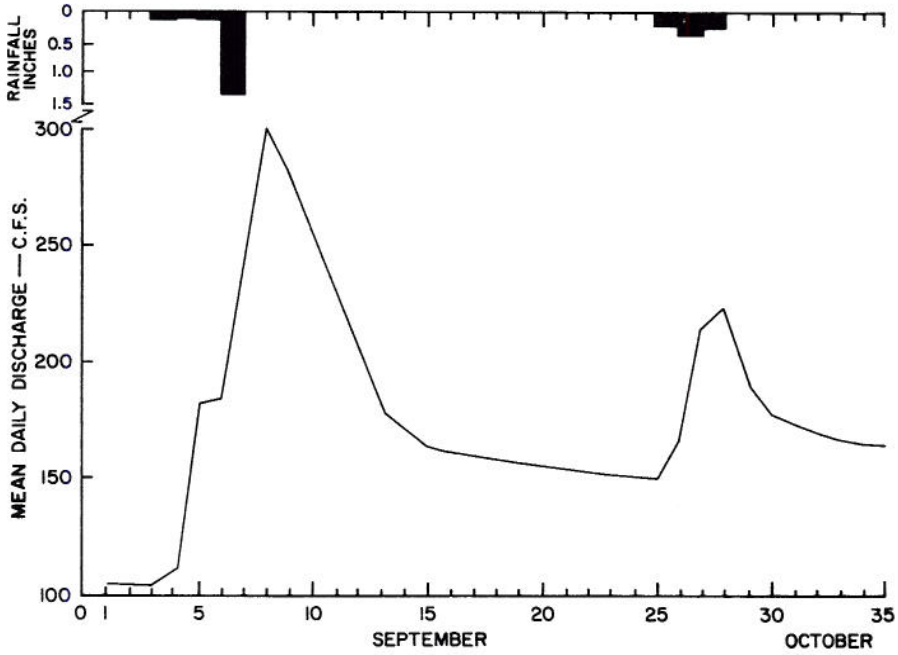

Fig. 24. Observed rainfall in inches and springflow in cubic feet per second for September 1 to October 5, 1952, Goodenough Springs, Comstock, Texas.

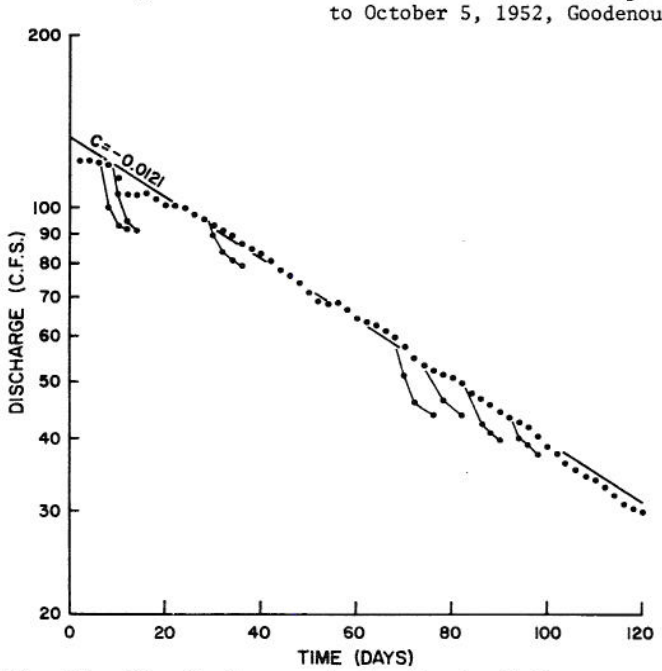

Fig. 25. Time-discharge relation for San Felipe Springs, Del Rio, Texas.

Goodenough Springs. The estimated area contributing to springflow at San Felipe Springs is less than 100 square miles.

A semi-log plot of discharge versus time for Big Springs near Van Buren, Missouri, is shown in Fig. 26. The curved recession line clearly indicates basically a two-slope relation of the recession curve. After 36 days, the recession is approximately a straight line. If the hypothesis of variable porosity, given earlier for Goodenough Springs, is true, there are apparently two types of flow regime and porosity in the Big Springs contributing area. The curvature is uniform and not highly erratic as was the recession for Goodenough Springs. The plotting for Big Springs also exhibits the rapid response to recharge as did Goodenough Springs and San Felipe Springs. The duration of recharge effect is relatively short for an estimated recharge area of approximately 200 square miles.

A study of the recession curves of the three springflow stations reveals that rapid percolation of recharge is characteristic of the two limestone formations studied. Two types of ground-water response are evident: (a) rapid response resulting from high percolation rates through the channels and (b) delayed response resulting from slow water movement through

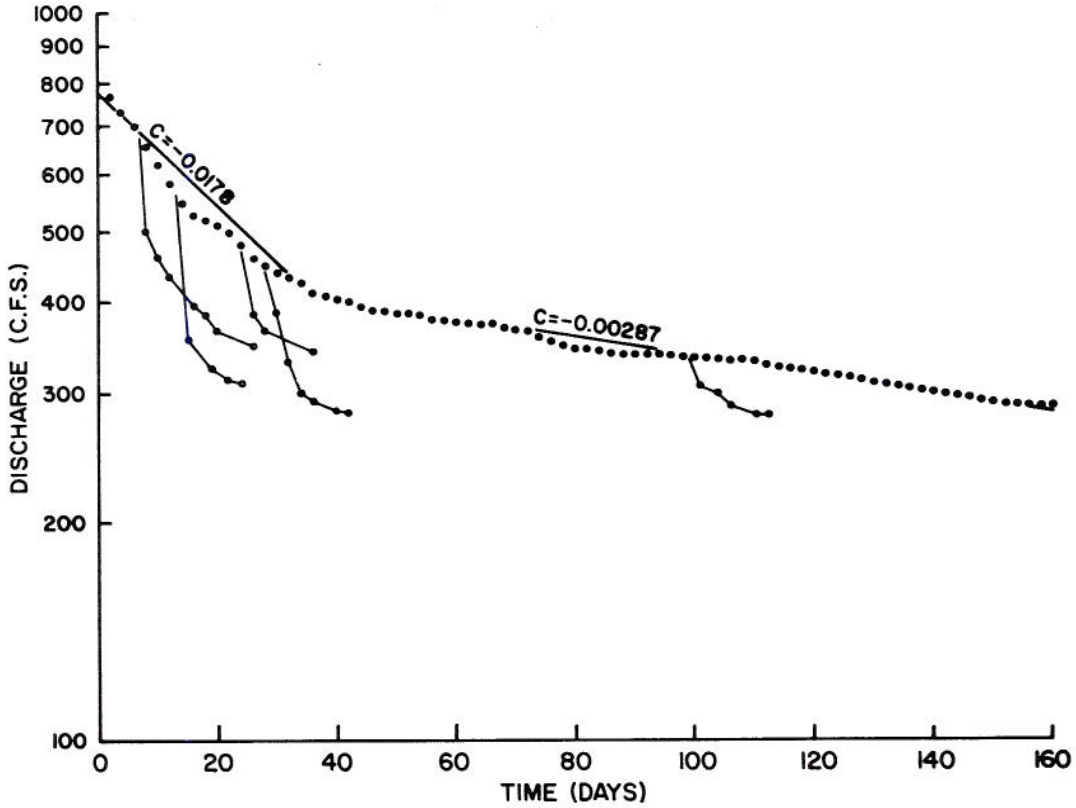

Fig. 26. Time-discharge relation for Big Springs near Van Buren, Missouri.

the limestone mass. It is hypothesized that all karstified topography will, in general, have similar characteristics. The relative degree of such responses depends upon the degree of karstification.

2. Autocorrelation of Springflow. The dependence in time of the daily springflow time series was determined for the three springflow stations used in the study. Autocorrelation coefficients were computed by Eq. (22). The first 30 autocorrelation coefficients were determined for each springflow station and the correlograms are shown in Figs. 27, 28, and 29. A high degree of dependence in time is indicated in the correlograms for the daily time series for each springflow station studied.

In view of the shape of the correlograms in Figs. 27, 28, and 29, the applicability of the first order Markov model was tested for each of the three springflow stations. The correlogram for the Markov I model follows the shape [24]

$$\rho_k = \rho_1^k \quad , \tag{53}$$

where ρ_1 is the first population autocorrelation coefficient and k is the lag. The population autocorrelation coefficient, ρ_1, can be estimated from the sample autocorrelation coefficient, r_1, and Eq. (53) becomes

$$r_k = r_1^k \quad . \tag{54}$$

The correlogram for Goodenough Springs and San Felipe fits the Markov I line well for a lag of approximately 5 to 10 days after which the lines diverge considerable above the Markovian line.

Fig. 29 shows that the correlogram for Big Springs falls below the Markov I line up to $k = 10$. For $k > 10$, the Markovian line is below the correlogram.

An important characteristic of the aquifer systems is indicated when the correlograms of rainfall time series and springflow time series are considered. As pointed out in Chapter IV, section 2, the rainfall series is relatively independent in time; i.e., rainfall occurrence represents isolated input to the ground-water systems. The ground-water system integrates the isolated input with time to produce a highly dependent time series. The discussion in the previous section, Recession Characteristics, pointed out some rapid response of springflow to recharge (Fig. 24). The high degree of dependence of springflow series in time indicates that not only is the system an integrator, the system has both a short "memory" as expressed in systems jargon and a long "memory". Since part of the memory is short and the input is isolated, the major portion is long memory and the springflow series represents sustained recession flow-thus the high degree of dependence and which can not be very well approximated with a first-order Markov Model.

The finite memory characteristic of springflow is important in systems analysis and simulation procedures to be presented later in the paper. The length of memory determines the limits of integration summation in systems analysis.

3. Cross Correlation of Rainfall and Springflow. The interdependence of rainfall and springflow time series was determined for the springflow and associated rain-

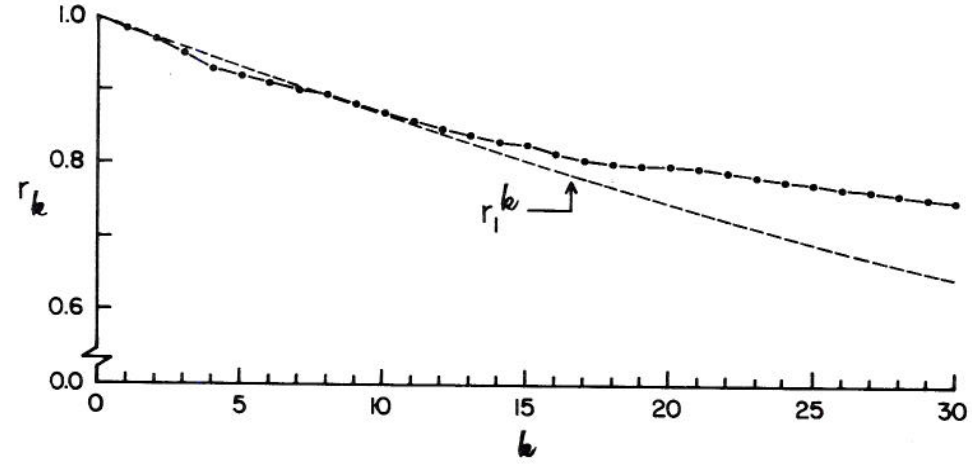

Fig. 27. Correlogram of autocorrelation coefficients of daily springflow for Goodenough Springs near Comstock, Texas.

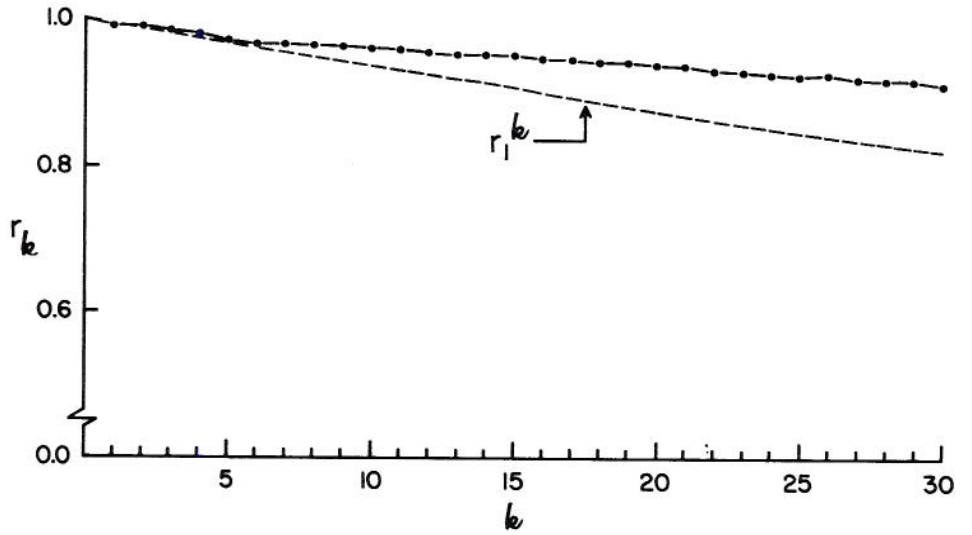

Fig. 28. Correlogram of autocorrelation coefficients of daily springflow for San Felipe Springs, Del Rio, Texas.

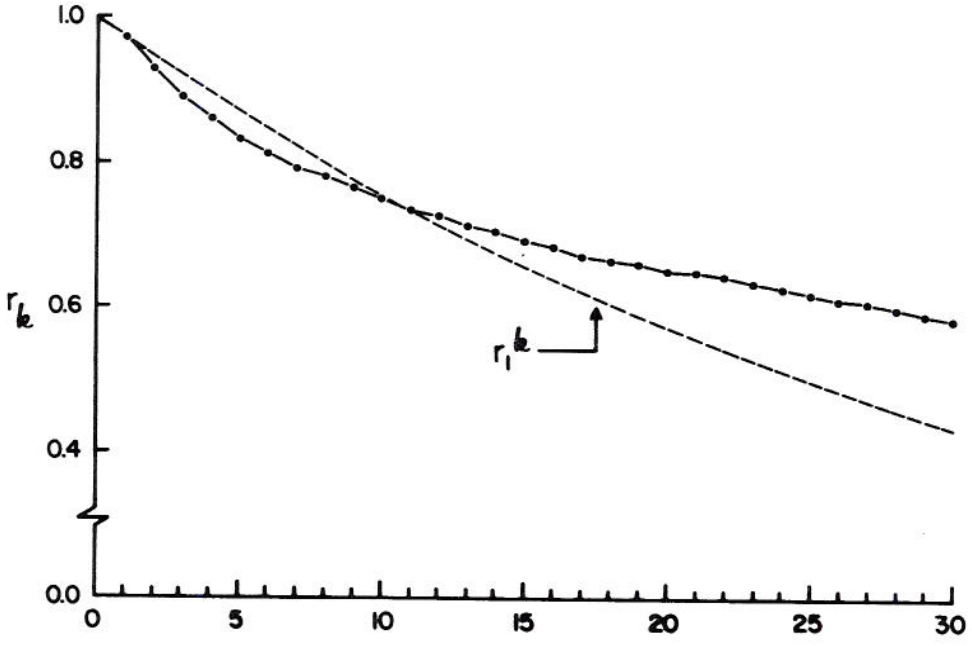

Fig. 29. Correlogram of autocorrelation coefficients of daily springflow for Big Springs near Van Buren, Missouri.

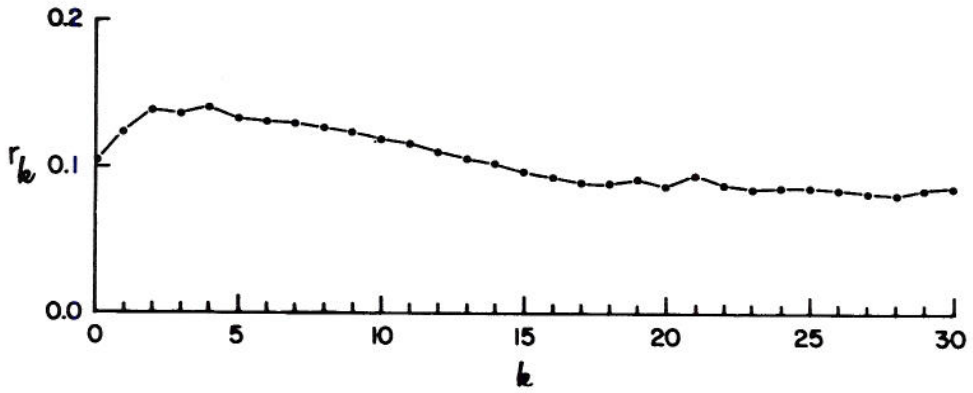

Fig. 30. Correlogram of cross correlation coefficients of rainfall and springflow at Goodenough Springs near Comstock, Texas.

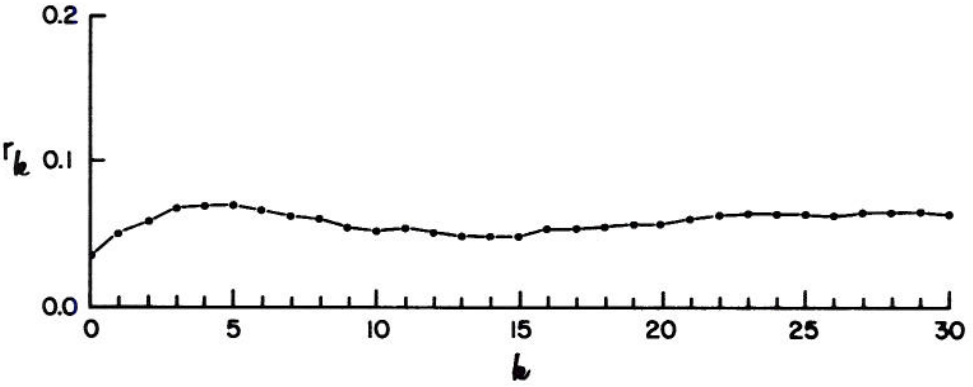

Fig. 31. Correlogram of cross correlation coefficients of rainfall and springflow at San Felipe Springs at Del Rio, Texas.

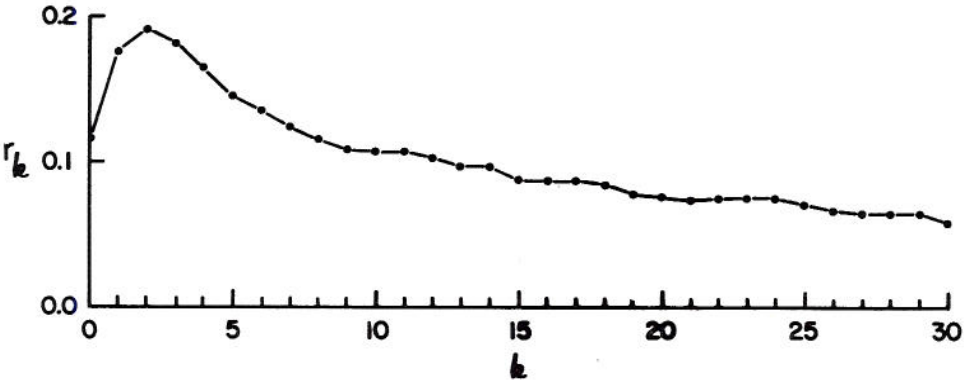

Fig. 32. Correlogram of cross correlation coefficients of rainfall and springflow at Big Springs near Van Buren, Missouri.

fall stations. Cross correlation coefficients (7) were determined by the relationship

$$r_k = \frac{\frac{1}{N-k}\sum_{i=1}^{N-k} X_i Y_{i+k} - \frac{1}{(N-k)^2}\left(\sum_{j=1}^{N-k} X_i\right)\left(\sum_{i=1}^{N-k} Y_{i+k}\right)}{\left[\frac{1}{N-k}\sum_{i=1}^{N-k} X_i^2 - \frac{1}{(N-k)^2}\left(\sum_{i=1}^{N-k} X_i\right)^2\right]^{1/2}\left[\frac{1}{N-k}\sum_{i=1}^{N-k} Y_{i+k}^2 - \frac{1}{(N-k)^2}\left(\sum_{i=1}^{N-k} Y_{i+k}\right)^2\right]^{1/2}} \quad (55)$$

The first 30 cross correlation coefficients were determined for each springflow and associated rainfall station. Correlograms of cross correlation coefficients are shown in Figs. 30, 31, and 32, for Goodenough Springs, San Felipe Springs, and Big Springs, respectively. The correlograms indicate a small degree of dependence between rainfall and springflow due to the large number of days with zero rainfall correlated with the sustained springflow recession. It should not be concluded that the two series are independent.

A notable characteristic of the system can be discerned from the cross correlation correlograms. The coefficients increase slightly and reach a maximum for a lag of 2 to 5 days. The lag for maximum coefficients indicates the short response time of the system response. Fig. 30 shows, for Goodenough Springs, that after reaching a maximum, the coefficients decrease consistently with little oscillation. For San Felipe Springs (Fig. 31), the coefficients increase to a maximum for a lag of 5 days, decrease to a minimum at a lag of 15 days, and again increases to a secondary maximum at a lag of 28 days. The significance of the secondary maximum is not known since both San Felipe Springs and Goodenough Springs are in a meteorologically homogeneous area.

4. Harmonic Analysis. Harmonic analyses were made to determine significant periodicities in the springflow time series. In order to compare springflow series properties with those of the rainfall series, averaging over time intervals of 1, 3, 7, and 14 days was made. The time intervals provide a means of possible extrapolation of data to shorter time intervals.

As in the case of the rainfall series, the basic data considered in the harmonic analyses of springflow were the means, the standard deviations, and the coefficients of variation. The statistics were determined by the relationships

$$m_\tau = \frac{1}{n}\sum_{p=1}^{n} y_{p,\tau} \quad , \quad (56)$$

$$s_\tau = \left[\frac{1}{n}\sum_{p=1}^{n}\left(y_{p,\tau} - m_\tau\right)^2\right]^{1/2} \quad , \quad (57)$$

and

$$Cv_\tau = \frac{s_\tau}{m_\tau} \quad , \quad (58)$$

where m_τ is the mean, s_τ is the standard deviation, Cv_τ is the coefficient of variation, τ is the interval of a year, p is the year index, n is the total years of record, and $y_{p,\tau}$ is the springflow for the p-th year and the τ-th interval.

Fourier series analyses were used to describe the periodic component for each statistic studied and time interval for the three springflow stations. Mathematical expressions for the periodic component of any parameter, the Fourier coefficients, and harmonic amplitudes are given by Eqs. (26), (27), (28), and (29), respectively. As in the case with rainfall, a total of 12 harmonics were determined for the springflow series.

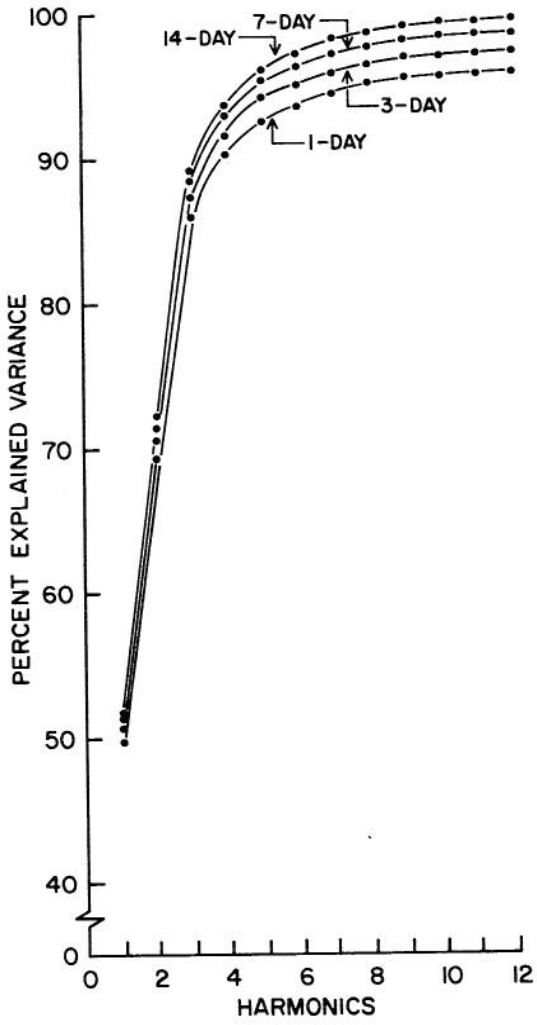

Fig. 33. Amount of variance of springflow interval means explained by harmonics for Goodenough Springs near Comstock, Texas, for 20 years of record (1947-66).

The variance of any periodic component, ν_τ, is given by

$$\text{var}\ \nu_\tau = \frac{1}{\omega} \sum_{\tau=1}^{\omega} \left(\nu_\tau - \nu_y \right)^2 \quad . \qquad (59)$$

The amount of variance of springflow interval means explained by each harmonic was determined for the 1-, 3-, 7-, and 14-day series for the three springflow stations studied. The results of the determination are shown in Figs. 33, 34, and 35 for Goodenough Springs, San Felipe Springs, and Big Springs, respectively.

Fig. 33 shows that 95 percent of the variance is explained by eight harmonics for the 1-day time interval at Goodenough Springs. The amount explained by eight harmonics for the 3-, 7-, and 14-day intervals is greater than for 1-day due to the effect of averaging in reducing sampling errors. Eight harmonics account for slightly more than 96, 97, and 98 percent of the explained variance for the 3-, 7-, and 14-day intervals, respectively.

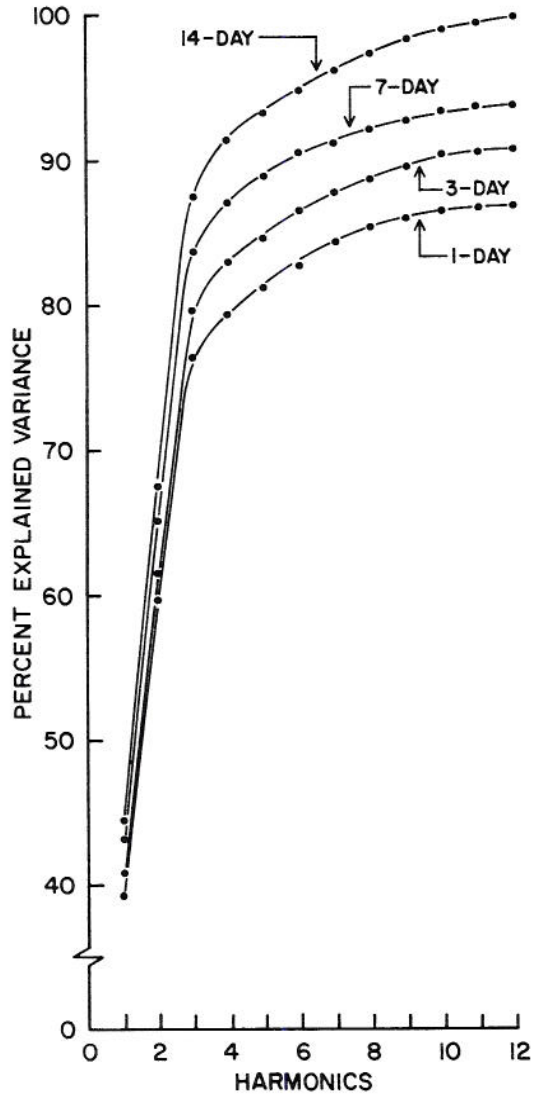

Fig. 34. Amount of variance of springflow interval means explained by harmonics for San Felipe Springs at Del Rio, Texas, for 6 years of record (1962-67).

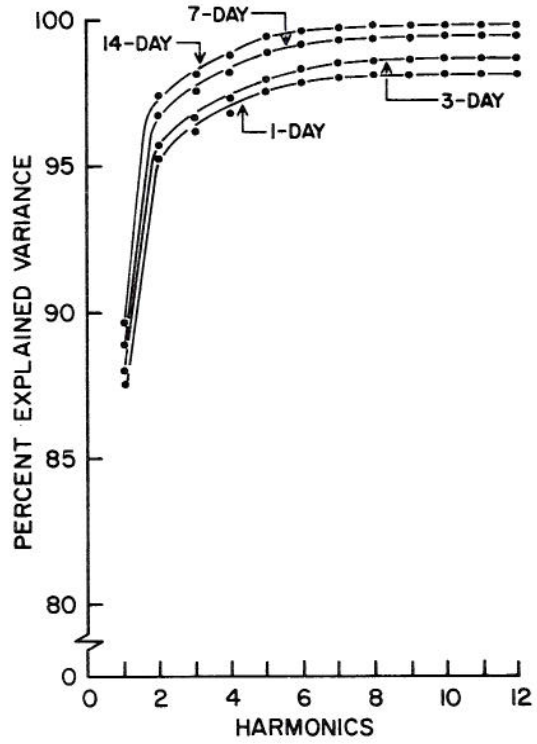

Fig. 35. Amount of variance of springflow interval means explained by harmonics for Big Springs near Van Buren, Missouri, for 20 years of record (1945-64).

Inspection of Fig. 34 shows that only 83 percent of the variance is explained by six harmonics for San Felipe Springs. Twelve harmonics explain only 87 percent of the variance for the 1-day interval. Also, the spread in amount of explained variance from the 1-day to 14-day interval is considerably more than that for Goodenough Springs and Big Springs (Fig. 35). The relative spread and amount of variance explained by the harmonics at San Felipe Springs is undoubtedly due to the short period of record, because only 6 years of record are available at San Felipe Springs, whereas 20 years of data are available for Goodenough Springs and Big Springs. Although 20 years is not a long record, the shape of the lines in Figs. 33 and 35 is very nearly alike and the characteristics of the curves are probably indicative of karst springflow data, showing the periodicity (first 2 or 3 harmonics) and high stochastic dependence.

Amount of variance explained by the first 2 or 3 harmonics for Big Springs (Fig. 35) is greater than for Goodenough Springs or San Felipe Springs. Only two harmonics explain more than 95 percent of the variance for all time intervals. The remaining 10 harmonics explain very little additional variance. A possible explanation for the difference in explained variance is that Big Springs is in a higher rainfall area with a more pronounced periodic distribution throughout the year.

In Chapter IV, section 3, the Fisher test (Eq. 32) was used to determine the number of significant harmonics in rainfall. The test utilized the square of the harmonic amplitude and variance of the component. In view of the large amount of variance explained by the first 2 or 3 harmonics for stations with long-term records, a better method of determining significance might be based on explained variance. A possible con-

sideration for significance might be 95, 96, 97, and 98 percent of variance explained for the 1-, 3-, 7-, and 14-day interval, respectively. These criteria appear to be relatively strict. Examination of Figs. 33 and 35 reveal that 2 to 3 harmonics will satisfy the conditions for both springflow stations. The 1-day period for Goodenough Springs (Fig. 33) shows 84 percent variance explained by three harmonics, but nine harmonics explain only 12 percent more variance. The same is true for time intervals 3, 7, and 14 days. Inspection of Fig. 35 shows similar results for Big Springs. Due to the short period of record for San Felipe Springs, Fisher's test shows no significant harmonics for the 1-, 3-, and 7-day time intervals, although this is not acceptable in view of Fig. 34. Fisher's test is not applicable.

For comparison with the above discussion, the Fisher test was applied to the springflow harmonic analyses. Table 4 gives the results of the comparison for each station by time interval. The Fisher test indicates more harmonics are significant than are needed to explain practically all the variance.

Figs. 36, 37, and 38, show the 1-day time interval fitted period component for daily springflow discharge mean, standard deviation and coefficient of variation, respectively, for Goodenough Springs. Eight harmonics (significant, Table 4) comprise the fitted periodic component. The number of harmonics used for the standard deviation and coefficient of variation are the same as for the mean, irrespective of explained variance for the specific parameter. In general, the number of harmonics determined significant by the Fisher test were the same for the three parameters: mean, standard deviation, and coefficient of variation.

Due to the high significance level (95 percent explained variance for the 1-day interval), the fitted periodic component closely approximates the density for all three parameters. The relative shapes of the three figures are similar with maxima occurring between 250 and 300 days. This corresponds to the normal high rainfall period for the area of September-October. Secondary peaks occur during the April-May-June period of normally second high rainfall for the area. The sharp peaks of Figs. 36, 37, and 38, cannot be approximated any more accurately with more harmonics due to the short duration.

Equally good fit of densities by the periodic component was obtained for the 3-, 7-, and 14-day time series. The amount of variance explained by harmonics for the three discrete 3-, 7-, and 14-day series relative to that for the 1-day series would indicate the relative goodness of fit by the periodic component. In the interest of space, Figs. for the 3-, 7-, and 14-day series are not shown.

5. Stochasticity in Springflow. The internal structure of the springflow time series was analyzed to determine any characteristics for possible use in system identification and springflow simulation. The original springflow series was shown to be highly dependent in time (section 1), and also was shown to contain periodicities (section 3).

In the harmonic analysis, the periodic means, m_τ , were determined for all τ . Then the coefficient of variation is also known for all τ , as given by Eq. (25), $Cv_\tau = s_\tau/m_\tau$, or

$$s_\tau = Cv_\tau m_\tau \quad , \tag{60}$$

where s_τ is the standard deviation, m_τ is the mean, Cv_τ is the coefficient of variation, and τ is the time interval within the year.

The periodicity of the y-series can be removed by standardization to give the new series

$$\xi_{p,\tau} = \frac{Y_{p,\tau} - m_\tau}{s_\tau} \quad , \tag{61}$$

or rather the original series can be written as

$$Y_{p,\tau} = m_\tau + s_\tau \xi_{p,\tau} \quad . \tag{62}$$

Substituting Eq. (60) for the standard deviation in Eq. (62) gives (with Cv_τ considered as a constant)

$$Y_{p,\tau} = m_\tau + m_\tau Cv_\tau \xi_{p,\tau} \quad . \tag{63}$$

Factoring Eq. (63) gives

$$Y_{p,\tau} = m_\tau \left[1 + Cv_\tau \xi_{p,\tau}\right] \tag{64}$$

where $E(\xi) = 0$ and the var $\xi = 1$. If

$$\theta_{p,\tau} = 1 + Cv_\tau \xi_{p,\tau} \quad , \tag{65}$$

where the $E(\theta) = 1$ and var $\theta = Cv^2$, then substitution into Eq. (64) gives

$$Y_{p,\tau} = m_\tau \quad \theta_{p,\tau} \quad . \tag{66}$$

Taking logarithms of Eq. (66) results in

$$\ln Y_{p,\tau} = \ln m_\tau + \ln \theta_{p,\tau} \quad . \tag{67}$$

Since $\mu_\tau = \ln m_\tau$, or $m_\tau = e^{\mu_\tau}$,

Eq. (67) can be written as

$$Y_{p,\tau} = e^{\mu_\tau} \quad \theta_{p,\tau} \quad . \tag{68}$$

A new series of θ was computed for the daily springflow time series at each station from Eq. (68). Autocorrelation coefficients were determined by Eq. (22) for the new θ-series. Autocorrelation was determined for each time series. Results are shown in Figs. 39, 40, and 41 for Goodenough Springs, San Felipe Springs, and Big Springs, respectively. These figures show that for time 3, 7, and 14 days series, the correlograms are not smooth in shape. For 7 and 14 days at Big Springs, the correlograms are irregular in shape with considerable oscillation. The Markov I model in general can approximate in a very rough manner the correlograms for 1, 3, and 7 days.

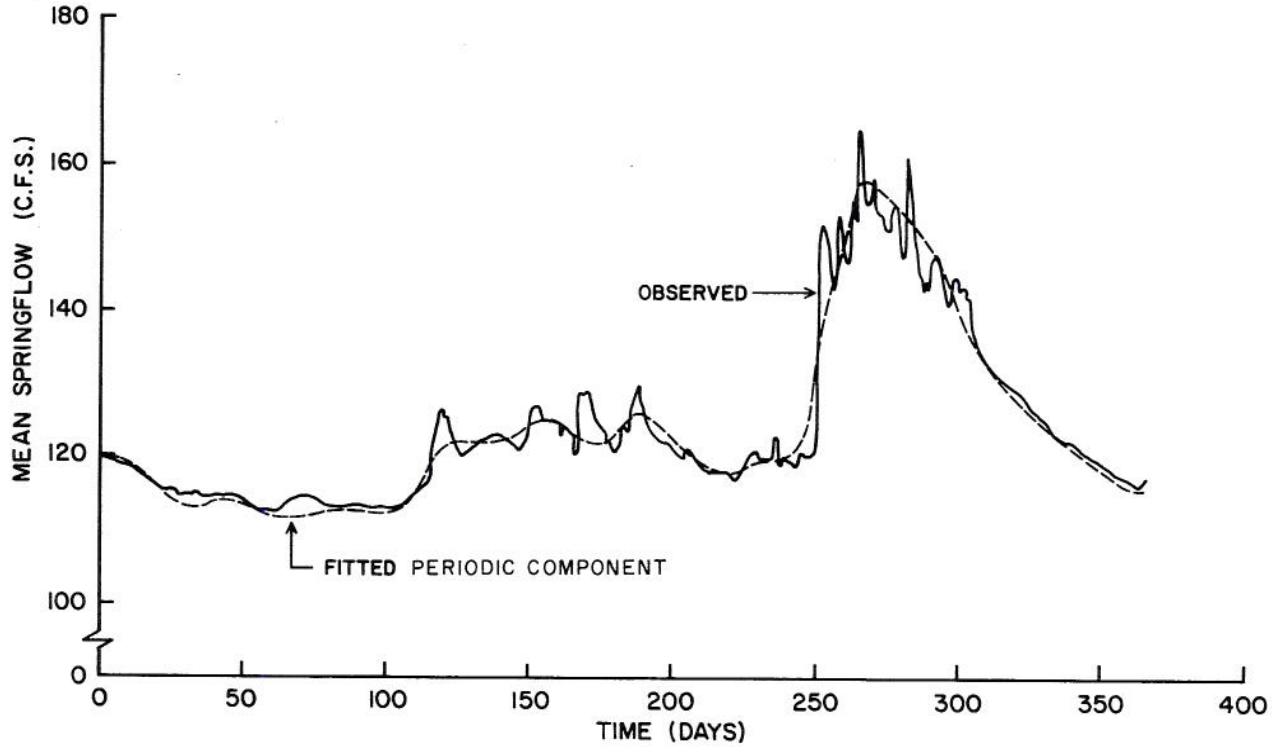

Fig. 36. Fitted periodic component for mean daily springflow by 8 harmonics for Goodenough Springs near Comstock, Texas.

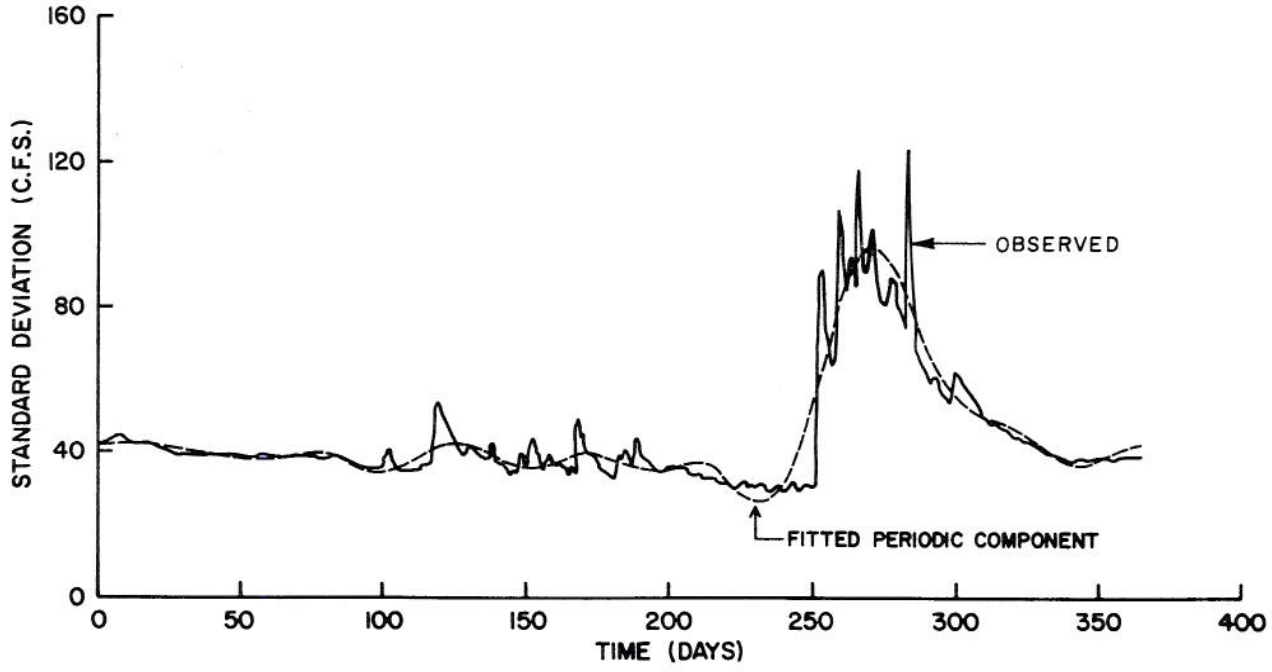

Fig. 37. Fitted periodic component for the daily standard deviation by 8 harmonics for Goodenough Springs near Comstock, Texas.

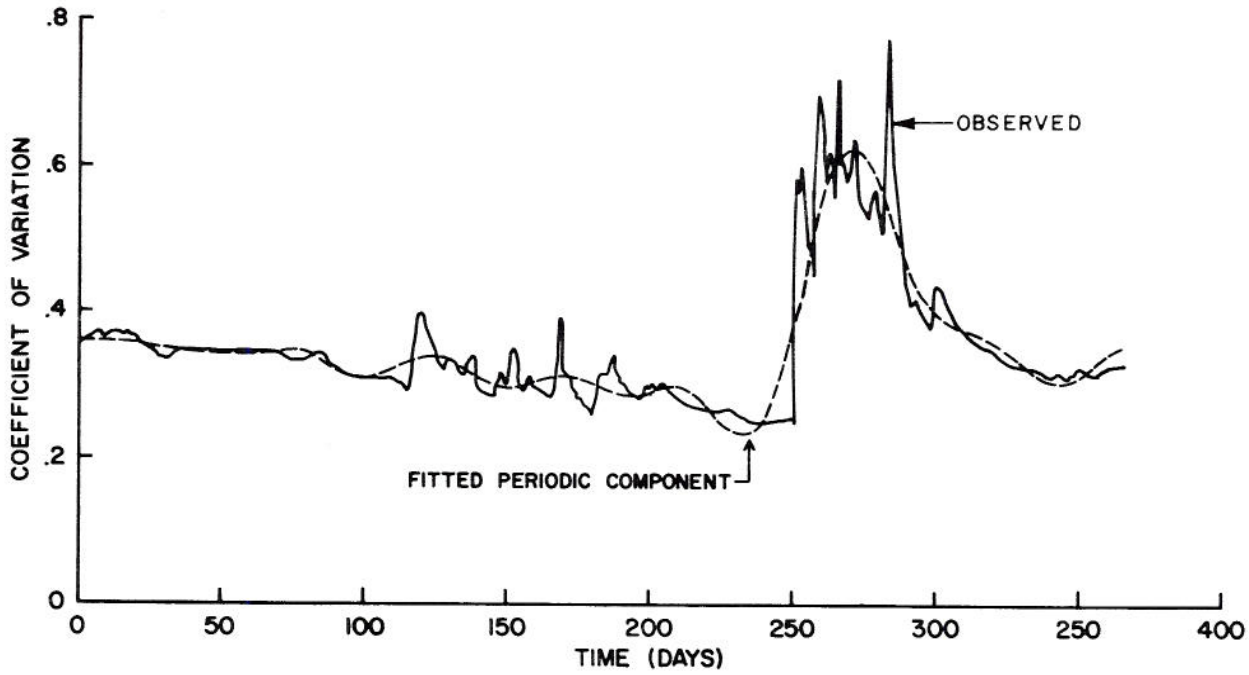

Fig. 38. Fitted periodic component for coefficient of variation of daily springflow by 8 harmonics for Goodenough Springs near Comstock, Texas.

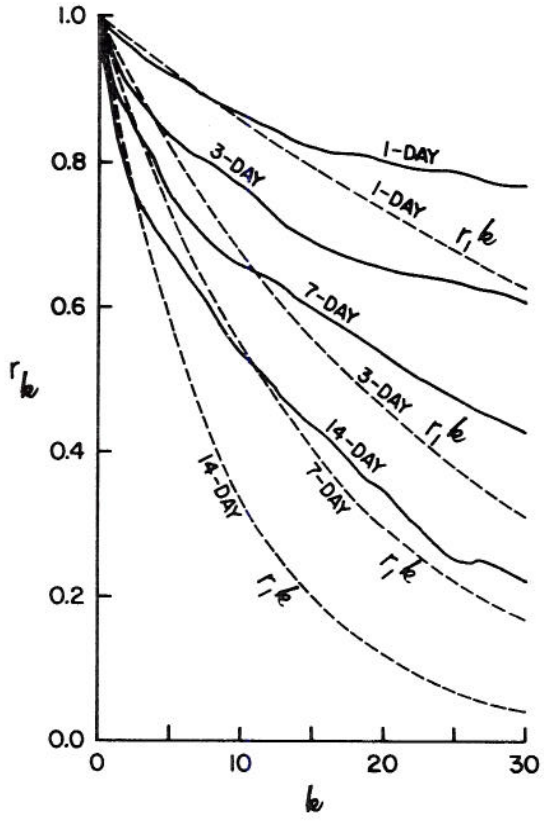

Fig. 39. Correlogram for θ-series and Markov I model for 1-, 3-, 7-, and 14-day intervals, Goodenough Springs near Comstock, Texas.

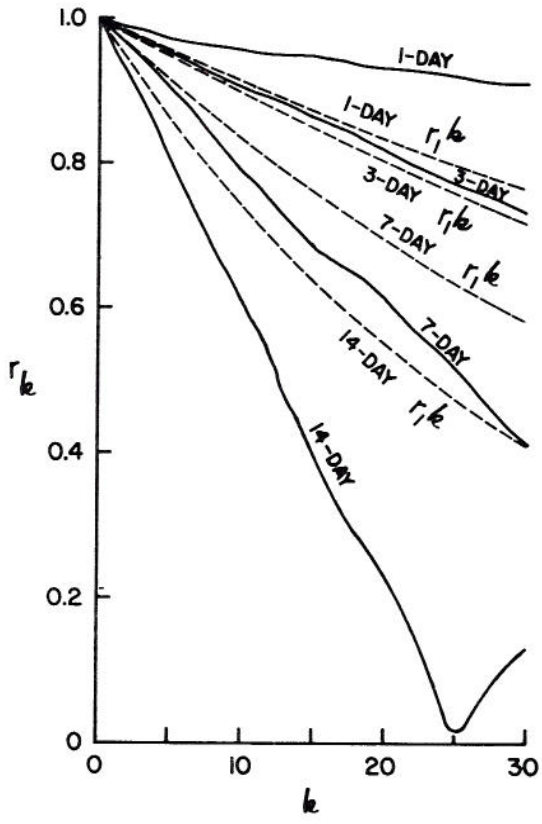

Fig. 40. Correlogram and Markov I model for θ-series of springflow, 1-, 3-, 7-, and 14-day intervals, San Felipe Springs at Del Rio, Texas.

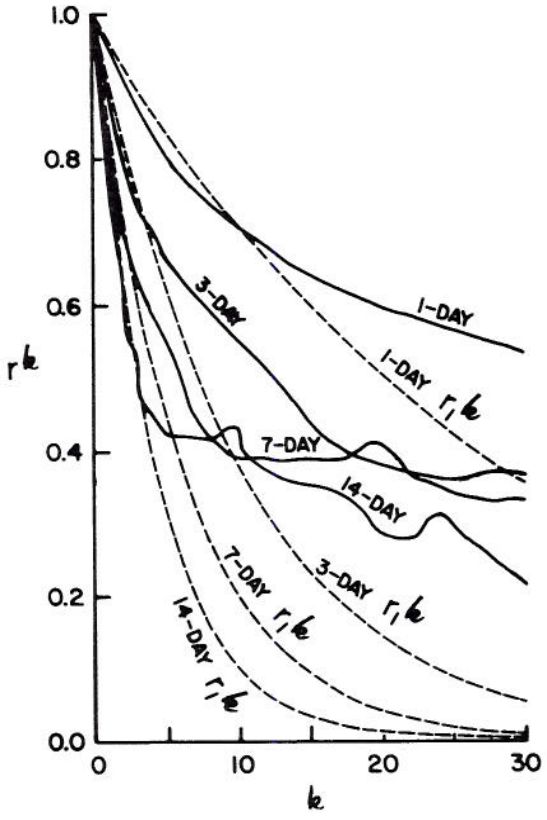

Fig. 41. Correlogram and Markov model for θ-series of springflow, 1-, 3-, 7-, and 14-day intervals, Big Springs near Van Buren, Missouri.

In view of the time dependence shown in Figs. 39, 40, and 41, Eq. (68) should be rewritten to include the Markov I model, thus

$$Y_{p,\tau} = e^{\mu_\tau}\left(r_1\theta_{p,\tau-1} + \delta_{p,\tau}\right) \qquad (69)$$

where $\theta_{p,\tau}$ represents the dependent component and $\delta_{p,\tau}$ represents the independent component.

Table 4. Significant harmonics based on Fisher test and explained variance criteria.

Time Interval	Number of Significant Harmonics					
	Goodenough Springs		San Felipe Springs		Big Springs	
	Fisher Test	Explained Variance*	Fisher Test	Explained Variance*	Fisher Test	Explained Variance*
1	8	8	12	**	6	2
3	6	8	12	**	6	3
7	6	8	12	**	6	3
14	6	8	9	9	6	3

*Number of harmonics to explain 95 percent variance for 1-day, 96 percent for 3-day, 97 percent for 7-day, and 98 percent for 14-day intervals.

**No significant harmonic was found.

CHAPTER VII

SYSTEM IDENTIFICATION

System identification is defined as that process of linking the system input to the system output; i.e., the determination of the function that distributes the excess precipitation in time into a discharge hydrograph. In surface runoff the input is precipitation excess--excess to soil moisture deficit and deep percolation. In ground water, the system input is excess infiltration or deep percolation. The linkage function is known by various names: unit hydrograph, impulse response function, transfer function, kernel function, distribution function. Regardless of the name, the purpose is the same--to distribute the effective or excessive precipitation in time.

The main problem in system identification is the accurate estimate of effective precipitation. Error-free data enable the determination of the same linkage function by several methods of identification. In view of this recognized importance, reiteration of some points made in earlier chapters is justified at this time.

In the ground-water systems under investigation, physical characteristics of the system cannot be clearly defined. The recharge area in karst formations contributing to springflow cannot be accurately determined. Neither can the "channel" system in the karst underground be defined. The lack of knowledge concerning the area makes it difficult to define areal distribution of rainfall. In areas without research instrumentation, there is a notable lack of adequate precipitation stations, particularly in the sparsely populated, semiarid areas. One rainfall station per county is the usual case. In addition to the problem of areal distribution of stations, only a small number of the available stations consist of recording gages where time distribution of rainfall is available. Furthermore, with all due respect to the proponents of infiltration theory and surface runoff modeling techniques, the determination of effective precipitation (recharge) from mass rainfall is subject to large errors.

In essence, the ground-water system is one for which the area and physical characteristics are unknown, over which an inexact rainfall amount is recorded over an unknown period of time. Unknown soil characteristics affect the transmission of water, the knowledge of which is an inexact science. Even if it is known on a limited number of points over the recharge area, the high variability of soil characteristics as it concerns the transmission and/or evaporation of water may make these points unrepresentative of the total area. These are a few of the problems that confront water resource planners and other hydrologists. Furthermore, hydrologic systems are known to be nonlinear. Linear systems are easier to model than nonlinear ones. There is little doubt that the system identification poses a difficult problem. It is the purpose in the following sections to describe the results of some methods of system identification used to determine linkage functions in karst aquifers.

1. Simplifying Assumptions. In order to solve the problem of system identification, some simplifying assumptions must be made. The assumptions not only will aid in overcoming the many vagaries previously described but will establish a reference plane for future studies. The assumptions are that a karst aquifer system is a lumped, linear, time-invariant system with a finite memory, causal in nature, and deterministic.

Linearity implies that the system has the property of superposition; i.e., the unit hydrograph can be applied anywhere in time. Linearity may be assumed in karst aquifers only as a rough approximation. Time invariance implies that the system behavior does not change in time. Because the chemical and physical erosion and sediment depositions are continuous processes in karst formations in which water circulates, the assumption of time invariance must be only a sufficient approximation at best. The finite memory implies that the system state and output can be expressed for dependence only on the history of the system for a previous length of time equal to the memory. Causality assumes that system output cannot occur earlier than the corresponding input. All hydrologic systems are causal and this assumption is actually not restrictive. A deterministic system is one in which the same input will always produce the same output. This assumption does not preclude that the input or output is stochastic. A lumped system implies that space variation can be ignored.

The first and last assumptions are the least realistic of all. Specifically, it is a well known fact that rainfall, over an area of any magnitude, is not uniform. Infiltrated rainfall effective for recharge is not uniform even if rainfall can be considered uniform. Furthermore, transmission rates through the mantle are not uniform over an area.

2. Effects of Errors in Data on System Identification. Although several papers cited in the literature review describe the effect of data errors in system identification, it is worthwhile at this point to refresh the readers' minds with an example before proceeding with identification of the systems studied. A better appreciation will be gained for the various procedures given later.

Dooge[1/] stated that if a system is truly linear and the data do not contain errors, the several methods system identification will produce the same results, i.e. the same response or transfer function. Therefore, the simplest method will be used to illustrate the effect of errors.

Assume a truly linear system with true input ordinates,

$$f = [f(1), f(2), f(3)] = [2, 6, 1] \qquad (70)$$

1/ Dooge, J.C.I. "Linear Theory of Hydrologic Systems," lecture series, University of Maryland in cooperation with the USDA Hydrograph Laboratory, August 1967, to be published as a USDA Technical Bulletin.

and true output ordinates,

$$g = [g(1), g(2), \ldots g(6)] = [4, 18, 24, 17, 8, 1]. \quad (71)$$

Using the simplest method of system identification, forward substitution, in Eq. (13),

$$g(i) = \sum_{k=1}^{i} h(k)f(i-k+1)\Delta k \quad (13)$$

solution for $h(k)$ with $\Delta k = 1$ gives

$$h(1) = \frac{g(1)}{f(1)} = 2$$

$$h(2) = \frac{g(2) - h(1)\, f(2)}{f(1)} = 3$$

$$h(3) = \frac{g(3) - [h(1)f(3) + h(2)f(2)]}{f(1)} = 2 \quad (72)$$

$$h(4) = \frac{g(4) - [h(2)f(3) + h(3)f(2)]}{f(1)} = 1$$

$$h(5) = \frac{g(5) - [h(3)f(3) + h(4)f(2)]}{f(1)} = 0$$

$$h(6) = \frac{g(6) - [h(4)f(3) + h(5)f(2)]}{f(1)} = 0$$

Then from Eq. (72), the response function ordinates are

$$h = [h(1), h(2), h(3), h(4)] = [2, 3, 2, 1]. \quad (73)$$

After determining the true impulse response function given by Eq. (73), assume that instead of the true input distribution, the data contain errors such that

$$f = [f(1), f(2), f(3)] = [3, 5, 1]. \quad (74)$$

The sum of input units is the same for both conditions, 9. Substitution in Eq. (72) results in response function ordinates

$$h = [h(1), h(2), \ldots h(6)]$$
$$= [1.33, 3.78, 1.26, 2.31, -1.60, 2.24]\ . \quad (75)$$

The result is an unrealistic negative ordinate and oscillations.

The previous example of error effect was in distribution only, with correct total. Now consider that the total is in error and the input data are given as

$$f = [f(1), f(2), f(3)] = [2, 5, 1]. \quad (76)$$

Solution by Eq. (72) gives

$$h = [h(1), h(2), \ldots h(6)] = [2, 4, 1, 4, -6.5, 14.75]. \quad (77)$$

As in the previous example, the error caused a non-realistic negative ordinate and oscillations.

The effect of erroneous output data on the impulse response function is shown in the following example. Assume an error occurred in the measurement of g(2) such that instead of the actual 18 the indicated value is 17. The determination of the impulse response function by Eq. (72) shows

$$h = [h(1), h(2), \ldots h(6)]$$
$$= [2, 2.5, 3.5, -3.25, 12, 33.88]\ . \quad (78)$$

As in the previous examples, the error in output again caused an unrealistic negative ordinate and oscillations.

In view of the previous examples, it is easily seen what effect errors in measurement can have in system identification. The examples given show errors in input and output, and the input represents precipitation excess (recharge in a ground-water system). Consider the fact that in a lumped system rainfall distribution is ignored, and it is realized that errors are commonplace. Furthermore, recharge must be estimated from total precipitation which increases the opportunities for errors. System identification, therefore, resolves to methods of coping with errors or optimization.

The remaining sections of this chapter will be devoted to specific methods of systems identification as applied to karst ground-water systems. In order to utilize actual hydrographs with associated recharge and without antecedent recession flow, the open-ended hydrograph above an extrapolated recession, shown in Fig. 7 of Chapter II, is used in succeeding sections. The recessions were extrapolated by Eq. (52) given in Chapter VI.

It is necessary to indicate the defining conditions for use of the open-ended hydrograph before proceeding to the determination of response functions. Response of the karst aquifer systems to recharge is both rapid and delayed in the same system, as indicated in Chapter VI. That is, rapid response to recharge quickly transcends into a sustained recession. Hydrograph truncation assumes that the rapid response portion is the total above the extrapolated base, and that the delayed response is represented by an instantaneous input at the truncation time, as shown in Fig. 42. The truncation point of rapid response represents

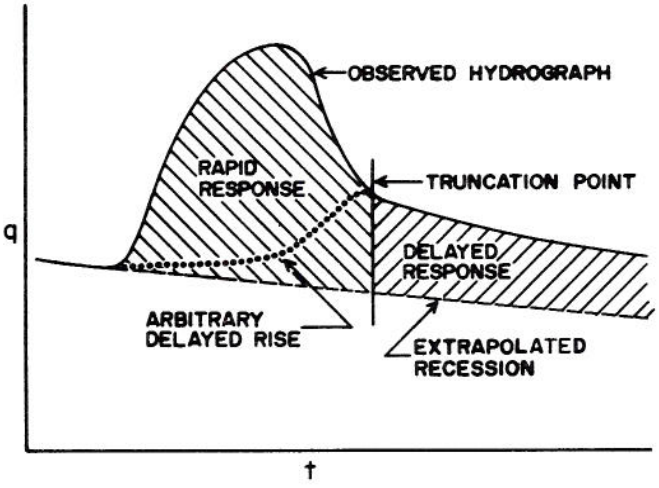

Fig. 42. Schematic representation of open-ended hydrograph indicating karst system responses.

the initial point of delayed response. This is not the true condition, but rather an increase in the delayed response is more nearly approximated by the dotted line, arbitrarily drawn, in Fig. 42. The increase in delayed response is analogous to baseflow increase in a total streamflow system. Since division of the two components of the karst aquifer response would be arbitrary, conjectural division is avoided by hydrograph truncation.

System identification using the truncated hydrograph provides a time distribution of only the rapid response portion of the karst springflow. The identification does not maintain the total volume of response. The conservation of volume is dependent upon the accurate duplication of the time distributed rapid response and accurate approximation of the sustained recession by the exponential equation. System identification is based on matching karst springflow rates rather than volumes. The validity of the analysis is not affected by the method of comparison.

5. System Identification Using Quantized Data.

a. Correlation and cross correlation functions. The optimization procedure of system identification used by Eagleson et al [12] for urban watersheds was reviewed in the literature of Chapter II. It is not necessary to repeat the development of procedure at this point, but for convenience, the Wiener-Hopf equation is repeated here, as

$$\phi_{fg}(j-1) = \sum_{k=1}^{\infty} h_{opt}(k)\phi_{ff}(j-k) \quad , \quad j \geq +1 \qquad (14)$$

where ϕ_{fg} is the cross correlation function of input, f , and output, g , ϕ_{ff} is the autocorrelation function of input, f , and h is the impulse response function.

Eagleson recognized that the data contained errors and the system was not truly linear. The procedure was modified to impose the constraint that the h-ordinates be equal to or greater than zero (no negative ordinates). In order to impose the constraints and be able to preserve the area under the hydrograph, slack variables were used to develop an underdetermined set of simultaneous equations. Linear programming was used to solve the equations under the condition that the sum of the slack variables be a minimum. The resulting impulse response function was characterized by a normal shape decreasing to zero and a disconnected secondary rise and recession. Such a response function was satisfactory in simulation of urban runoff. However, in a ground-water system the recession is the most predictable part of a hydrograph and the characteristic function shape is objectionable.

In the current study of karst ground-water systems, a large number of recharge periods were selected for analysis. A total of 16 recharge periods were selected from the record for Goodenough Springs and 18 periods were selected for Big Springs. Examination of the short record for San Felipe Springs revealed only four suitable recharge periods. The selection of hydrographs was made on the basis of: (1) a minimum of three consecutive days of rainfall, and (2) the recharge resulted in a significant increase of springflow. By selection of a large number of hydrographs, it was thought that normal solution of the Wiener-Hopf equation would result in a few solutions with all positive ordinates of the impulse response function.

The first step in the analysis was to determine the daily recharge amounts from daily rainfall amounts by applying the serpentine function, Eq. (47), Chapter V. The estimated recharge was considered to be the best estimate of system input.

After determining the system input (recharge), the next step was the determination of input autocorrelation functions and cross correlation functions by the relations

$$\phi_{ff}(i) = \sum_{j=1}^{N} f(i)f(i+j) \qquad i = 1, 2, \ldots, N \qquad (79)$$

and

$$\phi_{gf}(i) = \sum_{j=1}^{M} g(i)f(i+j) \qquad i = 1, 2, \ldots, M, \qquad (80)$$

respectively. The autocorrelation and cross correlation functions were substituted into Eq. (14) and a set of simultaneous equations were developed. Solution of the equations was performed by matrices rather than forward or backward substitution. The matrix convolution relationship can be written as

$$y_{P,1} = X_{P,N}\, h_{N,1} \qquad (81)$$

where y is the vector of cross correlation functions, X is the matrix of input autocorrelation functions, h is the vector of pulse response, P is the number of ordinates in the output vector and P = N + M - 1, N is the number of nonzero values of input, and M is the number of nonzero values of output. The least squares method of solving Eq. (81) arranges the data in the form

$$X^{-1}\, y = X^{-1}\, Xh \; . \qquad (82)$$

The product of a matrix and its inverse results in the identity matrix. The matrix equation can then be solved for the response function ordinates.

Determination of the impulse function was made for each hydrograph for the three springflow stations. Impulse functions with all positive ordinates resulted from only three hydrographs for Goodenough Springs, eight for Big Springs, and none for San Felipe Springs. Of the eight solutions for Big Springs, only three appeared to be realistic and those contained oscillations. The impulse functions derived for Goodenough Springs and Big Springs are shown in Figs. 43 and 44, respectively. Eagleson [12] suggested that an average impulse response function for a system should be determined by averaging the results from the several hydrographs as opposed to averaging hydrograph ordinates and then determining the response function. The average response functions for Goodenough Springs and Big Springs are shown on the respective figures.

The impulse response functions exhibit oscillations to some degree, but they are not completely erratic as were the examples in the previous section. The significance of the analysis rests in the fact that realistic impulse functions can be determined from several selected hydrographs.

b. Determination of angle points of impulse response function. It is recalled from the literature review of Chapter II that Snyder [27] determined angle points of the impulse response function of storm runoff by multiple regression techniques. The method provided a means of averaging over portions of the transfer function by interpolation in order to distri-

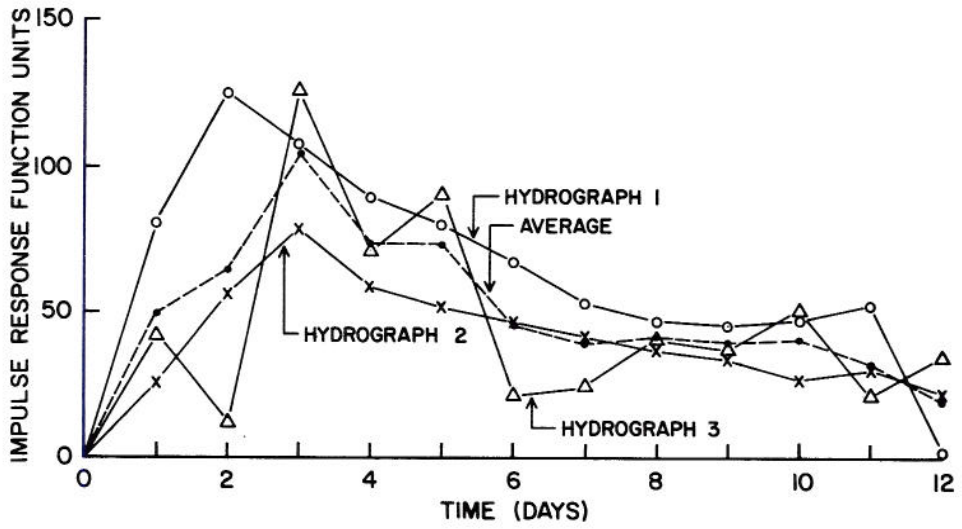

Figure 43. Impulse response function ordinates from autocorrelation and cross correlation functions, Goodenough Springs near Comstock, Texas.

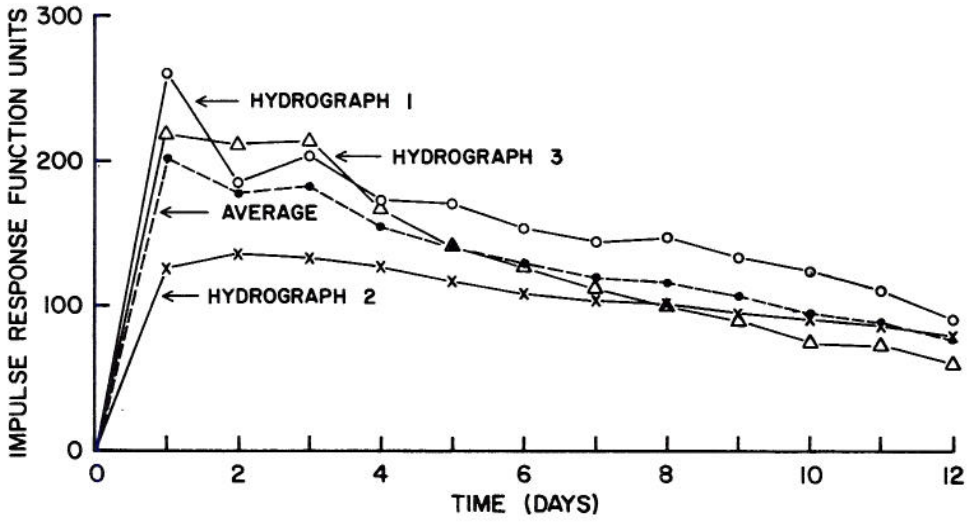

Figure 44. Impulse response function ordinates from autocorrelation and cross correlation functions, Big Springs near Van Buren, Missouri.

bute possible errors. Errors in the data are not eliminated by the procedure but are distributed in an optimization procedure.

For the purpose of distinguishing from the previous section, the discrete convolution equation is rewritten as

$$Q(i) = \sum_{k=0}^{i} u(k)\, R(i-k) \quad i = 0,1,\ldots, M \qquad (83)$$

where Q the springflow discharge rate, in cubic feet per second, R the ground-water recharge, in inches, and u is the transfer function ordinate. The order of summation can be reversed and Eq. (83) becomes

$$Q(i) = \sum_{k=0}^{i} R(k)\, u(i-k), \quad i = 0, 1,\ldots,M \qquad (84)$$

which is more convenient for future use. Eq. (84) is the condensed notation of Eq. (16) given in the literature review.

By applying Snyder's method to the karst groundwater systems under study, the appropriateness of the method for ground-water response can be determined. The hydrographs selected for analysis in the previous section were utilized in the multiple regression analysis.

Hydrograph peaks were given special consideration in the selection of angle points for each hydrograph. The peak ordinate and the ordinate immediately preceding and following the peak were selected as angle points. The initial and final ordinates of the hydrograph were also selected as angle points with additional intermediate points as considered necessary to define the impulse response function stage. An example of the procedure may be helpful to demonstrate the methodology. An actual hydrograph for Goodenough Springs will be used in the example, and the data are shown in Table 5.

The discharge data shown in column 3 of Table 5 are actual data. In order to determine the response to the recharge, the recession was extrapolated by Eq. (52). The extrapolated base was subtracted from the measured discharge (column 3) to obtain the response hydrograph discharge (column 4). Angle points (column 5) were arbitrarily selected at times 0, 2, 3, 4, 5, 8, and 10. The units 2, 3, and 4 define the hydrograph peak.

The transfer function ordinates can be expressed as

$$\begin{aligned}
u_0 &= \phi_0 + e_0 \\
u_1 &= \tfrac{1}{2}(\phi_0 + \phi_2) + e_1 \\
u_2 &= \phi_2 + e_2 \\
u_3 &= \phi_3 + e_3 \\
u_4 &= \phi_4 + e_4 \\
u_5 &= \tfrac{1}{2}(\phi_4 + \phi_6) + e_5 \\
u_6 &= \phi_6 + e_6 \\
u_7 &= \tfrac{1}{2}(\phi_6 + \phi_8) + e_7 \\
u_8 &= \phi_8 + e_8 \\
u_9 &= \tfrac{1}{2}(\phi_8 + \phi_{10}) + e_9 \\
u_{10} &= \phi_{10} + e_{10}
\end{aligned} \qquad (85)$$

Equation (85) is substituted into the convolution Eq. (84). The ordinate errors are not shown explicitly, but in the "averaging" solution, some error is considered attached to each ordinate which are combined with the convolution errors. The results of substitution are

$$\begin{aligned}
R_0\phi_0 &= Q_0 \\
\tfrac{1}{2}R_0(\phi_0 + \phi_2) + R_1\phi_0 &= Q_1 \\
R_0\phi_2 + \tfrac{1}{2}R_1(\phi_0 + \phi_2) + R_2\phi_0 &= Q_2 \\
R_0\phi_3 + R_1\phi_2 + \tfrac{1}{2}R_2(\phi_0 + \phi_2) &= Q_3 \\
R_0\phi_4 + R_1\phi_3 + R_2\phi_2 &= Q_4 \\
\tfrac{1}{2}R_0(\phi_4 + \phi_6) + R_1\phi_4 + R_2\phi_3 &= Q_5 \\
R_0\phi_6 + \tfrac{1}{2}R_1(\phi_4 + \phi_6) + R_2\phi_4 &= Q_6 \\
\tfrac{1}{2}R_0(\phi_6 + \phi_8) + R_1\phi_6 + \tfrac{1}{2}R_2(\phi_4 + \phi_6) &= Q_7 \\
R_0\phi_8 + \tfrac{1}{2}R_1(\phi_6 + \phi_8) + R_2\phi_6 &= Q_8 \\
\tfrac{1}{2}R_0(\phi_8 + \phi_{10}) + R_1\phi_8 + \tfrac{1}{2}R_2(\phi_6 + \phi_8) &= Q_9 \\
R_0\phi_{10} + \tfrac{1}{2}R_1(\phi_8 + \phi_{10}) + R_2\phi_8 &= Q_{10}
\end{aligned} \qquad (86)$$

Table 5. Recharge, hydrograph, and transfer function ordinates, hydrograph No. 2, for Goodenough Springs near Comstock, Texas

Time (days)	Recharge (Inches)	Discharge (CFS)	Discharge above Extrapolated Base (CFS)	Angle Points	Transfer Function Ordinates 1/ (CFS/Inch)
(1)	(2)	(3)	(4)	(5)	(6)
0	0	240	0	*	0
1	1.18	278	39		(79.6)
2	.28	340	102	*	159.1
3		392	155	*	126.1
4		375	139	*	108.1
5		351	116		(97.2)
6		338	104	*	86.3
7		326	93		(80.2)
8		316	84	*	74.1
9		305	74		(66.0)
10		292	62	*	58.0

1/ Ordinates in parentheses are linearly interpolated from adjacent ordinates.

Values of the R's and Q's from columns 2 and 4, respectively, of Table 5 are substituted into Eq. (86). The set of eleven equations contain seven unknowns, the Ø's. Eq. (86) can be rearranged to group the Ø's which provide the basic information for multiple regression analysis. From the multiple regression, the coefficients were solved and are shown in column 6 of Table 5. As shown in Eq. (85), only the angle ordinates were determined by multiple regression. The intermediate ordinates, in parenthesis in Table 5, were determined by linear interpolation.

Similar analyses were made for all of the selected hydrographs for each springflow station. Positive transfer function ordinates were obtained for five hydrographs for Goodenough Springs, five for Big Springs, and none for San Felipe Springs. Although solutions with positive ordinates were obtained for the stated number of hydrographs, all were not stable. The three stable solutions along with the average for Goodenough Springs are shown in Fig. 45. Only two functions for Big Springs were stable and are shown with the average in Fig. 46.

Solutions with some negative ordinates were obtained by the procedure as was the case with autocorrelation and cross correlation functions of the previous section. An assessment of the response functions cannot be made until simulation runs are made.

4. System Identification from Discrete Functions.

a. Harmonic function. It was demonstrated in Chapter VI that periodic discrete ouptut data can be approximated by trigonometric functions. The functions were effective in explaining a significant percentage of the total variance. It was shown in Chapter IV that trigonmetric functions were not significant in expressing discrete input data, although no periodicity is likely in output without a periodicity in input. In view of the significant periodicity in output, an equivalent number of harmonics can be imposed on the input system, even though a relatively small percentage of the variance is explained by the periodic component. The harmonic components were determined by averaging over an n-year period.

The periodic components of rainfall and springflow were super imposed and are shown for Goodenough Springs and Big Springs in Figs. 47 and 48, respectively. The periodic component contains eight harmonics for Goodenough Springs and contains two harmonics for Big Springs. The rainfall series for Goodenough Springs exhibit considerable oscillations as would be expected for eight harmonics. For Big Springs, Fig. 48 indicates springflow increases before associated increase in rainfall. This condition does not conform to that of a causal system such as the ground-water system under investigation. The rainfall Fourier series has been converted to equivalent springflow in CFS by assuming mean daily rainfall is equal to average mean daily discharge. This assumption and conversion merely permits a one-to-one comparison of springflow and rainfall.

O'Donnell [23] applied finite harmonic series to discrete rainfall excess and runoff for some British catchments. Rainfall excess was expressed by Fourier expansion as

$$x(\tau) = \sum_{k=0}^{\infty} a_k \cos k \frac{2\pi\tau}{T} + \sum_{k=0}^{\infty} b_k \sin k \frac{2\pi\tau}{T} \qquad (87)$$

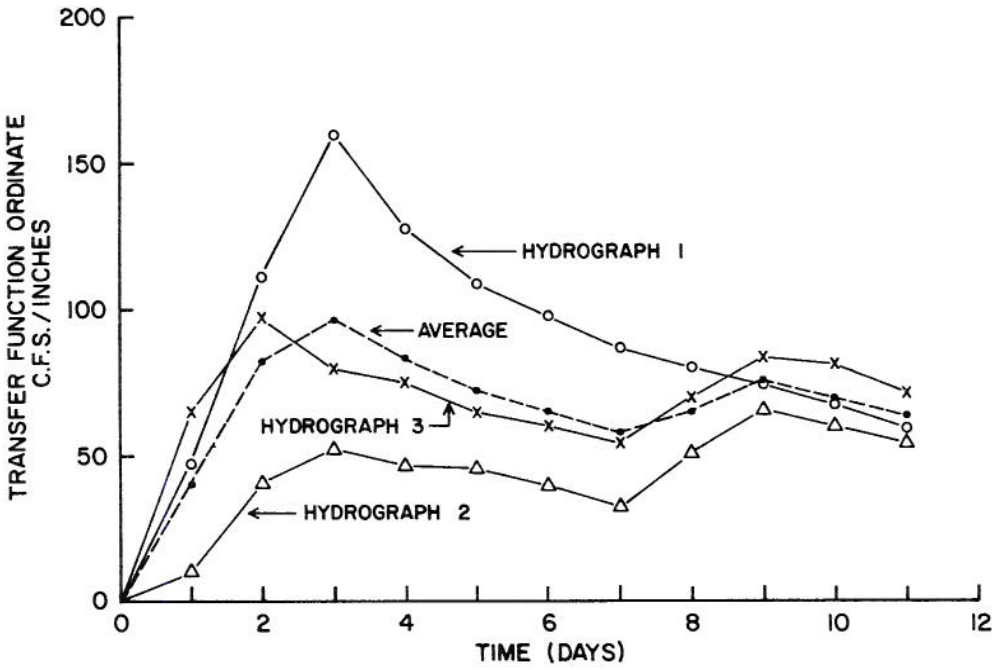

Figure 45. Transfer function ordinates determined by multiple regression methods, Goodenough Springs near Comstock, Texas.

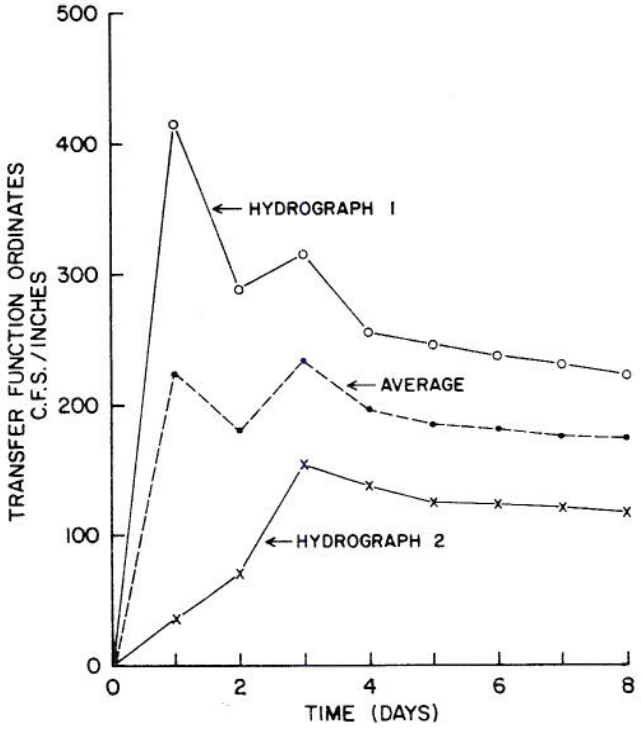

Figure 46. Transfer function ordinates determined by multiple regression methods, Big Springs near Van Buren, Missouri.

where a_k, and b_k are the Fourier coefficients, and T is the duration of runoff, or period. Likewise, Fourier expansion for runoff was given as

$$y(t) = \sum_{k=0}^{\infty} A_k \cos k \frac{2\pi\tau}{T} + \sum_{k=0}^{\infty} B \sin k \frac{2\pi\tau}{T} \qquad (88)$$

and the instantaneous unit hydrograph (IUH) was given as

$$h(t-\tau) = \sum_{k=0}^{\infty} \alpha_k \cos k \frac{2\pi(t-\tau)}{T} + \sum_{k=0}^{\infty} \beta_k \sin k \frac{2\pi(t-\tau)}{T} \qquad (89)$$

where A_k, B_k, α_k, and β_k are the Fourier coefficients. The limits of summation are shown as infinity. However, Dooge stated that truncation in hydrologic series to a finite number did not affect its accuracy materially. He further stated that the orthogonality of the Fourier series of rainfall excess and runoff provides simplicity in the solution of the linkage equations.

O'Donnell gave the linkage equations as

$$A_k = \frac{T}{2} (a_k \alpha_k - b_k \beta_k) \qquad (90)$$

and

$$B_k = \frac{T}{2} (a_k \alpha_k + b_k \beta_k) \qquad (91)$$

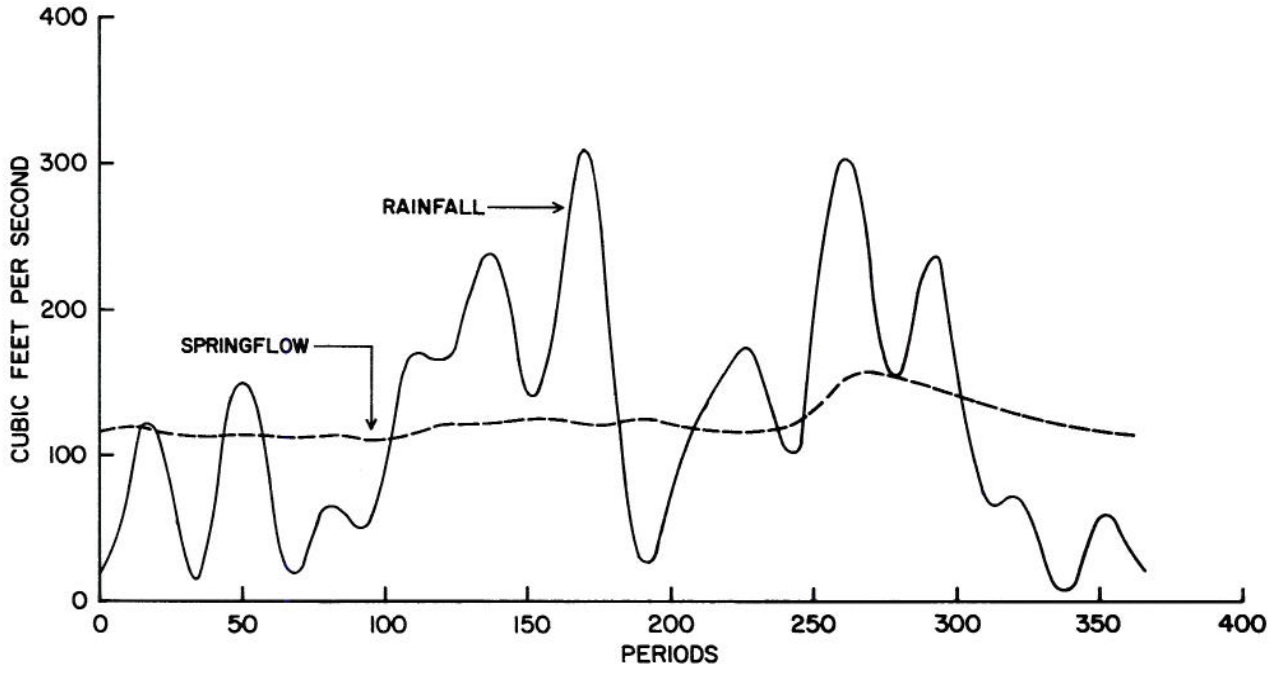

Figure 47. Fitted periodic component for rainfall and springflow for Goodenough Springs near Comstock, Texas.

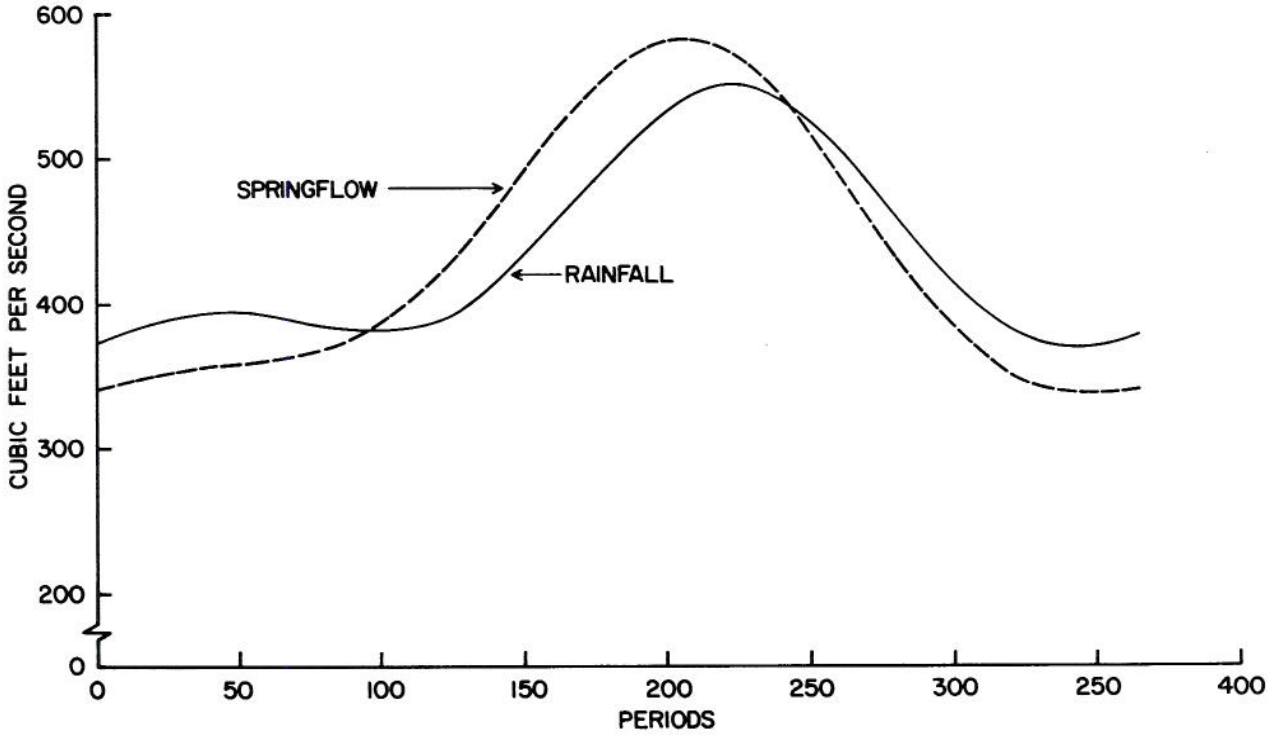

Figure 48. Fitted periodic component for rainfall and springflow for Big Springs near Van Buren, Missouri.

From Eqs. (90) and (91), the harmonic coefficients of the IUH can be determined by the relations

$$\alpha_k = \frac{2}{T} \frac{(a_k A_k + b_k B_k)}{a_k^2 + b_2^2} \qquad (92)$$

and

$$\beta_k = \frac{2}{T} \frac{(a_k A_k - b_k B_k)}{a_k^2 + b_k^2} \quad . \qquad (93)$$

The determination of α_k and β_k permit the determination of the ordinates of the IUH.

In order to determine the applicability of harmonic series to ground-water flow, the Fourier coefficients determined for rainfall and springflow for 1-day time series were used to determine the coefficients α and β in Eqs. (92) and (93). The IUH ordinates are shown in Figs. 49, 50, and 51 for Good-enough Springs, San Felipe Springs, and Big Springs, respectively. The conversion of rainfall to equivalent springflow, as mentioned earlier, provides a one-to-one comparison. Therefore, the IUH series have ordinate values of approximately unity as compared to an IUH from rainfall in inches and springflow in CFS. Although the surface runoff application of harmonic series was for individual storms, the application in the current ground-water study is shown for the mean daily flow series.

The harmonics are evident in the IUH series as shown in the figures. The range is quite small and only an exaggerated scale can show any deviation from unity. The harmonic IUH was determined for mean daily springflow rather than for selected hydrographs of karst aquifer rapid response, as was the determination by other methods. The relatively short periods of record and the highly variable rainfall precludes determination of the response function due to noise in the system.

b. Stochastic response function. The precipitation time series were analyzed in Chapter IV to determine the internal structure. The discussion and mathematical derivations in that chapter resulted in the description of the time series by Eq. (41). The rainfall time series was found to be nearly independent in time.

Springflow time series analysis in Chapter VI showed that mean daily discharge is highly dependent in time. As it was shown, the Markov I model provides only a first approximation for the series. The structure of the series was described by Eq. (69).

The convolution equation for the discrete functions can be written as

$$Y_{p,\tau} = \sum_{\tau=1}^{365} h_\tau X_{p,\tau}, \quad p = 1,2,\ldots,N \; . \qquad (94)$$

Substitution of Eqs. (41) and (69) for the respective components gives

$$e^{\mu_\tau} (r_1 \theta_{p,\tau-1} + \delta_{p,\tau}) = \sum_{\tau=1}^{365} h_\tau e^{\mu_\tau} \cdot \eta_{p,\tau}, \qquad (95)$$

$$p = 1,2,\ldots,N \; .$$

The duration of the transfer function as given by the limit of summation in Eq. (95) is necessary since the exponential was developed from daily data with $\Delta\tau$ equal to unity.

System identification from Eq. (95) represents a difficult mathematical manipulation. For system identification, the equation must be transformed from the time domain to the frequency domain for convenience of the solution. After the transfer function, h, is determined in the frequency domain, transformation back to the time domain will provide the transfer function for convolution with a stochastic input series.

The simplest method of determining the transfer function of Eq. (95) would be to use quantized data with forward substitution and determine the quantized ordinates. Since the system identification, as shown, is difficult to perform, and since it will be shown later that the total springflow simulation as a unit by discrete functions is very inaccurate, the method will not be pursued further.

5. Two-Parameter Gamma Function as System Transfer Function.

The two-parameter gamma function was proposed by Nash (22) as representative of the instantaneous unit hydrograph for surface runoff. The equation for the function was given in Chapter II as

$$q = \frac{1}{K\Gamma(n)} (t/k)^{(n-1)} e^{-t/k} \qquad (96)$$

where n is a dimensionless scale parameter, k is the shape parameter with dimensions of time, $\Gamma(n)$ is the gamma function with $\Gamma(n) = (n-1)$; for integer values of n, and K is the constant dependent upon the shape parameter, size of area, and runoff volume. Nash theorized that storm runoff hydrograph results from the equivalent of routing flow through linear reservoirs. The scale is dependent upon the dampening effect of the linear reservoirs, and thus the scale factor, n in Eq. (96) is representative of the number of linear reservoirs.

Since a ground-water system provides a dampening effect on the recharge, i.e., the response to recharge is not instantaneous, the gamma function should approximate the transfer function of the ground-water system. Although the aquifer system does provide a dampening, the springflow data indicate considerable increases in springflow from associated recharge. Based on a cursory examination of data, two linear reservoirs were thought to provide sufficient dampening.

Differentiating Eq. (96) with respect to time provides the determination of the slope of the hydrograph at any time, t. The slope is equal to zero at the hydrograph peak discharge, and the time to peak can be determined. For convenience, Eq. (96) can be rewritten as

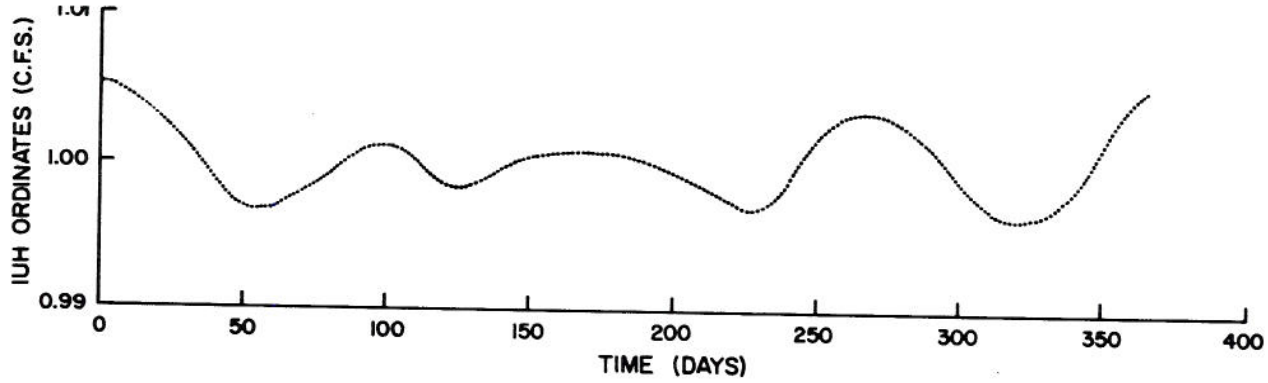

Figure 49. Harmonic series IUH with 8 harmonics, Goodenough Springs near Comstock, Texas.

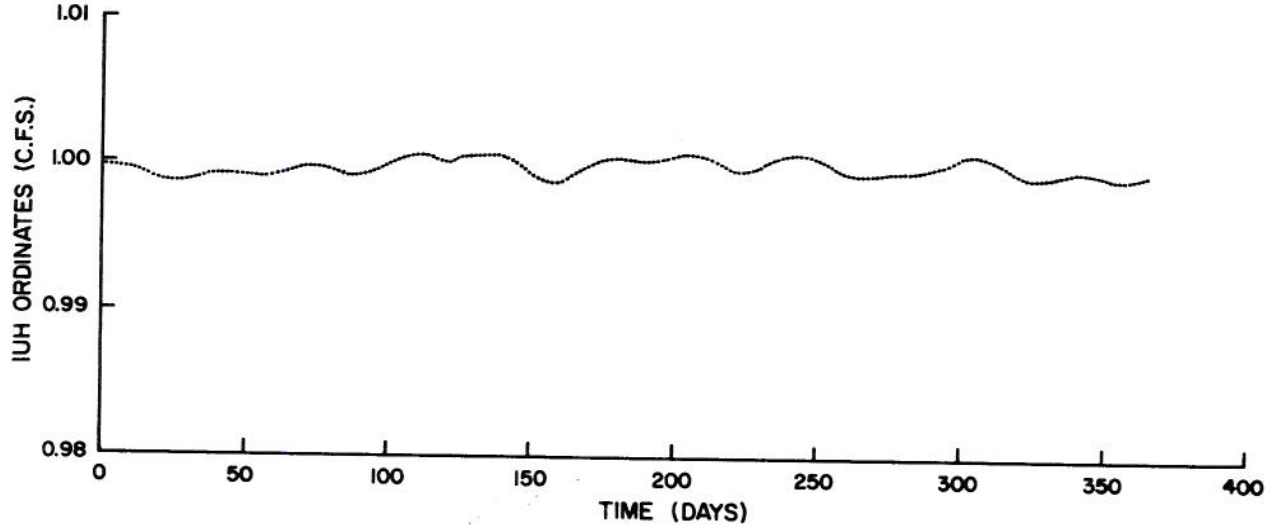

Figure 50. Harmonic series IUH with 12 harmonics, San Felipe Springs at Del Rio, Texas.

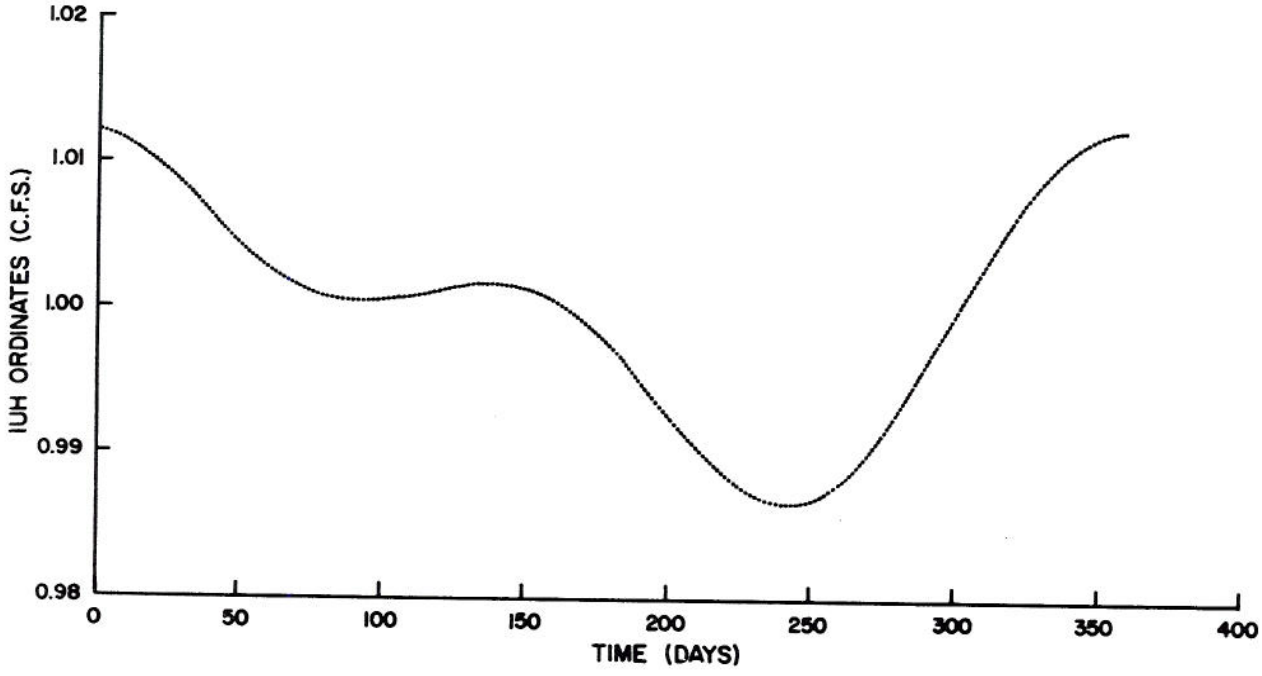

Figure 51. Harmonic series IUH with 2 harmonics, Big Springs near Van Buren, Missouri.

$$q = \frac{1}{K\, k^{(n-1)}\, \Gamma(n)}\, t^{(n-1)}\, e^{-t/k} \quad . \qquad (97)$$

Since K, k, and $\Gamma(n)$ are independent of t, Eq. (97) can be reduced further for differentiation purposes to

$$q = C\, t^{(n-1)}\, e^{-t/k} \quad . \qquad (98)$$

Differentiation with respect to time gives

$$\frac{dq}{dt} = 0 = C(n-1)\, t^{(n-2)}\, e^{-t/k} - Ct^{(n-1)}\, \frac{1}{k}\, e^{-t/k}. \qquad (99)$$

Dividing equation (99) by $C\, t^{(n-2)}\, e^{-t/k}$ results in

$$0 = (n-1) - \frac{t}{k} \qquad (100)$$

or

$$t = (n-1)k \quad , \qquad (101)$$

which, by definition is the time to peak. When n=2, a special case exists such that k is the time to peak.

Springflow discharge and recharge data were reviewed to select hydrographs resulting from rainfall for a single day. The selected data enabled the determination of time to peak, the k parameter in Eq. (96). the time to peak for all three springflow stations was two days. The determination of the two parameters left only the K-term to be evaluated.

The peak discharge rate was determined for each of the selected single input hydrographs for each station. The peak discharge rates were averaged for each station and the associated recharge was also averaged. The average peak discharge was divided by the average recharge to determine the unit peak discharge rate.

Values for unit peak discharge, n, and k were substituted into Eq. (96) with t = k and corresponding values of K were determined for each springflow station. The K values were determined to be 0.0148, 0.00194, and 0.0391 for Goodenough Springs, Big Springs, and San Felipe Springs, respectively.

It was stated earlier that the area contributing to springflow could not be determined. However, an estimate of area can be made by assuming no losses and that total rainfall is equivalent to total springflow. The average mean daily springflow is equivalent to the average daily rainfall for the period of record. In order to convert discharge in CFS to equivalent inches per day, dimensional analysis was made and the following relationship developed:

$$A = \frac{0.03719}{\bar{P}_d}\, \bar{q}_d \qquad (102)$$

where A is the area, square miles, $\bar{q}_d$ is the average mean daily discharge in CFS, and $\bar{p}_d$ is the average daily rainfall in inches per day. It is realized that the area determined by Eq. (102) is considerably less than actual. This is not important because it is used only as an indicator rather than a definite quantity. The areas determined by Eq. (102) for Goodenough Springs, Big Springs, and San Felipe Springs, are 128, 149, and 68 square miles, respectively.

The physical significance of differences between the previously determined K values can now be demonstrated. Fig. 52 shows the arithmetic relationship between K and the size of area. The least squares regression equation determined for the relationship is

$$K = 0.0735 - 0.000472\, A \qquad (103)$$

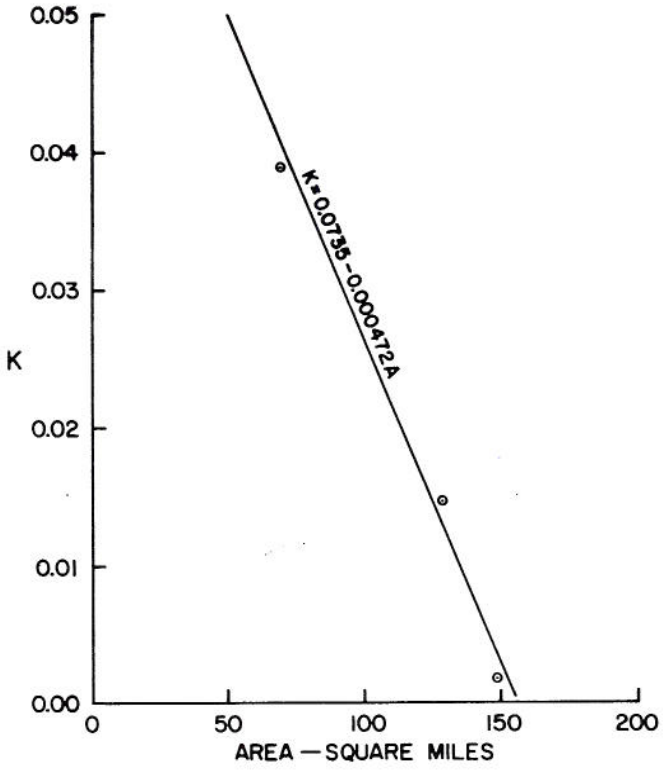

Figure 52. Relation between K in 2-parameter Γ-function and the springflow contributing area.

where A is the area in square miles. Using Eq. (103) to estimate K, the new K values were used to compute peak discharge by Eq. (96). Table 6 shows the comparison of peak discharge per inch of recharge determined by Eq. (96) with that determined by averaging of selected hydrograph peaks. The data in Table 6 compare well, but the effect of the change cannot be determined until springflow simulation is made.

Table 6. Comparison of hydrograph peak discharge rates with rates determined from Γ-function.

Springflow Station	K Value		Peak Discharge	
	Hydrograph	Figure 51	Hydrograph	Γ-function
Goodenough Springs	0.0148	0. 131	25	28
Big Springs	.00194	.00217	190	170
San Felipe Springs	.0391	.0413	9.4	8.9

CHAPTER VIII

SPRINGFLOW SIMULATION

The solving of systems identification problems in the preceding chapter leads to testing of hypotheses and assumptions, i.e., the testing of systems transfer functions. A most appropriate test is that of using rainfall data and predicting the resulting springflow. The test itself consists of a comparison of the predicted springflow with observed springflow to determine the goodness of fit.

An unbiased test of prediction techniques is one in which the test data were not used in the development procedure. This is particularly true where the total data set is used in development. If long periods of record are available, such as the 20 years for Goodenough Springs and Big Springs, and only selected portions of the record are used in the development procedure, a test using all the same data is not completely biased. In the case where all the 20-year period of record was used in development, such as the harmonic series, testing the same data is considerably biased. However, these are the only data available for the three springflow stations studied and the data are used in the test.

Several methods of system identification were presented in Chapter VII, and simulation is made for each method. Since the study is concerned with prediction techniques, a comparison of methods is made. A measure of the goodness of fit between observed and predicted springflow for comparison purposes is the computed chi-square. The computation is made by the equation

$$\chi^2 = \sum_{j=1}^{N} \frac{[q(j)_m - q(j)_p]^2}{q(j)_p} \qquad (104)$$

where $q(j)_m$ is the measured mean daily discharge of the j-th day in CFS, $q(j)_p$ is the predicted mean daily discharge of the j-th day in CFS, and N is the total number of days of record.

Such a test not only compares the observed and computed recharge-response hydrographs, but also compares observed and computed recession. The record was not separated as to recharge and recession for testing purposes. However, the same recession prediction was used with each hydrograph prediction technique, i.e.,

$$q_t = q_o e^{-ct} .$$

By using the same recession prediction irrespective of hydrograph prediction technique, the chi-square test provides a good comparison of hydrograph technique.

The prediction of springflow by transfer functions developed from total flow such as the harmonic function and stochastic function do not utilize the recession prediction of Eq. (52). That is, total springflow was used in the development of the procedure irrespective of recharge period and recession period. In this case, the computed chi-square compares both recharge-response and recession.

1. Comparison of Simulation with Recharge and Rainfall as Input. Derivation of the serpentine curve for estimating recharge from rainfall developed in Chapter V was not tested for accuracy. The only way to test the appropriateness is by simulation using impulse response functions derived from rainfall and those derived from recharge. Such a comparison was made for Goodenough Springs and Big Springs. As was stated in Chapter VII, impulse response functions derived for San Felipe Springs all contained unrealistic negative ordinates. The comparison of simulation could not be made for rainfall and recharge as input for San Felipe Springs.

Comparison of the results of simulation for rainfall and/or recharge as input is shown in Table 7. There is little difference between chi-square for the two inputs for Goodenough Springs and Big Springs. Realistic response functions could not be determined for San Felipe Springs. The short period of record did not afford enough hydrographs for analysis. The selected hydrographs were apparently not representative and input errors or output errors overshadowed the ability of the procedures to handle errors.

The method of recharge estimation derived obviously results in better accuracy of springflow simulation. This should not be misconstrued to mean that the rainfall-recharge relation is highly accurate. Only one conclusion can be drawn: the method of estimating recharge from rainfall provides a better estimate of input than does total rainfall. Optimization of the rainfall-recharge relation should be considered.

2. Impulse Function Determined by Multiple Regression. It was shown that recharge as an estimate of system input resulted in a more accurate prediction of springflow than rainfall as input. Therefore, recharge was used in simulation with the response function derived by multiple regression techniques using function angle points with linear interpolation. The few hydrographs available from the short record for San Felipe Springs again resulted in unrealistic negative ordinates and simulation was omitted for that station.

The data in Table 7 show that the chi-square for Goodenough Springs is only slightly less than for the optimized H-function when using recharge as estimated input. The computed chi-square for Big Springs using the transfer function derived by multiple regression techniques is almost double that for simulation using the optimized H-function with estimated recharge as input. The averaging of ordinates from the multiple regression determination may have been biased by selection of functions for averaging. The averaging process creates some subjectivity to any method. Perhaps a better fit of the measured data would have resulted from more selective screening of the solutions for averaging.

The method of treating errors by the multiple regression technique is probably the main reason for difference in results of the two prediction methods. The differences are small and are not significant. In view of the comparative results of the two methods of

Table 7. Computed chi-square for simulation of springflow by the derived impulse functions.

Impulse Function	Input	χ^2 Goodenough Springs	San Felipe Springs	Big Springs
H-optimized Eq. (14)	Rainfall	2.86×10^6	1/	2.36×10^6
	Recharge	5.89×10^5	1/	5.10×10^5
U-multiple regression Eq. (86)	Recharge	4.43×10^5	1/	8.33×10^5
Harmonic IUH Eq. (89)	Rainfall	4.70×10^{10}	6.81×10^9	1.52×10^{11}
2-Parameter Γ-fct. Eq. (96)	Recharge 2/	3.26×10^5	1.47×10^5	4.31×10^5
	Recharge 3/	3.00×10^5	1.48×10^5	3.69×10^5

1/ Realistic function could not be determined from short record.

2/ Simulation using initial determination of K from Eq. (96).

3/ Simulation using final determination of K from Eq. (103).

system identification, the selection of method is largely dependent upon ease of computation. There is little difference in degree of difficulty of computation when using a digital computer.

In the previous chapter on system identification, it was stated that the appropriateness of a method for ground-water application would be determined. Actually, both methods of system identification and simulation are applicable for recharge and response of ground-water systems. The large quantitative values of chi-square cannot be considered as a reason for rejecting the application of the methods of surface water systems to ground-water systems. It should be remembered that the 20-year period of simulation contains 7,300 daily values. A small difference between measured and predicted springflow for each day can accumulate as a large chi-square for the total period.

3. Harmonic Function. Total rainfall rather than recharge was used as input for the harmonic series development. After finding that estimated recharge resulted in more accurate simulation of springflow, recomputation of the input harmonic series was not made.

Relative accuracy of springflow simulation by the harmonic function is shown in Table 7.

The largest chi-square resulted for simulation using the harmonic IUH. This can be attributed mainly to two factors: (1) harmonics in rainfall are not significant but were imposed on the series based on harmonics in springflow, and (2) the harmonic functions for rainfall and springflow are averaged over the n-years of record, but convolution of the IUH is with actual daily values. As shown in Figs. 49, 50, and 51 in the previous chapter, by converting rainfall to equivalent springflow in CFS based on the means, the IUH is a harmonic series oscillating around unity. The one-to-one correspondence of rainfall and springflow causes the mean of the IUH to be unity.

Convolution of the 365-ordinate harmonic IUH does not provide natural recession of springflow during periods of no rainfall. The method, as used, simulates total springflow, i.e., sustained recession and recharge in a single step. This indicates that a one-step simulation procedure is not appropriate. Instead, the sustained recession in the absence of recharge should be simulated and superimposed with simulated hydrographs resulting from recharge as for the previous methods. Based on this reasoning, any model developed for total springflow, such as the hypothesized stochastic model of section 4b, Chapter VII, will not result in accurate simulation.

4. Two-Parameter Gamma Function. The two-parameter gamma function with n=2 was used for springflow simulation for the three stations studied. Two simulation runs were made for each station. The first simulation run included the initial estimate of K from estimated maximum discharge rate for unit recharge. After the initial determination, the K values were used in the area to K relation of Eq. (103). The adjustment of the K's by the equation could have had an adverse effect on accuracy of simulation. Therefore, a second simulation run was made to determine the effect of the adjustment of K.

Results of simulation using the two-parameter gamma function as the unit hydrograph are shown in Table 7. The chi-square for the initial run is listed first. As shown in the table, the second run had a smaller chi-square than the first run for Goodenough Springs and Big Springs. The difference for San Felipe Springs is reversed but not significant. The comparative results indicate there is a real relation between K and area. The relation shown by Eq. (103) can hardly be expected to be the actual relation when only three data points were available for the determination.

Another important feature of the results shown in Table 7 is the comparison of chi-square for simulation by the various functions with that for the two-parameter gamma function. Both simulation runs with the gamma function resulted in better accuracy than all other system transfer functions. The appropriateness of the two-parameter gamma function as an instantaneous unit hydrograph in ground-water systems is demonstrated by comparative simulations.

It is impossible to show graphical comparisons of measured and simulated discharge values or tabulations of the comparison values. A randomly selected period of 140 days for Goodenough Springs was taken from the total record to give the reader a view of relative results. The comparison is shown in Fig. 53. The period selected includes days with observed rainfall and days with zero rainfall. It should be remembered that observed rainfall may represent small areal coverage with little actual effect of recharge and resulting springflow. Likewise, nonobservance of rainfall may not mean that significant rainfall did not occur over an extensive portion of the recharge area. The result in the first case is an overestimate of springflow and in the second case an underestimate of springflow results. A view of Fig. 53 gives the reader an indication of why such large chi-square values were computed for 20 years of simulation as shown in Table 7.

A more meaningful comparison would be that for an individual hydrograph such that the ability of the method could be viewed. A recharge event was selected at random from the period of record for Goodenough Springs and Big Springs. The selected records contained more than one day of rainfall at each springflow station. The H-function, U-function, and Γ-function were used to simulate the springflow record from rainfall. Figs. 54 and 55 show the results of simulation for Goodenough Springs and Big Springs, respectively. Fig. 54 shows that the Γ-function more closely approximates the observed hydrograph than either the H-function or U-function. The delayed recession following the rapid response sumulation with the H-function and Γ-function flattens abruptly. A similar flattening occurred in the observed discharge, but it occurred later in time than the computed break point. The computed chi-square values for the predicted hydrographs were 1.90×10^3 for the H-function, 1.75×10^4 for the U-function, and 4.35×10^2 for the Γ-function.

Fig. 55 shows the same general results of prediction for Big Springs as that for Goodenough Springs. The Γ-function for Big Springs has a time base of sufficient length to prevent an abrupt change in shape from the Γ-function to the pure recession flow. The computed chi-square for the predicted hydrographs are 2.80×10^3, 5.14×10^3, and 5.77×10^2 for the H-function, U-function, and Γ-function, respectively.

The results of simulation shown in Figs. 54 and 55 are far from exact duplication of measured discharge. A much better fit of the data is desired, certainly. However, it must be remembered that input is represented by a single rain gage for an area of 128 and 149 square miles in Figs. 54 and 55, respectively (both are admittedly low), and aquifer recharge is estimated from the rainfall data. With these vagaries in mind, the two-parameter gamma function provides a reasonable estimate of springflow.

Methods heretofore applied only to surface water systems have been shown to be applicable to the karst ground-water systems by the current study. It has been demonstrated that somewhat different manipulations of the various techniques are necessary for application in ground-water systems. The two-parameter gamma function has been used extensively to represent the IU in surface water systems but has not been applied to aquifer systems. The measure of fit for each simulation procedure showed that the IUH is entirely satisfactory and resulted in the best accuracy.

It was also shown that rainfall can be adjusted by a serpentine curve to give an estimate of groundwater recharge. The resulting recharge is a more accurate input for springflow prediction than unadjusted rainfall.

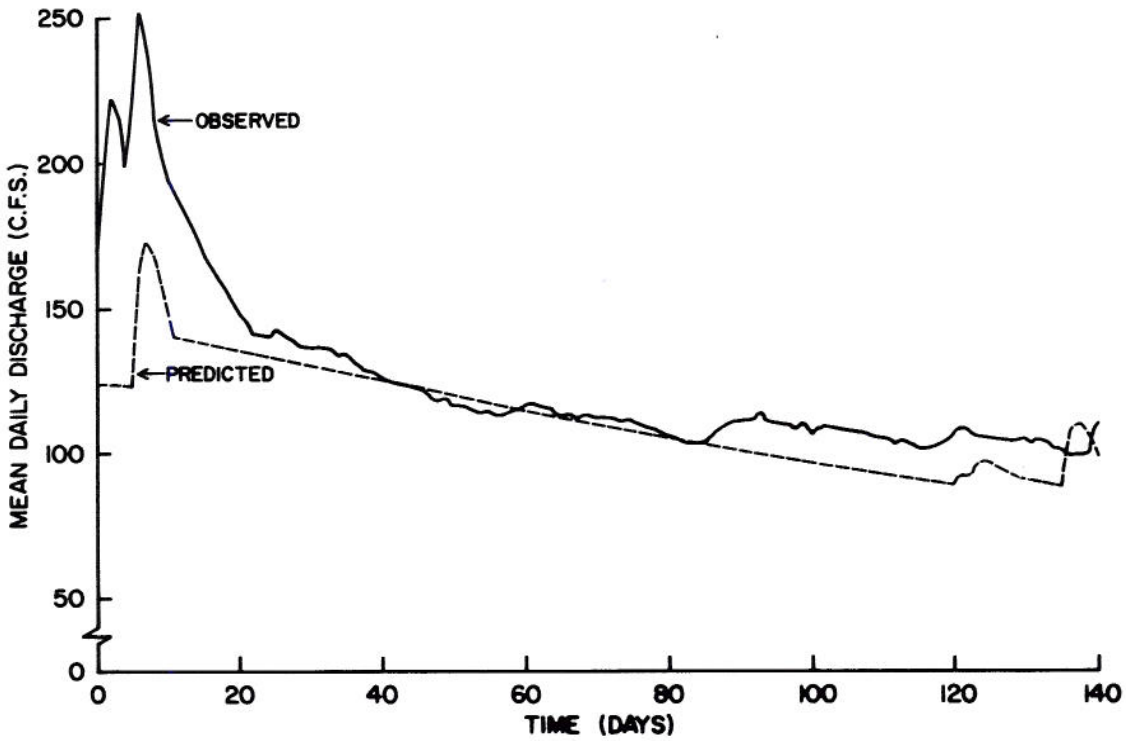

Figure 53. Observed and predicted springflow using 2-parameter Γ-function for selected period, Goodenough Springs near Comstock, Texas.

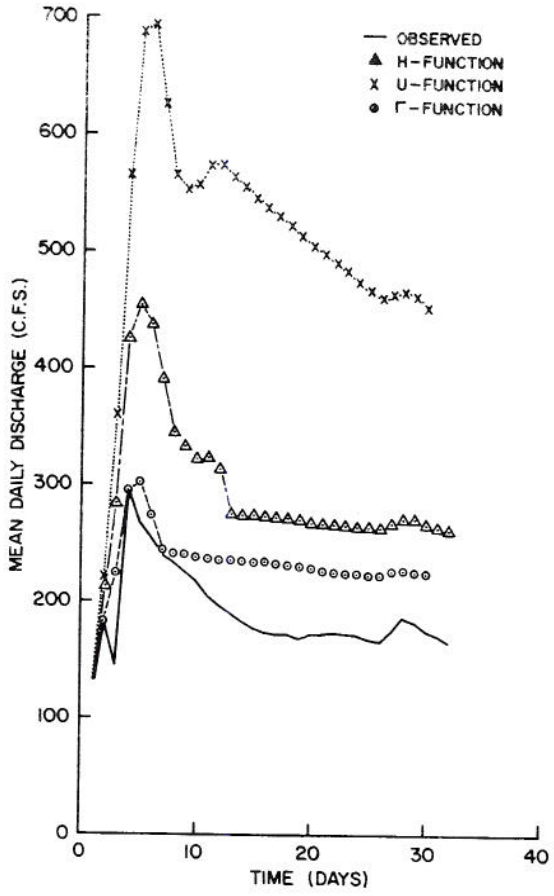

Figure 54. Comparison of observed and computed spring-flow, Goodenough Springs near Comstock, Texas.

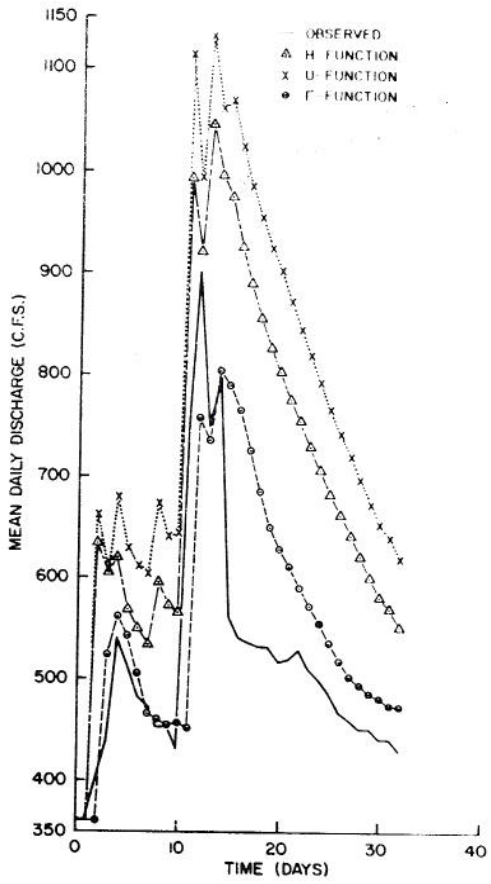

Figure 55. Comparison of observed and computed spring-flow, Big Springs near Van Buren, Missouri.

CHAPTER IX

SUMMARY AND RECOMMENDATIONS

Analyses of springflow data from limestone karst aquifers have revealed characterizing features. Recession analysis showed that karst ground-water systems have rapid and delayed response to recharge. The rapid response results from infiltrated water moving rapidly through large drainable pores, caverns, and channels. Delayed response results from water movement through the limestone mass. Recession plottings indicate considerable difference between aquifer systems in the same limestone and between different limestone formations. Limestone ground-water discharge may vary with depth of water in the aquifer system such that a single constant will not adequately describe the recession. An average recession constant cannot be used to represent limestone aquifers in general.

Time series analysis of daily rainfall and springflow data show that rainfall is a nearly time-independent variable and the limestone aquifer system acts as a filter that results in a highly time-dependent variable. Cross-correlation coefficients of rainfall and springflow indicate a low degree of dependence of the two variables in time. The low values result from the many zero values of rainfall, and nonzero values of rainfall correlated with both the rapid and delayed response of the aquifers. Daily rainfall time series did not show significant harmonics due to noise. The springflow time series contain significant periodicities. As much as 95 percent of the variance of mean daily springflow about the general mean can be explained by as few as two harmonics.

Inadequate rainfall station coverage of a study basin was shown to cause difficulties in estimating system input. A serpentine curve was found to approximate a hypothesized rainfall-recharge relation. The relation assumed a maximum of 80 percent recharge from a 3-inch rainfall. Rainfall less than 3 inches seldom has been found to produce surface runoff from large watersheds in Agricultural Research Service studies on a limestone area in Texas. Rainfall amounts greater than 3 inches generally result in some surface runoff. As rainfall increases over 3 inches, the percent recharge decreases, i.e., percent occurring as surface runoff increases.

The karst aquifer system was assumed to be represented by a linear, time-invariant system of finite memory with a lumped input. Based on these assumptions, several methods of system identification, proven satisfactory in surface-water hydrology, were applied to these karst ground-water systems. Since springflow continued throughout the period of record, sustained recession was extrapolated during periods of recharge to provide open-ended hydrographs for analysis.

Open-ended hydrograph ordinates were related to rainfall or recharge by: (a) optimized response function determined from autocorrelation functions of rainfall, or recharge, and cross correlation functions of rainfall and springflow, and (b) response function determined at angle points by multiple regression techniques with linear interpolation between angle points. A 6-year period of record was not sufficient for determination of impulse response functions.

The two-parameter gamma function was applied as an IUH to convolute with recharge for springflow determination. Hydrograph analysis enabled estimation of the parameters from which systems constants could be determined. Further estimation of springflow contributing area enabled determination of a functional relation between area and system constant. Use of the gamma function permits use of short periods of record.

Harmonic analysis was made to determine the IUH between total rainfall and total springflow. The number of significant harmonics in springflow was imposed in the rainfall series for system identification. Noise in the system prevented the determination of a valid IUH.

Springflow was simulated by convolution of rainfall and by convolution of estimated recharge with the optimized response function (H-function). Computed chi-square was used as a relative measure of fit for the two simulation procedures. Recharge as input gave the best fit with observed springflow.

Springflow simulation was made by convoluting input with (a) H-function, (b) U-function, (c) Γ-function, and (d) harmonic function. Chi-square was computed as a measure of fit between simulated and observed springflow. The best fit was obtained with the Γ-function and the poorest fit occurred with the harmonic function. There was little difference between the results obtained with the H-function and U-function.

The harmonic IUH represents the least subjectively determined transfer function of the methods studied. The method does not require hydrograph selection and recession extrapolation as do the other methods of system identification. A disadvantage is the length of record required for determination of the harmonic IUH. However, single-step simulation processes, such as the harmonic IUH and stochastic model, are not suitable for simulation of springflow.

Future studies should be concentrated on refining the rainfall-recharge relationship. Surface runoff data for limestone areas where adequate rainfall data are available should be analyzed for use in the refinement procedure. The effect of errors in input data on system response functions has been shown, and the effect of refinement of recharge determination can readily be seen.

An exhaustive search of U. S. and foreign data, beyond the realm of this study, should be made for other "pure springflow" stations in limestone karst. Additional stations should be studied in order to better establish the relation between contributing area and the K value of the gamma function.

Data for time intervals less than 1 day, where available, should be analyzed to provide better estimation of gamma function parameters. Due to the rapid response of limestone aquifers to recharge, time intervals of 12 hours and 6 hours should be investigated for improvement of the parameter determination.

A long-term research project should be developed to provide instrumentation for adequate rainfall, surface runoff, and springflow data collection in a limestone karst region. Such a study should be established in a humid area to provide the most information in the shortest time.

LITERATURE CITED

[1] Amorocho, J. "Measures of the Linearity of Hydrologic Systems." Journal Geophysical Research, Vol. 68, No. 8, 1963, pp. 2237-2249.

[2] Amorocho, J. and Orlob, G. T. "Nonlinear Analysis of Hydrologic Systems." Water Resources Center, University of California, Contribution No. 40, Berkeley, California, 1961.

[3] Barnes, B. S. "The Structure of Discharge-Recession Curves." Transactions American Geophysical Union, Vol. 20, 1939, pp. 721-725.

[4] Becker A. "Threshold Considerations and their General Importance for Hydrologic Systems Investigation." Proceedings, The International Hydrology Symposium, Vol. 1, Fort Collins, Colorado, Sept. 6-8, 1967.

[5] Blank, H. R., Knisel, W. G., and Baird, R. W. "Geology and Groundwater Studies in Part of the Edwards Plateau of Texas Including Sutton and Adjacent Counties." U. S. Department of Agriculture, Agricultural Research Service, ARS 41-103, Beltsville, Maryland, 1966, 41 pp.

[6] Cheng, D. K. "Analysis of Linear Systems." Addison-Wesley Publishing Company, Reading, Massachusetts, 1959.

[7] Dawdy, D. R. and Matalas, N. C. "Statistical and Probability Analysis of Hydrologic Data." Handbook of Applied Hydrology, Edited by V. T. Chow. McGraw-Hill Book Company, New York, Section 8-III, 1964, pp. 8:68-8:90.

[8] DeCoursey, D. G. "A Runoff Hydrograph Equation," U. S. Department of Agriculture, Agricultural Research Service, ARS 41-116, Beltsville, Maryland, 1966, 23 pp.

[9] Dooge, J. C. I. "A General Theory of the Unit Hydrograph." Journal Geophysical Research, Vol. 64, No. 2, 1959, pp. 241-256.

[10] Dooge, J. C. I. "The Routing of Groundwater Recharge Through Typical Elements of Linear Storage." International Association of Scientific Hydrology, Publication No. 52, Helsinki, Finland, 1960, pp. 286-300.

[11] Downer, R. N. "The Effect of the Time Distribution of Rainfall Intensities on Small Watershed Floods." Technical Report CER67-68RND14, Civil Engineering Department, Colorado State University, Fort Collins, Colorado, September 1967, 117 pp.

[12] Eagleson, P. S., Mejia, R. R., and March, F. "Computation of Optimum Realizable Unit Hydrograph." Water Resources Research, Vol. 2, No. 4, 1966, pp. 755-764.

[13] Gass, S. I. "Linear Programming." McGraw-Hill Book Company, Inc., New York, 1964, 280 pp.

[14] Green, M. G. "Artificial Recharge to the Edwards Limestone Aquifer in South Texas." Proceedings of the Dubrovnik Symposium, Hydrology of Fractured Rocks, Vol. II, International Association of Scientific Hydrology, Publication No. 74, 1965, pp. 465-481.

[15] Gupta, V. "Cross-Spectral Analysis of Precipitation and Streamflow Data Systems." Paper No. H-5, Section of Hydrology, American Geophysical Union, National Fall Meeting, San Francisco, California, December 7-10, 1970.

[16] Holt, C. L. R., Jr. "Geology and Ground-Water Resources of Medina County, Texas." Texas Water Development Board, Bulletin B5601, 1956, 289 pp.

[17] Knisel, W. G., Jr. "Baseflow Recession Analysis for Comparison of Drainage Basins and Geology," Journal of Geophysical Research, Vol. 68, No. 12, 1963, pp. 3649-3653.

[18] Knisel, W. G., Jr. "Groundwater Studies in the Edwards Plateau of Texas." U. S. Department of Agriculture, Agricultural Research Service, ARS 41-100, Beltsville, Maryland, 1956, 12 pp.

[19] Knisel, W. G., Jr., and Baird, R. W. "Field and Laboratory Experimental Approaches (panel)." Annual Meeting of the American Society of Agricultural Engineers, Paper No. 68-215B, Logan, Utah, June 1968, 15 pp.

[20] Kraijenhoff van de Leur, D. A. "A Study of Non-Steady Groundwater Flow with Special Reference to a Reservoir Coefficient." De Ingenieur, No. 19 1958, pp. B87-B94.

[21] Linsley, R. K., Jr., Kohler, M. A., and Paulhus, J. L. H. "Hydrology for Engineers." McGraw-Hill Book Company, New York, 1958, 340 pp.

[22] Nash, J. E. "The Form of the Instantaneous Unit Hydrograph." International Association of Scientific Hydrology, Proceedings General Assembly of Toronto, Vol. 3, 1957, pp. 114-121.

[23] O'Donnell, T. "Instantaneous Unit Hydrograph Derivation by Harmonic Analysis." International Association of Scientific Hydrology, Publication No. 57, 1960, pp. 546-557.

[24] Quimpo, R. G. "Stochastic Model of Daily River Flow Sequences." Colorado State University, Hydrology Paper No. 18, February 1967, 30 pp.

[25] Sherman, L. K. "Streamflow from Rainfall by the Unit-Graph Method." Engineering News-Record, Vol. 108, 1932, pp. 501-505.

[26] Snyder, W. M. "Hydrograph Analyses by the Method of Least Squares." Proceedings American Society of Civil Engineers, Vol. 81, Separate No. 793, 1955, pp. 1-25.

[27] Snyder, W. M. "Subsurface Implications from Surface Hydrograph Analysis. Proceedings, Second Seepage Symposium, Phoenix, Arizona, U.S. Department of Agriculture, Agricultural Research Service, ARS 41-147, March 25-27, 1968, pp. 35-45.

[28] Snyder, W. M., Mills, W. C., and Stephens, J. C. "A Method of Derivation of Nonconstant Watershed Response Functions." Water Resources Research, Vol. 6, No. 1, 1970, pp. 261-274.

[29] Stringfield, V. T. and LeGrande, H. B. "Hydrology of Carbonate Rock Terrandes--A Review with Spe-

cial Reference to the United States." Journal of Hydrology, Vol. 8, 1969, pp. 349-417.

[30] Thornbury, W. D. "Principles of Geomorphology." John Wiley and Sons. New York, 1959, 336 pp.

[31] Todd, D. K. "Ground Water Hydrology." John Wiley and Sons, New York, 1959, 336 pp.

[32] Todorovic, P. and Yevjevich, V. M. "Stochastic Processes in Precipitation." Colorado State University, Hydrology Paper No. 35, September 1969, 61 pp.

[33] United States Department of Agriculture, Soil Conservation Service. "National Engineering Handbook," Section 4, Hydrology, Part 1, Watershed Planning, U. S. Government Printing Office, 1964.

[34] United States Department of Commerce, Weather Bureau. "Climatological Data, Texas," Asheville, North Carolina, available from 1946 through 1967.

[35] United States Department of Commerce, Weather Bureau. "Climatological Data, Missouri." Asheville, North Carolina, available from 1945 through 1966.

[36] United States Department of Interior, Geological Survey. "Lower Mississippi River Basins." Water Supply Paper, Part 7, U. S. Government Printing Office, Washington, D. C., available from 1945 through 1966.

[37] United States Department of State, International Boundary and Water Commission, United States and Mexico. "Flow of the Rio Grande and Related Data." Water Bulletin Numbers 16 through 37, available from 1946 through 1967, El Paso, Texas

[38] Wiener, N. "The Interpolation, Extrapolation and Smoothing of Stationary Time Series." John Wiley and Sons, Inc., New York, 1949, 163 pp.

[39] Williams, J. R. "Runoff Hydrographs from Small Texas Blacklands Watersheds." U. S. Department of Agriculture, Agricultural Research Service, ARS 41-143, Beltsville, Maryland, 1968, 24 pp.

[40] Yevjevich, V. M. "Analytical Integration of the Differential Equation for Water Storage." Journal of Research of the National Bureau of Standards--B, Mathematics and Mathematical Physics, Vol. 63B, No. 1, 1959, pp. 43-52.

KEY WORDS: Response of karst aquifers, karst aquifers, karst hydrology, unit hydrograph of karst aquifers.

ABSTRACT: Systems analysis was applied to determine system identification for springflow simulation. Convolution transfer functions were estimated by four methods: (1) optimization by the Wiener-Hopf equation, (2) optimization by multiple regression techniques, (3) harmonic series for total springflow, and (4) two-parameter gamma function. Recharge-response hydrographs, above extrapolated recessions, were used with methods 1,2, and 4. Average convolution transfer functions were determined from the Wiener-Hopf equations and from multiple regression techniques with estimated recharge as input. Parameters of the gamma function were estimated from hydrograph analysis. Aquifer constants were determined for each springflow station using estimated parameters and hydrograph peak discharges. One-to-one correspondence of rainfall and springflow enabled determination of

KEY WORDS: Response of karst aquifers, karst aquifers, karst hydrology, unit hydrograph of karst aquifers.

ABSTRACT: Systems analysis was applied to determine system identification for springflow simulation. Convolution transfer functions were estimated by four methods: (1) optimization by the Wiener-Hopf equation, (2) optimization by multiple regression techniques, (3) harmonic series for total springflow, and (4) two-parameter gamma function. Recharge-response hydrographs, above extrapolated recessions, were used with methods 1,2, and 4. Average convolution transfer functions were determined from the Wiener-Hopf equations and from multiple regression techniques with estimated recharge as input. Parameters of the gamma function were estimated from hydrograph analysis. Aquifer constants were determined for each springflow station using estimated parameters and hydrograph peak discharges. One-to-one correspondence of rainfall and springflow enabled determination of

KEY WORDS: Response of karst aquifers, karst aquifers, karst hydrology, unit hydrograph of karst aquifers.

ABSTRACT: Systems analysis was applied to determine system identification for springflow simulation. Convolution transfer functions were estimated by four methods: (1) optimization by the Wiener-Hopf equation, (2) optimization by multiple regression techniques, (3) harmonic series for total springflow, and (4) two-parameter gamma function. Recharge-response hydrographs, above extrapolated recessions, were used with methods 1,2, and 4. Average convolution transfer functions were determined from the Wiener-Hopf equations and from multiple regression techniques with estimated recharge as input. Parameters of the gamma function were estimated from hydrograph analysis. Aquifer constants were determined for each springflow station using estimated parameters and hydrograph peak discharges. One-to-one correspondence of rainfall and springflow enabled determination of

KEY WORDS: Response of karst aquifers, karst aquifers, karst hydrology, unit hydrograph of karst aquifers.

ABSTRACT: Systems analysis was applied to determine system identification for springflow simulation. Convolution transfer functions were estimated by four methods: (1) optimization by the Wiener-Hopf equation, (2) optimization by multiple regression techniques, (3) harmonic series for total springflow, and (4) two-parameter gamma function. Recharge-response hydrographs, above extrapolated recessions, were used with methods 1,2, and 4. Average convolution transfer functions were determined from the Wiener-Hopf equations and from multiple regression techniques with estimated recharge as input. Parameters of the gamma function were estimated from hydrograph analysis. Aquifer constants were determined for each springflow station using estimated parameters and hydrograph peak discharges. One-to-one correspondence of rainfall and springflow enabled determination of

springflow contributing area. A linear relation was developed between size of area and aquifer constant.

Springflow simulation was made with convolution transfer functions determined for rainfall and for recharge using the optimized Wiener-Hopf equation. The chi-square test of goodness of fit was made to determine that recharge which as input gave the better results.

The two-parameter gamma function with estimated recharge provided the best results of simulation as determined by the computed chi-square. The harmonic function was the least accurate of the simulation procedures.

Response of Karst Aquifers to Recharge
Walter G. Knisel
Hydrology Paper #60
Colorado State University

springflow contributing area. A linear relation was developed between size of area and aquifer constant.

Springflow simulation was made with convolution transfer functions determined for rainfall and for recharge using the optimized Wiener-Hopf equation. The chi-square test of goodness of fit was made to determine that recharge which as input gave the better results.

The two-parameter gamma function with estimated recharge provided the best results of simulation as determined by the computed chi-square. The harmonic function was the least accurate of the simulation procedures.

Response of Karst Aquifers to Recharge
Walter G. Knisel
Hydrology Paper #60
Colorado State University

springflow contributing area. A linear relation was developed between size of area and aquifer constant.

Springflow simulation was made with convolution transfer functions determined for rainfall and for recharge using the optimized Wiener-Hopf equation. The chi-square test of goodness of fit was made to determine that recharge which as input gave the better results.

The two-parameter gamma function with estimated recharge provided the best results of simulation as determined by the computed chi-square. The harmonic function was the least accurate of the simulation procedures.

Response of Karst Aquifers to Recharge
Walter G. Knisel
Hydrology Paper #60
Colorado State University

springflow contributing area. A linear relation was developed between size of area and aquifer constant.

Springflow simulation was made with convolution transfer functions determined for rainfall and for recharge using the optimized Wiener-Hopf equation. The chi-square test of goodness of fit was made to determine that recharge which as input gave the better results.

The two-parameter gamma function with estimated recharge provided the best results of simulation as determined by the computed chi-square. The harmonic function was the least accurate of the simulation procedures.

Response of Karst Aquifers to Recharge
Walter G. Knisel
Hydrology Paper #60
Colorado State University

LIST OF PREVIOUS 25 PAPERS

No. 35 Stochastic Process of Precipitation, by P. Todorovic and V. Yevjevich, September 1969.

No. 36 Suitability of the Upper Colorado River Basin for Precipitation Management, by Hiroshi Nakamichi and H. J. Morel-Seytoux, October 1969.

No. 37 Regional Discrimination of Change in Runoff, by Viboon Nimmanit and Hubert J. Morel-Seytoux, November 1969.

No. 38 Evaluation of the Effect of Impoundment on Water Quality in Cheney Reservoir, by J.C. Ward and S. Karaki, March 1970.

No. 39 The Kinematic Cascade as a Hydrologic Model, by David F. Kibler and David A. Woolhiser, February 1970.

No. 40 Application of Run-Lengths to Hydrologic Series, by Jaime Saldarriaga and Vujica Yevjevich, April 1970.

No. 41 Numerical Simulation of Dispersion in Groundwater Aquifers, by Donald Lee Reddell and Daniel K. Sunada, June 1970.

No. 42 Theoretical Probability Distribution for Flood Peaks, by Emir Zelenhasic, December 1970.

No. 43 Flood Routing Through Storm Drains, Part I, Solution of Problems of Unsteady Free Surface Flow in a Storm Drain, by V. Yevjevich and A. H. Barnes, November 1970.

No. 44 Flood Routing Through Storm Drains, Part II, Physical Facilities and Experiments, by V. Yevjevich and A. H. Barnes, November 1970.

No. 45 Flood Routing Through Storm Drains, Part III, Evaluation of Geometric and Hydraulic Parameters, by V. Yevjevich and A. H. Barnes, November 1970.

No. 46 Flood Routing Through Storm Drains, Part IV, Numerical Computer Methods of Solution, by V. Yevjevich and A. H. Barnes, November 1970.

No. 47 Mathematical Simulation of Infiltrating Watersheds, by Roger E. Smith and David A. Woolhiser, January 1971.

No. 48 Models for Subsurface Drainage, by W. E. Hedstrom, A. T. Corey and H. R. Duke, February 1971.

No. 49 Infiltration Affected by Flow of Air, by David B. McWhorter, May 1971.

No. 50 Probabilities of Observed Droughts, by Jaime Millan and Vujica Yevich, June 1971.

No. 51 Amplification Criterion of Gradually Varied, Single Peaked Waves, by John Peter Jolly and Vujica Yevjevich, December 1971.

No. 52 Stochastic Structure of Water Use Time Series, by Jose D. Salas-La Cruz and Vujica Yevjevich, June 1972.

No. 53 Agricultural Response to Hydrologic Drought, by V. J. Bidwell, July 1972.

No. 54 Loss of Information by Discretizing Hydrologic Series, by Mogens Dyhr-Nielsen, October 1972.

No. 55 Drought Impact on Regional Economy by Jaime Millan, October 1972.

No. 56 Structural Analysis of Hydrologic Time Series, by Vujica Yevjevich, November 1972.

No. 57 Range Analysis for Storage Problems of Periodic-Stochastic Processes, by Jose Salas La Cruz, November 1972.

No. 58 Applicability of Canonical Correlation in Hydrology, by Padoong Torranin, December 1972.

No. 59 Transposition of Storms, by Vijay Kumar Gupta, December 1972.